Engineering with Computers (2022) 38:1581–1625
https://doi.org/10.1007/s00366-020-01120-w

ORIGINAL ARTICLE

HMPA: an innovative hybrid multi-population algorithm based on artificial ecosystem-based and Harris Hawks optimization algorithms for engineering problems

Saeid Barshandeh[1] · Farhad Piri[2] · Simin Rasooli Sangani[3]

Received: 6 May 2020 / Accepted: 18 July 2020 / Published online: 28 July 2020

Abstract
Optimization algorithms have made considerable advancements in solving complex problems with the ability to be applied to innumerable real-world problems. Nevertheless, they are passed through several challenges comprising of equilibrium between exploration and exploitation capabilities, and departure from local optimums. Portioning the population into several sub-populations is a robust technique to enhance the dispersion of the solution in the problem space. Consequently, the exploration would be increased, and the local optimums can be avoided. Furthermore, improving the exploration and exploitation capabilities is a way of increasing the authority of optimization algorithms that various researches have been considered, and numerous methods have been proposed. In this paper, a novel hybrid multi-population algorithm called HMPA is presented. First, a new portioning method is introduced to divide the population into several sub-populations. The sub-populations dynamically exchange solutions aiming at balancing the exploration and exploitation capabilities. Afterthought, artificial ecosystem-based optimization (AEO) and Harris Hawks optimization (HHO) algorithms are hybridized. Subsequently, levy-flight strategy, local search mechanism, quasi-oppositional learning, and chaos theory are utilized in a splendid way to maximize the efficiency of the HMPA. Next, HMPA is evaluated on fifty unimodal, multimodal, fix-dimension, shifted rotated, hybrid, and composite test functions. In addition, the results of HMPA is compared with similar state-of-the-art algorithms using five well-known statistical metrics, box plot, convergence rate, execution time, and Wilcoxon's signed-rank test. Finally, the performance of the HMPA is investigated on seven constrained/unconstrained real-life engineering problems. The results demonstrate that the HMPA is outperformed the other competitor algorithms significantly.

Keywords Hybrid optimization · Multi-population · Chaos theory · Levy flight · Local search · Engineering problems · Wilcoxon signed-rank test · CEC 2017 test functions

1 Introduction

Optimization algorithms are the most efficient approaches for solving time-consuming and complex real-world scientific, medical, engineering, and other NP-complete problems [1]. In the optimization process, the value of a target function is minimized or maximized [2, 3]. Meta-heuristic algorithms provide new techniques in discovering optimal or near-optimal solutions in a reasonable amount of time [4]. In recent years, researchers have increasingly focused on these algorithms, and they developed numerous algorithms inspired by various phenomena. For instance, Smart Flower Optimization Algorithm (SFOA) [5], Group Teaching Optimization Algorithm (GTOA) [6], Locust Swarm Optimization (LSO) [7], Manta Ray Foraging Optimization (MRFO) [8], Supply–Demand-Based Optimization (SDO)

✉ Saeid Barshandeh
saeid_barshandeh@yahoo.com

Farhad Piri
Farhad.peeri@aut.ac.ir

Simin Rasooli Sangani
simin.rasooli@gmail.com

[1] Afagh Higher Education Institute, Urmia, Iran

[2] Electrical Engineering Department, Amirkabir University of Technology, Hafez Avenue, Tehran 15875-4413, Iran

[3] Computer Engineering Department, Urmia Branch, Islamic Azad University, Urmia, Iran

[9], Artificial Electric Field Algorithm (AEFA) [10], Equilibrium Optimizer (EO) [11], Sooty Tern Optimization Algorithm (STOA) [12], Henry Gas Solubility Optimization (HGSO) [13], Fitness Dependent Optimizer (FDO) [14], Parasitism-Predation algorithm (PPA) [15], Emperor Penguin Optimizer (EPO) [16], Multi-Objective Spotted Hyena Optimizer (MOSHO) [17], Seagull Optimization Algorithm (SOA) [18], Spotted Hyena Optimizer (SHO) [19, 20], and Marine Predators Algorithm (MPA) [21] are among the most recently published meta-heuristic algorithms. These algorithms are widely used in complex problems such as time series [22–24], industrial applications [25], non-linear applications [26–29], clustering and feature selection [30].

Considering the inspiring phenomenon, meta-heuristic algorithms can be divided into different categories. Figure 1 illustrates a possible classification of the meta-heuristic algorithms and provides some representative algorithms for each category.

Artificial Ecosystem-based Optimization (AEO) [31], and Harris Hawks Optimization (HHO) [32] algorithms are two influential and potent population-based meta-heuristic algorithms, which are inspired by the flow of energy in the ecosystem of the Earth, and intelligence cooperative behavior of Harris' hawks in nature, respectively. These algorithms, like other optimization algorithms, start with a randomly generated set of solutions within the problem space [33, 34]. Then, the solutions are updated according to the historical data and the other solutions' information in the limited iteration [35]. In this gradual process, the quality of the solutions is increased, and further optimal solutions are found for the given problem. These algorithms were applied to various problems, and tested on abundant test functions, attaining promising results.

However, they have several deficiencies. For example, the convergence rate of them is scant in some high-dimensional and complex problems, and they do not have full confidence in finding an optimal solution in a reasonable time. In addition, the AEO algorithm has insufficient exploration capability and has inadequate performance on multimodal problems. Besides, they fall into local optimums easily. Once a solution gets stuck on a local optimum, it cannot search other areas of the problem space with more iterations. This observation is exceptionally unfavorable for real-world NP-Hard applications.

To compensate for the above-mentioned and other shortcomings, the notable creation and successful development of new optimization algorithms is still a challenging task. Researchers have provided various techniques to overcome these weaknesses (e.g., taking advantage of the chaos theory [36–38], hybridizing supplementary algorithms [39–44], using the memory in solutions [45–48], applying greedy or hill climbing selection methods [49–52], dividing the population into several sub-populations [53–56], utilizing of orthogonal learning [57–59], using quantum-based strategy [60–62], employing oppositional learning [63–65], taking benefits of information sharing mechanisms [66–68], etc.).

In this paper, the following strides have been taken to overcome the stated deficiencies of the AEO and HHO algorithms.

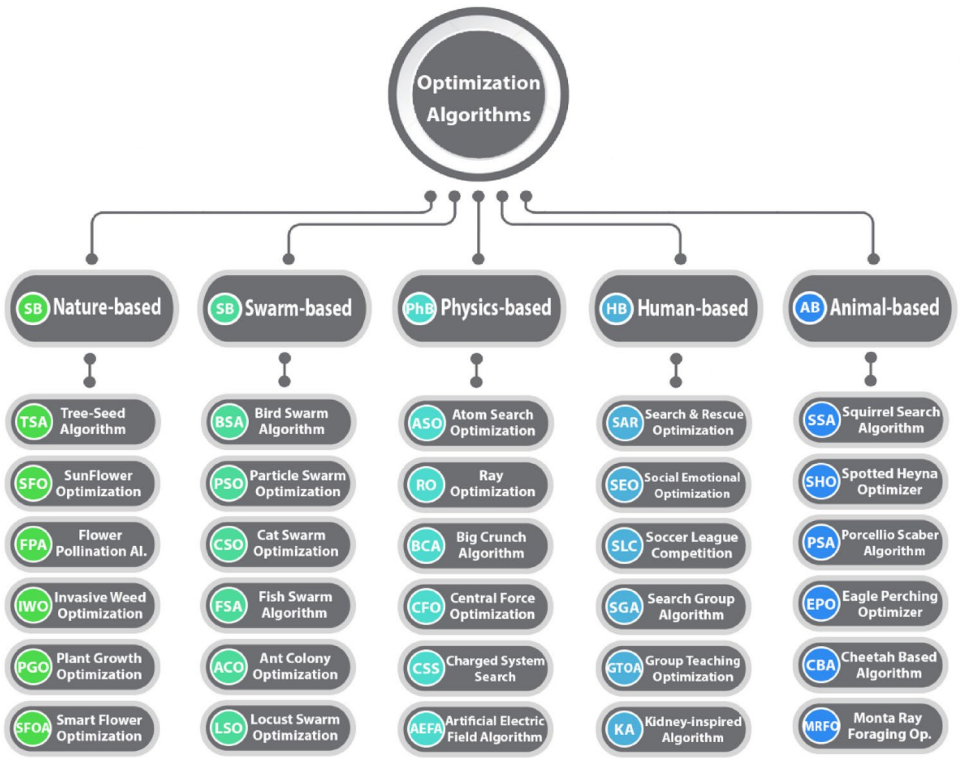

Fig. 1 Classification of meta-heuristic algorithms

Initially, a multi-population technique has been introduced to enhance the population diversity. The Multi-population technique significantly increases the exploration capability by scattering the solutions over the entire search space. This dispersion allows solutions to search for more areas of problem space and find promising areas. With this technique, the population is divided into several sub-populations, and each sub-population searches independently. Nonetheless, the number of solutions in the sub-populations are changed dynamically.

Next, the quasi-oppositional mechanism is utilized to increase exploration capability further. The quasi-oppositional mechanism is an expansion of opposite position-based learning that many papers have considered the phenomenon [69–71].

Afterwards, a chaotic-based local search (CLS) approach is adopted in the proposed algorithm to increase the exploitation capability of it. The CLS, using the advantages of the chaotic maps, probes around a solution to find better ones. This behavior dramatically increases the exploitation ability [72, 73]. Furthermore, for improving the exploitation as much as possible, the levy-flight random walk has also been exploited. According to the obtained results of the levy-flight based optimization algorithms, it can be concluded that levy-flight is an efficient technique to improve efficiency [74–76].

Next, the greedy selection strategy has been introduced to accelerate the convergence speed. The greedy selection mechanism can mitigate excessive differentiation and preserve the excellent characteristics of the solution [57]. Additionally, this strategy can also achieve further targeted search process. However, it can cause solutions to get stuck in local optimums and prevent them from jumping out. Hence, a mechanism is required to take solutions out of local optimums.

Finally, a mechanism is introduced to bring the trapped solution out. The effectiveness of the mechanism has been evidenced in our previous work [1].

The resulting multi-population hybrid algorithm is extensively evaluated over forty-five unconstrainted single-objective test functions from different categories. The evaluations are conducted with statistically comparing the resulting algorithm with numerous similar meta-heuristic algorithms. Moreover, the Wilcoxon signed-rank test is used to investigate the possible significant difference between the proposed algorithm and the competitor algorithms. In the end, the superiority of the proposed multi-population algorithm is tested on seven widely-used constrained and unconstrained engineering problems.

The key contributions of this paper can be summarized as follow:

- AEO algorithm has been hybridized with HHO in an innovative way.
- A novel multi-population model has been introduced to the resulting algorithm.
- A new levy-flight based function has been presented.
- Two neoteric local search algorithms have been provided.
- The quasi-oppositional learning technique has been used.
- The proposed algorithm has been tested on fifty classical and CEC 2017 test functions.
- The proposed algorithm has been applied on several real-life applications.
- The proposed algorithm has been compared with state-of-the-art algorithm statistically and visually.
- The obtained results have been proved by Wilcoxon signed-rank test.

The rest of the paper is organized as follows. Section 2 reviews some of the multi-population and multi-swarm algorithms. Sections 3 and 4 present a concise description of artificial ecosystem-based optimization, and Harris Hawks optimization algorithms, respectively. Section 5 provides the mathematical details and different parts of the proposed algorithm. In Sect. 6, the experimental results of the algorithms are provided on the test functions. Section 7 gives the results of real-world problems experiments, and finally, Sect. 8 propounds the conclusion and future perspectives.

2 Literature review

This section aims at giving a brief review of the presented multi-population algorithms. Many pieces of research attempted to improve the performance of meta-heuristic algorithms using multi-swarming or multi-populating techniques. For instance, in [77], Qiu proposed a novel multi-swarm particle swarm optimization algorithm. In the proposed algorithm, the population is divided into several sub-swarms, and the particles of each sub-swarm update their positions according to the corresponding best particle of the swarm.

Besides, Rao et al. suggested an adaptive multi-team perturbation Jaya algorithm in [53]. In the suggested schema, the multiple teams of the population are used to explore search scopes efficiently, and the teams have the same size with different perturbation or movement equations. The supremacy of the solutions of the teams are investigated based on the fitness value and boundary violations.

Furthermore, in [55], Rao and Pawar presented self-adaptive multi-population Rao algorithms for solving engineering design problems. In this study, the initial population of Rao algorithms is divided into several sub-population to keep the diversity of the population. In addition, the number and members of sub-populations are changed over time. The resulting algorithms are evaluated on 25 test functions and several constrained engineering problems.

Additionally, in [78], the authors propounded a multi-swarm multi-objective hybrid algorithm called MSMO/2D. In MSMO/2D, the particle swarm optimization algorithm

is integrated with decomposition and dominance strategies. This algorithm has been proposed to reduce the gap between solutions in the Pareto Front, and maximize the solutions' diversity.

Moreover, a new multi-swarm hybrid optimization algorithm has been presented in [79] by Nie, and Xu for solving dynamic optimization problems. In the presented multi-swarm algorithm, the particle swarm algorithm is combined with the simulated annealing algorithm and a prediction strategy. Afterwards, the resulting algorithm has been applied to the CEC 2009 test functions. These changes enhanced the adaptability of individual evolution and balanced exploration and exploitation.

Similarly, in [80], Li et al. proposed a multi-swarm cuckoo search algorithm named MP-QL-CS, which is enhanced by the Q-learning strategy. In Q-Learning, the optimal action is learned by selecting the action of enlarging the accumulative benefits with a discount. Additionally, to evaluate the multi-stepping evolution effect and learn the optimal step size, Q function value used a step size control in the proposed algorithm. The Q function is defined as diminished, the maximum expected, and cumulative reward.

In addition, in [81], the authors developed a novel multi-population differential evolution algorithm. In the proposed algorithm, the diversity of the population increases while the simplicity is preserved. The diversity is achieved by dividing the population into independent subpopulations, which each subpopulation has the different mutation and update equations. A new mutation strategy, which utilizes information on the best solution or a randomly selected one, is used as another contribution to balance exploration and exploitation by generating better individuals. Moreover, in the proposed algorithm, function evaluations are divided into epochs. At the end of each epoch, solutions of the sub-populations are exchanged.

In a similar study, Biswas et al. proposed a new multi-swarm artificial bee colony algorithm for global searching [82]. In this study, the swarm of bees is divided into multiple sub-swarms, which are characterized using different and unique perturbation mechanisms. Also, the reinitializing operator has been replaced with a set of criteria for detecting impotent sub-swarms. Whenever an impotent bee is detected in a sub-swarm, the foragers mitigation strategy is performed considering the minimum member constraint.

Likewise, in [83], Di Carlo et al. provided a novel multi-population adaptive inflationary differential evolution algorithm. In the inflationary differential evolution algorithm, some of the restart, and local search techniques of monotonic basin hopping have been used. In addition, in the proposed adaptive differential evolution algorithm, the CR, and F parameters are adopting with each other automatically with the size of local restart bubble, and the number of local restarts of monotonic basin hopping. The multi-swarming technique in the proposed algorithm avoids trapping in the local optimums.

Withal, Xiang and Zhou offered a multi-colony artificial bee colony algorithm in [84]. In the offered algorithm, a multi-deme model and a dynamic information technique are used to handle multi-objective problems. The colonies in the algorithm search the problem space independently by exchanging useful information. The colonies have the same number of employed and onlooker bees, and the bees search the space by neighboring information and use the greedy mechanism to keep better solutions.

Correspondingly, in [85], the authors propounded a new hybrid multi-swarm particle swarm optimization and shuffled frog leaping algorithm to improve particle communications and enhance their searching ability. Accompanying the multi-swarming, and updating along with a cooperating strategy have been proposed in the propounded algorithm. The particles of the sub-swarms update their positions using the equations morphed from the shuffled frog leaping algorithm.

In addition, Wu et al. proposed a multi-population differential evolution algorithm with different mutation strategies [86]. The mutation strategies are current particle to best particle, current particle to random particle, and random mutation. In the proposed algorithm, four sub-populations are used: three sub-populations with a smaller size and one with a larger size. After a specified number of rounds, the best mutation strategy can be determined using the fitness improvements and consumed functions evaluated. Subsequently, the reward sub-population will dynamically be allocated to the determined best performing mutation strategy.

3 Artificial ecosystem-based optimization

The artificial ecosystem-based optimization (AEO) is a novel nature-inspired meta-heuristic algorithm, which is presented in [31] by Zhao et al. AEO is a population-based algorithm inspired from the energy flow in the ecosystem of Earth, and has three main operators: production, consumption, and decomposition. The details of the AEO algorithm, along with the exposition of its operators, have been presented in the [31]. However, a brief overview of the operator's head with its equations is presented here.

3.1 Production

The first operator of the AEO algorithm is production. Through using this operator, a new individual is produced using Eq. (1) between the best individual and a randomly selected individual from the current population.

$$\mathrm{New}X_1^{\mathrm{It}+1} = (1-a)\cdot \mathrm{Best}X + a\cdot X_r^{\mathrm{It}} \tag{1}$$

$$a = \left(1 - \frac{\text{It}}{\text{Max\_it}}\right) \cdot r_1 \tag{2}$$

$$X_r^{\text{It}} = \text{Lb} + r \cdot (\text{Ub} - \text{Lb}) \tag{3}$$

where Best$X$ is the best individual found so far, It is the current iteration, r and r_1 are random number vectors within (0,1) whose sizes are Dim and one, respectively. Furthermore, Dim is the dimension of the problem, Lb and Ub are the lower and upper bounds of problem space, respectively. The a is a coefficient, which decreases linearly over time and specifies the exploration or exploitation of the New$X_1^{\text{It+1}}$.

3.2 Consumption

The second operator of the AEO is the consumption operator. The consumer individuals are divided into three species: Herbivore, Carnivore, and Omnivore, and are updated by Eqs. (4)–(6), respectively.

$$\text{New}X_i^{\text{It+1}} = X_i^{\text{It}} + C \cdot \left(X_i^{\text{It}} - \text{New}X_1^{\text{It+1}}\right) \tag{4}$$

$$\text{New}X_i^{\text{It+1}} = X_i^{\text{It}} + C \cdot \left(X_i^{\text{It}} - X_j^{\text{It}}\right) \tag{5}$$

$$\text{New}X_i^{\text{It+1}} = X_i^{\text{It}} + C \cdot r_2 \cdot \left(X_i^{\text{It}} - \text{New}X_1^{\text{It+1}}\right) + \left(1 - r_2\right)\left(X_i^{\text{It}} - X_j^{\text{It}}\right) \tag{6}$$

where r_2 is a random number in range (0,1), X_j is a randomly chosen solution from the current population, and C can be obtained as below:

$$C = \frac{1}{2} \cdot \frac{u}{v} \tag{7}$$

where u and v are normally distributed random numbers. It is worth mentioning that the second-best individual is in the Herbivore category.

3.3 Decomposition

The last operator of the AEO is a decomposition operator, which models the decomposition process in ecosystems. This process is formulated as Eq. (8). In other words, the individuals in this phase are updated by Eq. (8).

$$\text{New}X_i^{\text{It+1}} = X_N^{\text{It}} + D \cdot \left(e \cdot X_N^{\text{It}} - h \cdot X_i^{\text{It}}\right) \tag{8}$$

where X_N^{It} is the best individual in the current iteration, D, e, and h are calculated using Eqs. (9)–(11), respectively.

$$D = 3u \tag{9}$$

$$e = r_3 \cdot \text{rand}i([12]) - 1 \tag{10}$$

$$h = 2 \cdot r_3 - 1 \tag{11}$$

where u is a normally distributed random numbers, and r_3 is a random number in (0,1). The flowchart of the AEO has been illustrated in Fig. 2.

4 Harris Hawks optimization

Harris Hawks optimization (HHO) algorithm is another powerful population-based meta-heuristic algorithm, which is motivated by the behavior of Harris' hawks in nature [32]. As with the previous algorithm, a summary of the HHO algorithm is given with its update equations (for more details, refer to [32]). HHO models the intelligence cooperative behavior and chasing style of Harris hawks mathematically. The HHO consists of two main phases: exploration and exploitation, which are characterized in the next subsections. In addition, these phases are selected by parameter E, which can be obtained by Eq. (12).

$$E = 2E_0\left(1 - \frac{\text{It}}{\text{Max\_it}}\right) \tag{12}$$

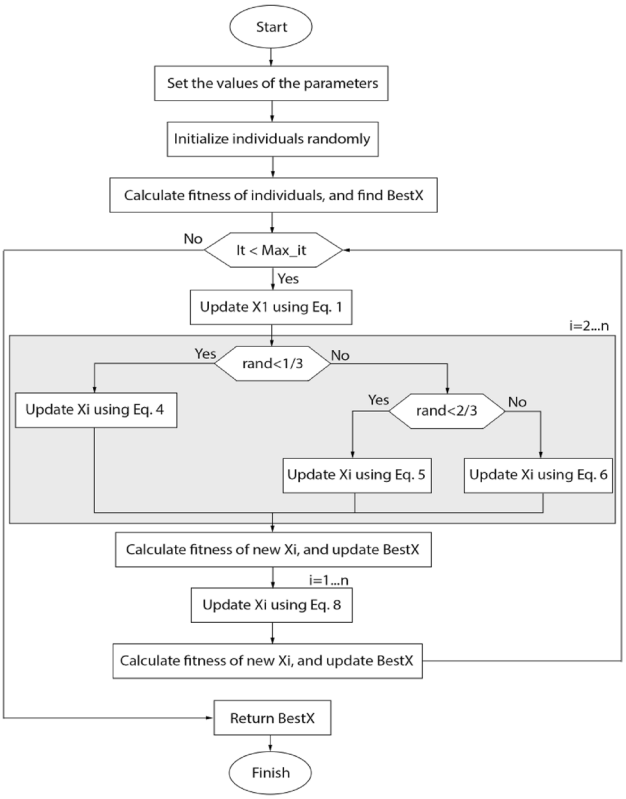

Fig. 2 Flowchart of the basic AEO

where E_0 is the initial energy of the prey, It and Max_it are the current, and maximum number of iterations, respectively. Whenever $|E| \geq 1$, the exploration phase is selected, and when $|E| < 1$, the exploitation phase is going to be selected.

4.1 Exploration phase

The current phase presents the exploration mechanism of HHO. In this phase, the solutions are updated by the perching strategy of Harris hawks that is simulated by Eq. (13).

$$\mathrm{New}X_i^{\mathrm{It}+1} = \begin{cases} X_r^{\mathrm{It}} - r_1\left|X_r^{\mathrm{It}} - 2r_2X_i^{\mathrm{It}}\right| & q \geq 0.5 \\ \left(\mathrm{Best}X - X_m^{\mathrm{It}}\right) - r_3\left(\mathrm{Lb} + r_4(\mathrm{Ub} - \mathrm{Lb})\right) & q < 0.5 \end{cases} \tag{13}$$

In Eq. (13), X_i^{It} is the current position of ith solution in iteration It, $\mathrm{New}X_i^{\mathrm{It}+1}$ is the updated position of ith, X_r^{It} is a randomly chosen solution from the population, r_1, r_2, r_3, r_4, and q are random numbers in (0,1), Best$X$ is the best solution found so far, Lb and Ub are the lower and upper bounds of problem space, and X_m^{It} is the average of the solutions in the current population, and can be calculated using Eq. (14).

$$X_m^{\mathrm{It}} = \frac{1}{N}\sum_{i=1}^{N} X_i^{\mathrm{It}} \tag{14}$$

where N is the number of solutions in the population.

4.2 Exploitation phase

This phase models the surprising pounce of the Harris hawks. Given that the preys try to escape from the menacing situation, the Harris hawks use different chasing styles for hunting. In this phase, four possible strategies are suggested to simulate the attacking behaviors: soft besiege, hard besiege, soft besiege with progressive rapid dives, and hard besiege with progressive rapid dive, which are briefly described in the next subsections. Two parameters are used in HHO to choose one of these four strategies. First parameter is r, which is a random number inside (0,1), and the second one is E, which is calculated using Eq. (12).

4.2.1 Soft besiege

When $r \geq 0.5$ and $|E| \geq 0.5$, the soft besiege phase is selected, and the solution is updated by Eq. (15).

$$X_i^{\mathrm{It}+1} = \Delta X^{\mathrm{It}} - E\left|J \cdot \mathrm{Best}X - X_i^{\mathrm{It}}\right| \tag{15}$$

$$\Delta X^{\mathrm{It}} = \mathrm{Best}X - X_i^{\mathrm{It}} \tag{16}$$

$$J = 2\left(1 - r_5\right) \tag{17}$$

where r_5 is a random number between [0, 1].

4.2.2 Hard besiege

When $r \geq 0.5$ and $|E| < 0.5$, the hard besiege phase is used, and the solution is updated by Eq. (18).

$$X_i^{\mathrm{It}+1} = \mathrm{Best}X - E\left|\Delta X^{\mathrm{It}}\right| \tag{18}$$

4.2.3 Soft besiege with progressive rapid dives

When $r < 0.5$ and $|E| \geq 0.5$, the third strategy is selected, and the solution is updated using Eq. (19).

$$X_i^{\mathrm{It}+1} = \begin{cases} Y & F(Y) < F\left(X_i^{\mathrm{It}}\right) \\ Z & F(Z) < F\left(X_i^{\mathrm{It}}\right) \end{cases} \tag{19}$$

$$Y = \mathrm{Best}X - E\left|J \cdot \mathrm{Best}X - X_i^{\mathrm{It}}\right| \tag{20}$$

$$Z = Y + S \times L \tag{21}$$

$$LF(x) = 0.01 \times \frac{u \times \sigma}{|v|^{\frac{1}{\beta}}} \tag{22}$$

$$\sigma = \left(\frac{\Gamma(1+\beta) \times \sin\left(\frac{\pi\beta}{2}\right)}{\Gamma\left(\frac{1+\beta}{2}\right) \times \beta \times 2\left(\frac{\beta-1}{2}\right)}\right)^{\frac{1}{\beta}} \tag{23}$$

where F is the fitness of the given solution, S is a random vector, L is the levy-flight function, u and v are random values in (0,1), and β is a constant value of 1.5.

4.2.4 Hard besiege with progressive rapid dives

When $r < 0.5$ and $|E| < 0.5$, the solution is updated using the last phase, which is modeled by Eq. (24).

$$X_i^{\mathrm{It}+1} = \begin{cases} Y & F(Y) < F\left(X_i^{\mathrm{It}}\right) \\ Z & F(Z) < F\left(X_i^{\mathrm{It}}\right) \end{cases} \tag{24}$$

$$Y = \mathrm{Best}X - E\left|J \cdot \mathrm{Best}X - X_m^{\mathrm{It}}\right| \tag{25}$$

$$Z = Y + S \times L \tag{26}$$

where X_m^{It}, and L are calculated using Eqs. (14) and (22), respectively. The flowchart of the HHO algorithm is represented in Fig. 3.

5 Proposed hybrid multi-population algorithm (HMPA)

As mention earlier, the main challenge of the meta-heuristic algorithms is enhancing the exploration and exploitation capabilities and balancing them. In addition, providing an approach to avoid or jump out of local optimums is another challenge relevant to the so-called algorithms. In the proposed hybrid multi-population algorithm (HMPA), the whole list of these issues is considered, and a solution is provided for each of them, which are described below in detail. Figure 4 outlines the schematic view of the HMPA.

5.1 Proposed multi-population technique

First, a novel multi-population technique has been utilized to propagate the diversity of solutions. This technique helps to make the solutions more scattered and search for more space of the problem. For this intension, three sub-populations are considered in the proposed method, which exchanges the solutions dynamically. The first sub-population is responsible for independently searching the entire space of the problem, which initially includes 60% of the solutions. This process improves exploration significantly. The solutions in the first sub-population update their position using Eq. (27). Additionally, this equation is used in the initialization phase to initialize the solutions.

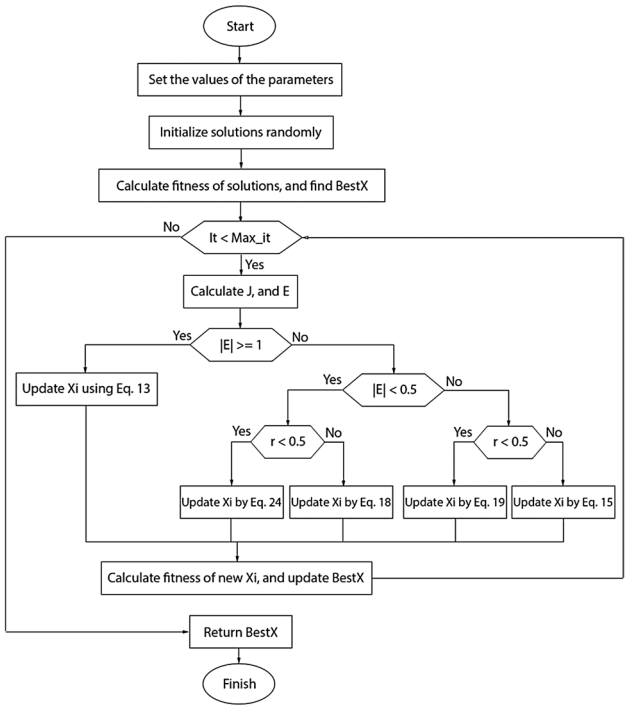

Fig. 3 Flowchart of the basic HHO

$$\text{new}X_i^{\text{It}} = \text{Lb} + \text{rand}(0,1) \times (\text{Ub} - \text{Lb}) \tag{27}$$

To make this random search process more efficient, the new solution that is being produced will replace the previous solution only if it has better fitness. The greedy selection mechanism dramatically increases efficiency. Figure 5 presents the pseudo-code of the greedy selection mechanism that is used in HMPA.

Moreover, in each H iterations, the best solution of the first sub-population is selected and added to one of the second or third sub-populations. Thenceforth, the selected solution will be eliminated from the first sub-population. In this way, the number of solutions in the first sub-population is reduced, and the solutions for the next two sub-populations increased over time. This makes the algorithm more searchable in the initial iterations and more exploitable in the final iterations.

Afterwards, the remained 40% of initial solutions are divided into two sub-populations equally. The solutions of each sub-population update their positions according to the best solution (local best of the sub-population) and other solutions of the corresponding sub-population. Consequently, the solutions are converged to two different areas, instead of converging only to one point. Besides, there is a counter in the solutions of second and third sub-populations, which counts the unsuccessful updates of the solutions. With this parameter, the trapped solutions in the local optimal points can be detected. The details of this parameter and its effectiveness are entirely stated in our previous work [1]. Similarly, in each H iterations, if the counter of a solution exceeds a threshold (Thr), and the members of the sub-population (NM) were more than specified minimum numbers (MNM), the solution will be transmitted into the first sub-population to reinitialize. Maintaining the minimum number of solutions in the sub-populations are for retaining the successful functioning of the sub-populations. As it is vividly apparent, the size of the sub-populations is changed dynamically, and they can exchange the solutions. Figure 6 illustrates the exchange mechanism between sub-populations.

The solutions of the second and third sub-populations are updated either with AEO or HHO algorithm.

5.2 Quasi-oppositional learning

The quasi-oppositional position technique (QOPP) is used in the HMPA to enhance the searching ability. The QOPP is a learning-based technique, which can improve the searching ability by generating the symmetrical position of a solution [87]. In HMPA, the QOPP has been used only in the autonomous solutions of the first sub-population. The pseudo-code of the QOPP is presented in Fig. 7.

Fig. 4 Flowchart of HMPA

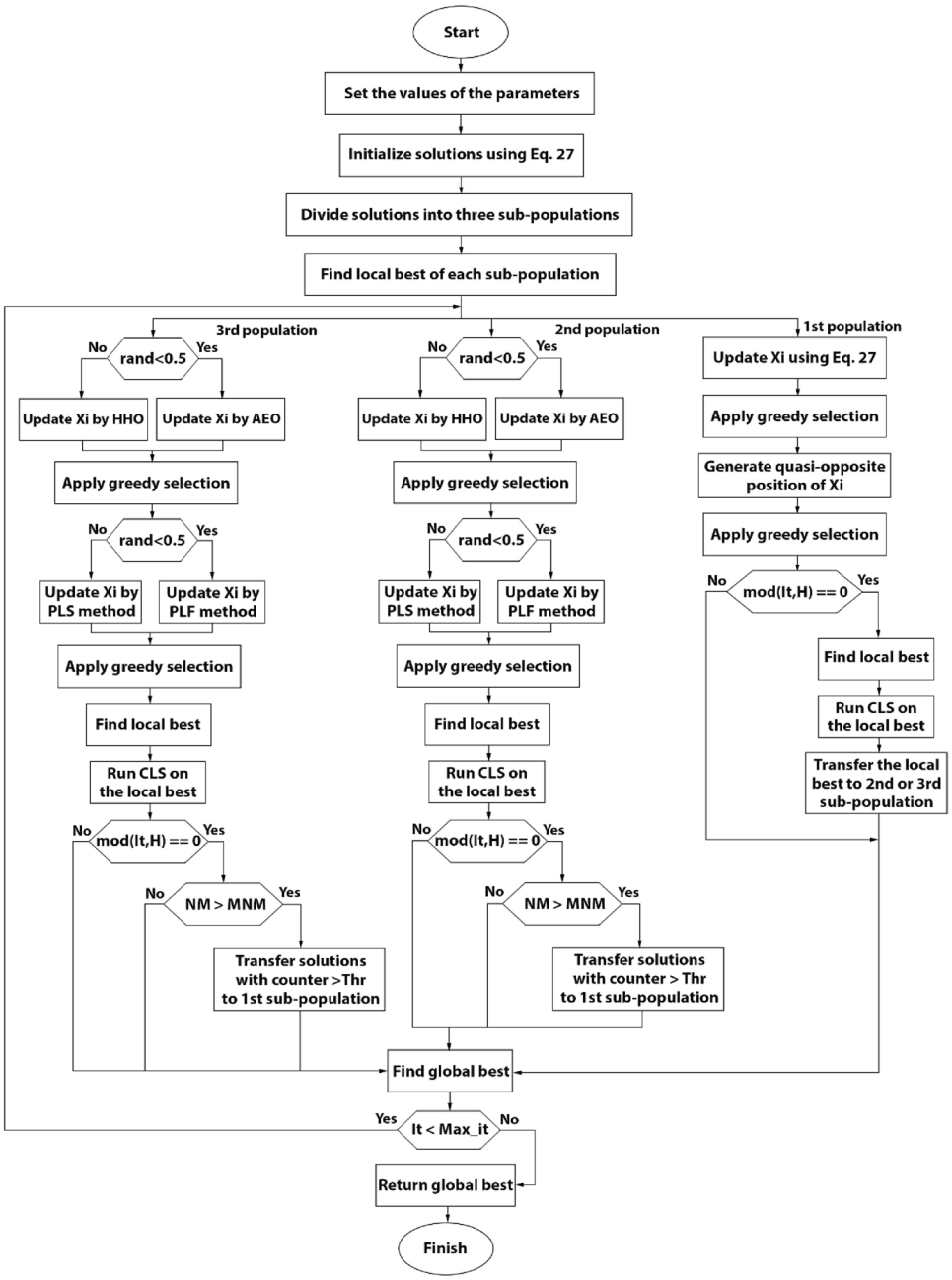

In pseudo-code of Fig. 7, D is the dimension of the problem, and $\mathrm{QOp}X_i^{\mathrm{It}}$ is the quasi-opposite position of X_i^{It}. In addition, as shown in Fig. 4, after generating new solutions using the QOPP, the greedy selection mechanism is used yet again.

5.3 Chaotic local search strategy

Chaotic local search (CLS) strategy explores the nearby of a solution to discover promising areas [69]. Therefore, this

```
if fitness(newX_i^It) < fitness(X_i^It)
    X_i^It = newX_i^It
    Counter(i) = 0
else
    % only for the solutions of 1st, 2nd sub-populations
    Counter(i) = Counter(i) + 1
end if
```

Fig. 5 Pseudo-code of the greedy selection mechanism

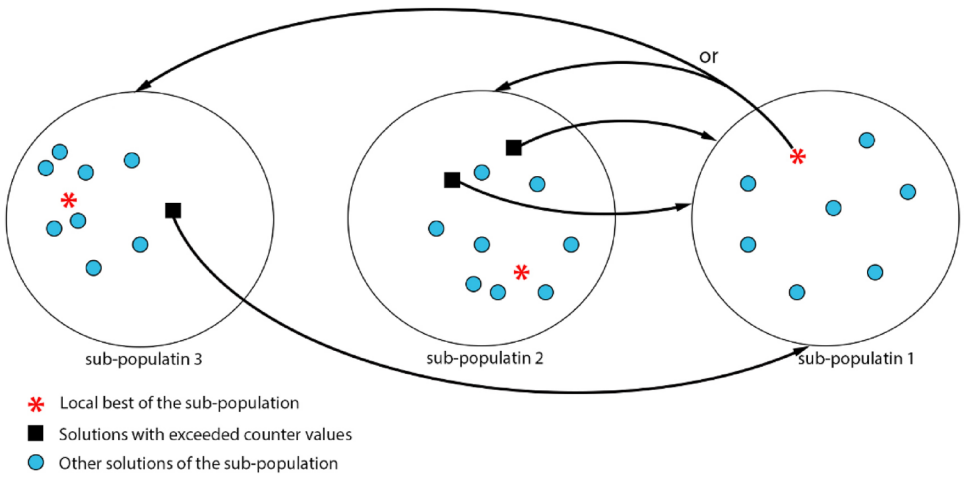

Fig. 6 Solution exchange mechanism between sub-populations

for $j = 1$ to D
$OpX_{i,j}^{It} = Lb + Ub - X_{i,j}^{It}$
$C_j = (Lb_j + Ub_j)/2$
if $X_{i,j}^{It} < C_j$
$QOpX_{i,j}^{It} = C_j + (OpX_{i,j}^{It} - C_j) \times rand(0,1)$
else
$QOpX_{i,j}^{It} = OpX_{i,j}^{It} + (C_j - OpX_{i,j}^{It}) \times rand(0,1)$
end if
end for

Fig. 7 Pseudo-code of the QOPP

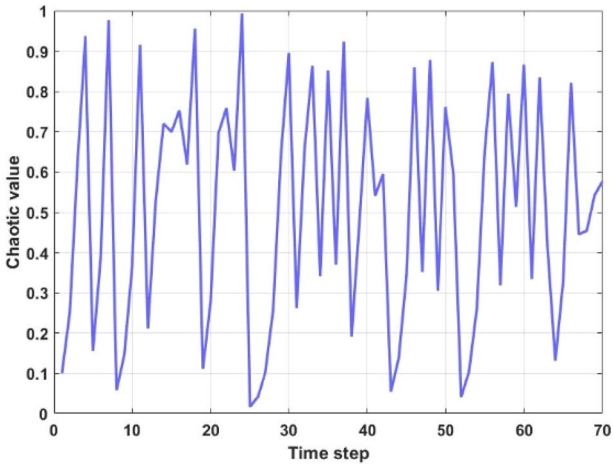

Fig. 8 Distribution of the piecewise map over time

strategy enhances exploitation capability. Besides, taking advantages of chaos theory increases the potency of the strategy. In HMPA, the CLS strategy is just applied to the local best of the sub-populations. In this way, only around the best solutions will be explored, and the execution time will be reduced. In the CLS, a new local best solution can be calculated using Eq. (28).

$$\text{newBest}X = \text{Best}X + \left(\text{CV}^{k+1} - 0.5\right) \times \left(X_{r1}^{\text{It}} - X_{r2}^{\text{It}}\right) \quad (28)$$

where X_{r1}^{It} and X_{r2}^{It} are two randomly selected solutions from the corresponding sub-population, and CV^{k+1} is the chaotic value generated by the chaotic map. In the HMPA, the piecewise map has been selected as the chaotic map, which is a well-known chaotic map and generates random numbers between (0,1). The piecewise chaotic map is modeled mathematically as below:

$$\text{CV}^{k+1} = \begin{cases} \frac{\text{CV}^k}{P} & 0 \le \text{CV}^k \le P \\ \frac{\text{CV}^k - P}{0.5 - P} & P \le \text{CV}^k < 0.5 \\ \frac{1 - P - \text{CV}^k}{0.5 - P} & 0.5 \le \text{CV}^k < 1 - P \\ \frac{1 - \text{CV}^k}{P} & 1 - P \le \text{CV}^k < 1 \end{cases} \quad (29)$$

P = 0.4

Figure 8 shows the distribution of the piecewise map over time.

Similarly, the pseudo-code of the CLS strategy is provided in Fig. 9.

After producing a new local best using the proposed CLS strategy, the greedy selection mechanism is used to increase profitability.

for $k = 1$ to K
  Update CV using Eq. 29
  Select X_{r1}^{It} and X_{r2}^{It} from the sub-population randomly
  Generate new local best using Eq. 28
  Apply the greedy selection mechanism
end for

Fig. 9 Pseudo-code of the CLS strategy

5.4 Proposed levy-flight function (PLF)

The levy-flight random walk function has been introduced earlier in Sect. 4 in the HHO algorithm. The levy-flight random walk is an advantageous approach to enhance the performance of the algorithms by increasing exploitation. This approach has been used in the state-of-the-art algorithms in various ways. In HMPA, this approach is used in a novel way, as illustrated in Fig. 10.

In the PLF, the first command can speed up the convergence, and the second command improves the exploitation capability. Additionally, LF is the value obtained by the Eq. (22).

5.5 Proposed local search mechanism (PLS)

To increase the searching strength of the HMPA, a local search mechanism denoted as PLS is also proposed, which searches the space between solutions of the sub-population more accurately to discover better solutions. In PLS, a new solution is generated using Eq. (30).

$$X_i^{\mathrm{It}+1} = \begin{cases} X_i^{\mathrm{It}} + \mu \cdot \left(X_i^{\mathrm{It}} - X_j^{\mathrm{It}}\right) & \delta < \mathrm{CP2} \\ X_i^{\mathrm{It}} + \mu \cdot (\mathrm{Best}X - NX) & \text{otherwise} \end{cases} \tag{30}$$

where μ is coefficient between $(-L, +L)$, L and δ are random numbers in (0,1), X_j^{It} is a randomly chosen solution from the sub-population, CP2 is a control parameter with a value of 0.5, and NX is a solution vector produced by Eq. (27). The pseudo-code of the PLS is provided in Fig. 11.

if $CP1 < \rho$
  $X_i^{It+1} = X_i^{It} \times LF$
else
  $X_i^{It+1} = X_i^{It} + LF$
end if

Fig. 10 Proposed levy-flight function (PLF)

for i = 1 : N
  update X_i^{It} using Eq. 30
  apply greedy selection mechanism
end

Fig. 11 Proposed local search mechanism (PLS)

5.6 Computational complexity

In this subsection, the computational complexity of HMPA is discussed in terms of time complexity on three main process of the algorithm: initialization, fitness evaluation, and updating phase.

The complexity of the initialization phase is $O(N)$, where N is the total number of solutions. The evaluating fitness of solutions requires $O(T \times (N \times N + 3 \times K))$ time, since the fitness of each solution is evaluated twice in each iteration, and three local best solutions are evaluated K times in each iteration. The T is the maximum number of iterations.

The updating phase of the proposed algorithm is consisting of three branches; therefore, the complexity of the updating phase is discussed for each branch.

The complexity of the first branch is $O\left(T \times \left(N_1 + D \times N_1 + K\right)\right)$, which N_1 is the number of solutions in the first sub-population, and D indicates the dimension of the problem.

For the second and third branches the approximate complexity must be expressed, since the AEO or HHO, and PLS or PLF algorithms are selected randomly in each iteration. The approximate complexity of the second and third branches are $O\left(T \times (N_2 \times (A_1 + A_2) + K)\right)$ and $O\left(T \times (N_3 \times (A_1 + A_2) + K)\right)$, respectively. Where, A_1 is the average complexity of HHO and AEO algorithms, A_2 is the average complexity of PLS and PLF methods, N_2 and N_3 are the number of solutions in the second and third sub-populations, respectively. The complexity of PLS is $O\left(N_n\right)$, PLF is $O(1)$, HHO is $O(N \times (T + T \times D + 1))$, and AEO is $O(T \times N \times N)$. It is worth to mention that $\sum_{n=1}^{3} N_n = N$.

6 Experimental results

To substantiate the superiority of the proposed HMPA, the performance of HMPA is evaluated on fifty widely-used test functions comprising unimodal, multimodal, fix-dimension, shifted rotated, hybrid, and composite functions. The results of the HMPA is compared with several state-of-the-art metaheuristic algorithms in terms of the best, worst, median, average, standard deviation, average execution time (AET) in second, and box plot metrics over the results of 30 independent executions. Furthermore, the convergence speed

of the algorithms is compared graphically. Moreover, the Wilcoxon signed-rank test is used to prove the supremacy of HMPA. The *R* column in the tables of Wilcoxon signed-rank test presents the result of the test, which '+', '− show the HMPA is significantly is better, or worse than the competitor algorithm, respectively. When the results of the algorithms are equal or very close to each other, the difference between algorithms cannot be determined using this test (The '=' sign in *R* column).

Harris hawks optimization (HHO) [32], artificial ecosystem-based optimization (AEO) [31], spotted hyena optimizer (SHO) [88], farmland fertility algorithm (FFA) [89], Salp swarm algorithm (SSA) [90], moth-flame optimization (MFO) [91], and antlion optimizer (ALO) [92] have been selected as competitor algorithms. The number of solutions in the algorithms is set to 50, and stopping criteria in them is considered to reach 1000 rounds of iteration. The values of other parameters of these algorithms are presented in Table 1, which are the default values proposed by the authors in the original papers.

The specifications of the system by which the experiments are conducted are shown in Table 2.

6.1 Experiments on unimodal test functions

In this subsection, the performance of the HMPA is evaluated on a set of standard unimodal test functions illustrated in Table 3. These test functions challenge the exploitation capability of the algorithms and categorized into separable and non-separable functions. The statistical results of the algorithms on unimodal test functions are specified in Table 4.

According to Table 4, the proposed HMPA has achieved better results on all unimodal test functions. To further evaluate the obtained results, the box plot metric is used, and the graphical results are provided in Fig. 12.

According to Table 4, the proposed HMPA has achieved better results on all unimodal test functions. To further evaluate the obtained results, the box plot metric is used, and the graphical results are provided in Fig. 12.

Figure 12 states that the HMPA has reached better and more coherent results in the independent runs. The convergence rate of algorithms is also significant in evaluating the efficiency of optimization algorithms. Figure 13 represents the convergence rates comparison of the algorithms visually.

Figure 13 expresses the HMPA started with better solutions and converged quickly in the early iterations. Moreover, the Wilcoxon signed-rank test is performed on the HMPA versus other competitor algorithms, and the results are provided in Table 5 for investigating the significant differences among the algorithms.

The p-values presented in Table 5 declare that the HMPA has a significant difference with other algorithms on all test

Table 1 Parameter values of the algorithms

Algorithm	Parameter	Value
HMPA	Thr	100
	H	5
	MNM	10
	K	10
	CP1, and CP2	0.5
	$\rho, \delta,$ and L	rand
AEO	r_1, r_2, and r	rand
	h	2 × rand-1
HHO	r_1,r_2, r_3, r_4, and q	rand
	E_0	(− 1,1)
	J	2 × (1 − rand)
SHO	$\vec{h}$	5 to 0
	$\vec{M}$	[0.5, 1]
FFA	k	2
	α	0.6
	β	0.4
	Q	0.7
ALO	Selection method	Roulette wheel
SSA	c_1,c_2, c_3	rand
MFO	Spiral constant	1
	Converge constant	− 1 to − 2
	Number of flames	$N - l \times \frac{N-1}{T}$
STOA	C_f	2
	S_A	2 to 0
	C_B	0.5 × rand
	u, v	1
MRFO	α	$2r \times \sqrt{\lvert\log(r)\rvert}$
	r_1,r_2, r_3, and r	rand
	ω	rand
	s	2
SCA	r_1,r_2, r_3, and r_4	rand
WOA	α	2 to 0
	r, p	rand
	A, l	[− 1,1]

* rand is a random number inside [0,1]

Table 2 Running platform specifications

Name	Value
Hardware	
CPU	Core i5
Frequency	3.1 GHz
RAM	8 GB
Hard drive	1 TB + 250 SSD
Software	
Operating system	Windows 10
Language	MATLAB R2017a

Table 3 Details of the unimodal test functions

	Function	dim	Range	$F_{\min}$
TF1	$f(x) = \sum_{i=1}^{d} x_i^2$	30	$[-100, 100]^d$	0
TF2	$f(x) = \sum_{i=1}^{d} \lvert x_i \rvert + \prod_{i=1}^{d} \lvert x_i \rvert$	30	$[-10, 10]^d$	0
TF3	$f(x) = \sum_{i=1}^{d} \left(\sum_{j=1}^{i} x_j \right)^2$	30	$[-100, 100]^d$	0
TF4	$f(x) = \max_i \{ \lvert x_i \rvert, 1 \le i \le d \}$	30	$[-100, 100]^d$	0
TF5	$f(x) = \sum_{i=1}^{d-1} \left[100 \left(x_{i+1} - x_i^2 \right)^2 + \left(x_i - 1 \right)^2 \right]$	30	$[-30, 30]^d$	0
TF6	$f(x) = \sum_{i=1}^{d} \left(\lvert x_i + 0.5 \rvert \right)^2$	30	$[-100, 100]^d$	0
TF7	$f(x) = \sum_{i=1}^{d} i x_i^4 + \text{random}[0, 1)$	30	$[-1.28, 1.28]^d$	0

functions, except on TF1-TF4 with SHO, and TF1-TF2 with AEO algorithms.

6.2 Experiments on multimodal test functions

This subsection evaluates the performance of the HMPA on six widely used standard multimodal test functions. The multimodal test functions are demonstrated in Table 6.

These test functions have a lot of local optima points and challenge the exploration capability of the algorithm. The statistical results of the algorithms on multimodal test functions are presented in Table 7.

As it is evident from the results of Table 7, the HMPA attained better results in all test functions. For further in-depth scrutinizing the obtained results of the algorithms on multimodal test functions, the box plot graphs are plotted and shown in Fig. 14.

As depicted in the diagrams of Fig. 14, unlike other algorithms that have diverse results in each execution, the obtained results in the proposed algorithm are closer to each other. In addition, the comparisons of the convergence rate of the algorithms are provided in Fig. 15.

The graphs of Fig. 15 represent that the HMPA is converged with more agility than other competitor algorithms in all multimodal test functions. Besides, the results of algorithms are further investigated statistically by the nonparametric Wilcoxon signed-rank test, and the consequence is presented in Table 8.

As it is evident from Table 8, the HMPA has a significant difference from other algorithms, except in TF9-TF11 from HHO, SHO, and AEO algorithms. Although the results of the algorithms are similar, considering the convergence rate of the algorithms, it can be inferred that the HMPA is premier than the other algorithms in all multimodal test functions.

6.3 Experiments on fix-dimension test functions

Fix-dimension test functions are kind of standard test functions with constant and unchangeable dimensions. This subsection presents the results of experiments on ten well-known fix-dimension test functions. The details of the test functions are provided in Table 9.

Similarly, the statistics of the obtained results by the algorithms on these test functions are presented in Table 10.

The statistical results presented in Table 10 indicate that the HMPA algorithm outperforms the competitor algorithms. Additionally, the box plot graphs of the algorithms on fix-dimension test functions are depicted in Fig. 16.

The box plots of Fig. 16 affirm the authenticity of the statistical results of the algorithms. Moreover, the convergence speeds of the algorithms are examined on fix-dimension test functions, and the results are illustrated in Fig. 17. Likewise, the non-parametric Wilcoxon signed-rank test results are provided in Table 11 to investigate the possible superiority of the HMPA with further confidence.

6.4 Experiments on CEC 2017 test functions

These test functions are the most complicated test functions, which comprise three categories: shifted and rotated hybrid, and composite. Shifted and rotated test functions are the result of rotating the optimal points around a particular axis, which complicates the optimization process. Hybrid and composite test functions are the results of combining several test functions. To achieve satisfactory results

Table 4 Statistical results obtained by the algorithms on the unimodal test functions

	Algorithm	Best	Median	Average	Worst	STD	AET(s)
TF1	HHO	1.0000e−323	2.5000e−323	3.5000e−323	8.4000-323	0.0000e+00	10.0097
	FFA	1.6369e−15	6.0574e−15	8.0388e−15	2.1586e−14	5.6259e−15	4.70663
	MFO	3.3689e−06	3.8259e−05	2.0000e+04	1.0000e+04	4.0824e+03	2.34953
	ALO	1.1823e−07	5.1007e−07	7.3696e−07	2.2146e−06	5.7755e−07	98.3398
	SHO	**0.0000e+00**	**0.0000e+00**	**0.0000e+00**	**0.0000e+00**	**0.0000e+00**	12.9254
	SSA	5.5065e−09	8.0706e−09	8.0563e−09	1.3163e−08	1.8566e−09	3.88224
	AEO	**0.0000e+00**	**0.0000e+00**	**0.0000e+00**	**0.0000e+00**	**0.0000e+00**	4.60428
	HMPA	**0.0000e+00**	**0.0000e+00**	**0.0000e+00**	**0.0000e+00**	**0.0000e+00**	19.0020
TF2	HHO	5.1979e−206	1.7512e−197	1.8512e−190	4.9795e−189	0.0000e+00	11.2838
	FFA	2.9715e+03	3.8991e+03	4.0797e+03	5.6537e+03	8.1891e+03	4.68083
	MFO	4.9049e+02	1.5404e+04	1.7750e+04	4.5014e+04	1.2734e+04	2.45368
	ALO	6.1435e+01	1.9159e+02	2.9953e+02	1.0512e+03	2.4488e+02	41.0972
	SHO	**0.0000e+00**	**0.0000e+00**	**0.0000e+00**	**0.0000e+00**	**0.0000e+00**	6.50187
	SSA	1.2186e−02	1.2476e−01	2.3641e−01	1.0632e+00	2.8210e−01	3.73297
	AEO	**0.0000e+00**	**0.0000e+00**	**0.0000e+00**	**0.0000e+00**	**0.0000e+00**	4.76564
	HMPA	**0.0000e+00**	**0.0000e+00**	**0.0000e+00**	**0.0000e+00**	**0.0000e+00**	20.3771
TF3	HHO	1.4522e−212	4.8138e−196	2.3876e−182	7.12616e−181	0.0000e+00	14.7399
	FFA	6.2985e+00	1.0327e+01	1.0496e+01	1.4887e+01	2.2956e+00	8.27796
	MFO	3.4044e+01	5.9916e+01	5.8078e+01	8.1314e+01	1.1906e+01	3.96288
	ALO	2.4086e+00	8.0520e+00	8.0912e+00	2.5570e+01	5.0478e+00	39.8589
	SHO	**0.0000e+00**	**0.0000e+00**	**0.0000e+00**	**0.0000e+00**	**0.0000e+00**	8.63975
	SSA	7.4633e−01	2.7721e+00	3.3223e+00	1.0269e+01	2.3172e+00	3.44956
	AEO	1.3784e−194	1.6972e−188	1.1399e−182	2.2171e−181	0.0000e+00	6.60229
	HMPA	**0.0000e+00**	**0.0000e+00**	**0.0000e+00**	**0.0000e+00**	**0.0000e+00**	30.5945
TF4	HHO	1.6793e−114	2.5701e−108	6.7150e−104	2.0077e−102	3.6652e−103	11.8984
	FFA	2.6937e−11	6.6793e−11	8.5617e−11	2.1259e−10	5.1696e−11	4.50707
	MFO	1.6907e−04	3.0000e+01	3.2000e+01	6.0000e+01	1.6329e+01	1.76030
	ALO	1.7437e−02	4.4840e+00	2.1912e+01	1.0910e+02	3.8137e+01	42.6791
	SHO	**0.0000e+00**	**0.0000e+00**	**0.0000e+00**	**0.0000e+00**	**0.0000e+00**	7.23653
	SSA	5.5213e−05	2.6504e−01	4.0761e−01	1.9738e+00	5.1345e−01	3.10988
	AEO	1.0355e−198	3.2118e−193	2.2896e−189	5.6003e−188	0.0000e+00	3.71831
	HMPA	**0.0000e+00**	**0.0000e+00**	**0.0000e+00**	**0.0000e+00**	**0.0000e+00**	18.3284
TF5	HHO	8.3815e−06	9.7890e−05	2.2322e−04	1.2350e−03	3.1150e−04	12.7046
	FFA	4.1162e+00	6.0000e+00	5.8803e+00	6.6667e+00	5.4078e−01	4.84226
	MFO	3.6068e−02	4.8846e+00	2.6352e+02	3.0228e+03	8.3396e+02	2.15418
	ALO	8.0219e−05	5.3664e+00	8.3663e+01	1.0148e+03	2.4137e+02	42.7115
	SHO	2.8689e+01	2.8704e+01	2.8762e+01	2.8976e+01	1.0644e−01	6.70522
	SSA	1.1144e+00	4.4050e+00	6.8853e+00	5.5888e+01	1.0464e+01	3.38507
	AEO	7.0413e−12	4.8640e−07	7.2525e−06	7.4446e−05	1.6008e−05	3.46068
	HMPA	**2.6430e−22**	**2.0135e−19**	**7.3912e−18**	**1.5420e−16**	**3.0772e−17**	22.5178
TF6	HHO	4.3626e−07	1.8420e−05	2.9232e−05	1.1375e−04	3.0713e−05	12.1314
	FFA	1.2877e−15	9.3170e−15	1.0636e−14	3.4602e−14	7.5780e−15	4.66573
	MFO	1.6901e−06	3.0841e−05	1.2040e+03	1.0100e+04	3.3279e+03	1.66695
	ALO	4.7917e−08	8.1258e−07	9.0834e−07	3.8749e−06	7.9537e−07	44.3519
	SHO	9.2260e−03	4.6681e−01	2.2458e+00	6.9165e+00	2.7662e+00	5.18416
	SSA	4.2972e−09	7.5869e−09	8.0025e−09	1.4509e−08	2.2793e−09	2.88100
	AEO	6.8362e−13	4.3952e−10	2.2861e−09	3.2404e−08	6.7688e−09	2.78123
	HMPA	**0.0000e+00**	**0.0000e+00**	**1.2326e−33**	**1.2326e−32**	**3.0814e−33**	19.6652

Table 4 (continued)

	Algorithm	Best	Median	Average	Worst	STD	AET(s)
TF7	HHO	2.3273e−06	2.6054e−05	5.0525e−05	2.3625e−04	5.9026e−05	10.9908
	FFA	7.8302e−03	1.9475e−02	1.8355e−02	3.0869e−02	5.2235e−03	5.14018
	MFO	2.0341e−02	2.5288e−01	5.0071e+00	3.2248e+01	8.1182e+00	2.18480
	ALO	3.1288e−02	5.3176e−02	5.6774e−02	1.0049e−01	2.0556e−02	42.9241
	SHO	4.9675e−06	1.9173e−05	4.0058e−05	2.5764e−04	5.9995e−05	5.32082
	SSA	2.5333e−02	4.6630e−02	5.4026e−02	1.0453e−01	2.1156e−02	2.92922
	AEO	2.0266e−05	1.3109e−04	1.5704e−04	4.8868e−04	1.1154e−04	2.96990
	HMPA	**2.6040e−07**	**1.0774e−05**	**1.3767e−05**	**5.3285e−05**	**1.3687e−05**	17.5846

The best results have been written in bold

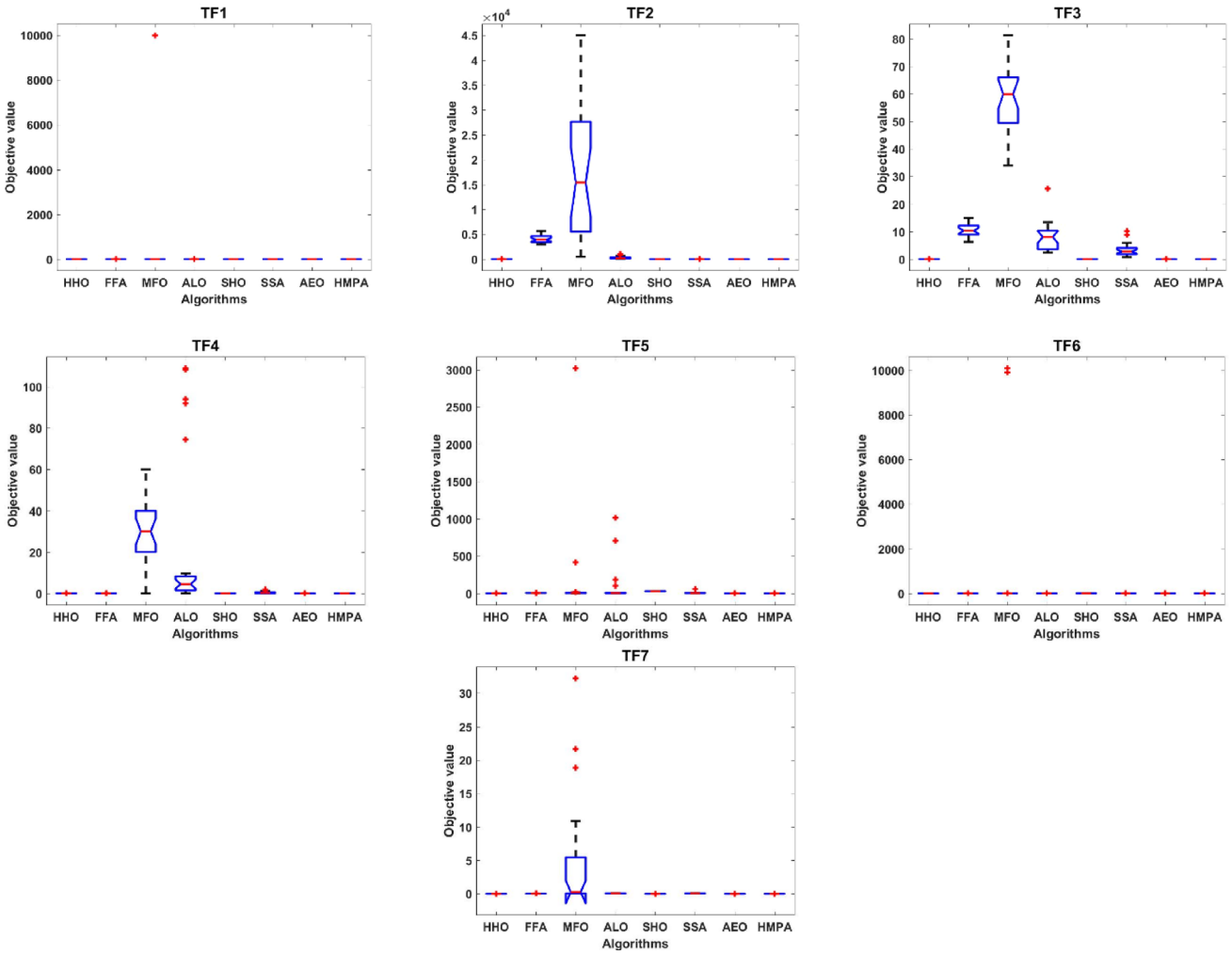

Fig. 12 Box plots of the obtained results from the algorithms on the unimodal test functions

in these test functions, the algorithms must have superior exploitation and exploration capabilities along with local optima avoidance ability. CEC 2017 includes twenty-nine single-objective test functions, which the second and twenty-second test functions have been removed in the recent update [93]. The brief description of CEC 2017 test functions is

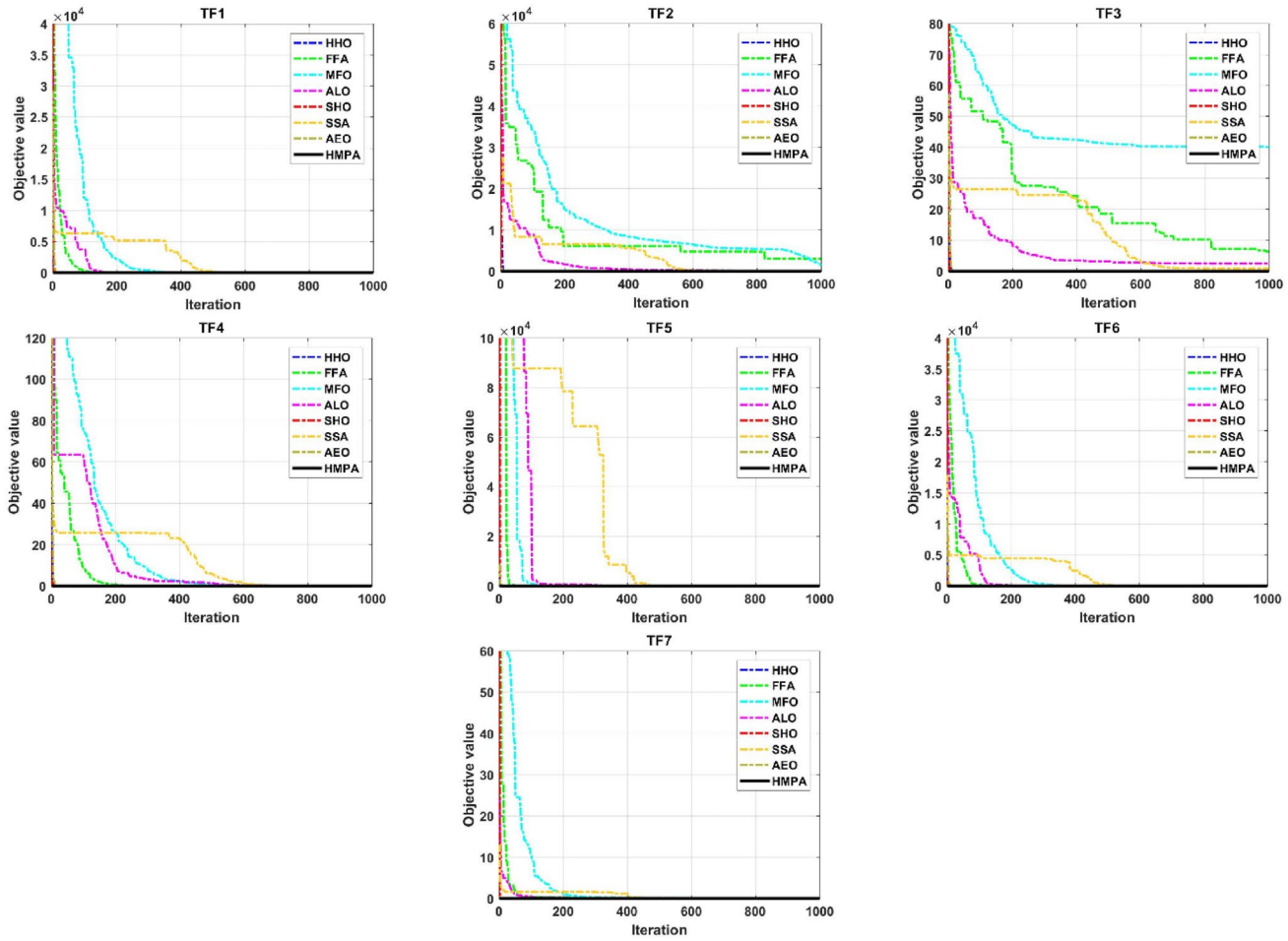

Fig. 13 Convergence graphs of the algorithms on the unimodal test functions

Table 5 Wilcoxon signed-rank test results of the HMPA versus the competitor algorithms with 5% significance level on the unimodal test functions

	HMPA vs.HHO		HMPA vs.FFA		HMPA vs.MFO		HMPA vs.ALO		HMPA vs.SHO		HMPA vs.SSA		HMPA vs.AEO	
	P value	*R*	*P* value	*R*	*P* value	*R*	*P* value	*R*	*P* value	*R*	*P* value	*R*	*P* value	R
TF1	2.726e−06	+	1.229e−05	+	1.229e−05	+	1.229e−05	+	–	=	1.229e−05	+	–	=
TF2	1.229e−05	+	1.229e−05	+	1.229e−05	+	1.229e−05	+	–	=	1.229e−05	+	–	=
TF3	1.229e−05	+	1.229e−05	+	1.229e−05	+	1.229e−05	+	–	=	1.229e−05	+	1.229e−05	+
TF4	1.229e−05	+	1.229e−05	+	1.229e−05	+	1.229e−05	+	–	=	1.229e−05	+	1.229e−05	+
TF5	1.229e−05	+	1.229e−05	+	1.229e−05	+	1.229e−05	+	1.229e−05	+	1.229e−05	+	1.229e−05	+
TF6	1.229e−05	+	1.229e−05	+	1.229e−05	+	1.229e−05	+	1.229e−05	+	1.229e−05	+	1.229e−05	+
TF7	0.0049	+	1.229e−05	+	1.229e−05	+	1.229e−05	+	0.0264	+	1.229e−05	+	1.389e−05	+

presented in Table 12. Similar to the previous subsections, the statistical results of the algorithms are provided in Table 13.

In line with the statistics presented in Table 13, the HMPA found better solutions for all CEC 2017 test functions. The box plot graphs are depicted in Fig. 18 for additional examination.

The box plots of Fig. 18 confirm the statistical results of Table 13 and expose the superiority of the HMPA. Besides, Box charts show that the HMPA is less dependent on the initial solutions, and it demonstrated better achievements

Table 6 Details of the multimodal test functions

	Function	dim	Range	$F_{\min}$
TF8	$f(x) = -\sum_{i=1}^{d}\left(x_i \sin\left(\sqrt{\lvert x_i\rvert}\right)\right)$	30	$[-500, 500]^d$	− 12569.5
TF9	$f(x) = 10d + \sum_{i=1}^{d}\left[x_i^d - 10\cos\left(2\pi x_i\right)\right]$	30	$[-5.12, 5.12]^d$	0
TF10	$f(x) = -20\exp\left(-0.2\sqrt{\frac{1}{d}\sum_{i=1}^{d}x_i^2}\right) - \exp\left(\frac{1}{d}\sum_{i=1}^{d}\cos 2\pi x_i\right) + 20 + e$	30	$[-32, 32]^d$	0
TF11	$f(x) = \frac{1}{4000}\sum_{i=1}^{d}x_i^2 - \prod_{i=1}^{d}\cos\left(\frac{x_i}{\sqrt{i}}\right) + 1$	30	$[-600, 600]^d$	0
TF12	$f(x) = \frac{\pi}{d}\left\{10\sin\left(\pi y_1\right) + \sum_{i=1}^{d-1}\left(y_i - 1\right)^2\left[1 + 10\sin^2\left(\pi y_{i+1}\right)\right] + \left(y_d - 1\right)^2\right\} + \sum_{i=1}^{d}U\left(x_i, 10, 100, 4\right)$ $y_i = 1 + \frac{x_i+1}{4}, U\left(x_i, a, k, m\right) = \begin{cases} k\left(x_i - a\right)^m & x_i > a \\ 0 & -a < x_i < a \\ k\left(-x_i - a\right)^m & x_i < -a \end{cases}$	30	$[-50, 50]^d$	0
TF13	$f(x) = 0.1\left\{\sin^2\left(3\pi x_1\right) + \sum_{i=1}^{d}\left(x_i - 1\right)^2\left[1 + \sin^2\left(3\pi x_i + 1\right)\right] + \left(x_d - 1\right)^2\left[1 + \sin^2\left(2\pi x_d\right)\right]\right\}$ $+ \sum_{i=1}^{d}U\left(x_i, 5, 100, 4\right)$	30	$[-50, 50]^d$	0

than the rest of the algorithms. Likewise, the convergence speeds of the algorithms are compared, and the results are established in Fig. 19.

The graphs of Fig. 19 indicate that the HMPA outperforms the other comparative algorithms in terms of convergence rate, in all CEC 2017 test functions except TF32. In addition, it can be inferred that HMPA has the ability to go out of the local optimum points. Besides, the results of the Wilcoxon signed-rank test on these test functions are disclosed in Table 14.

Drawing on the results of Figs. 18, 19, and Tables 13, 14, it can be concluded that the HMPA could find optimal or near-optimal solutions for CEC 2017 test functions, and have a significant difference from other representative algorithms.

According to the results of experiments on the vast set of test functions, it can be concluded that the HMPA outperforms in all test functions.

7 Real-world engineering applications

To further investigate the superiority of the HMPA, in this section, the algorithms have been utilized to solve real-life engineering problems. For this purpose, the algorithms are applied to seven constrained and unconstrained real-world engineering problems of minimization and maximization nature. Besides, the results of HMPA is compared statistically with the results of the algorithms used in Sect. 6, as well as Tree Seed Algorithm (TSA) [95], Manta Ray Foraging Optimization (MRFO) [8], Sine Cosine Algorithm (SCA) [96], and Whale Optimization Algorithm (WOA) [97]. The values of the parameters of the algorithms are provided in Table 1. It is worth mentioning that, in the constrained engineering problems, the death penalty mechanism is utilized as a constraint handling method, in which a considerable positive/negative number is added to the objective value as a penalty. As a result, the infeasible solutions would be rejected.

7.1 Welded beam design problem

The welded beam design problem is a constrained optimization problem, the objective of which is to minimize the fabrication cost of welding. The constraints are shear stress (τ) and bending stress (θ) in the beam, buckling load (P_c) on the bar, and deflection (δ) of the beam. Additionally, the thickness of the weld (h), length of the clamped bar (l), height of the bar (t), and thickness of the bar (b) are the design variables of the problem. The welded beam design problem is illustrated in Fig. 20.

Below is outlined the problem's constraints as well as mathematical formulation.Consider:

Table 7 Statistical results obtained by the algorithms on the multimodal test functions

Algorithm	Best	Median	Average	Worst	STD	AET(s)
TF8						
HHO	− 12568.7987	− 11955.4152	− 11503.3821	− 8131.4065	1311.77832	12.4664
FFA	− 8336.5535	− 6872.4861	− 6805.3727	− 4337.8464	1110.6248	4.93968
MFO	− 9956.2579	− 8876.6594	− 8794.5104	− 7559.0769	602.7702	2.07681
ALO	− 12569.4862	− 5537.5832	− 5830.718	− 5417.6747	1432.9433	37.6073
SHO	− 3703.5540	− 2672.2821	− 2797.3806	− 2103.6576	507.9239	1.51219
SSA	− 8611.5961	− 7495.9671	− 7522.6963	− 6407.7053	603.1958	3.00812
AEO	− 11951.7028	− 11403.2147	− 11296.5607	− 10437.5459	382.6176	3.28673
HMPA	**− 12569.4866**	**− 12569.4866**	**− 12569.4866**	**− 12569.4866**	**7.9200e−12**	24.8868
TF9						
HHO	**0.0000e+00**	**0.0000e+00**	**0.0000e+00**	**0.0000e+00**	**0.0000e+00**	11.7496
FFA	2.7809e+01	6.4123e+01	7.2483e+01	1.4118e+02	3.0201e+01	4.67649
MFO	8.5566e+01	1.3531e+02	1.4153e+02	2.1924e+02	3.3390e+01	1.83756
ALO	4.3778e+01	6.8652e+01	7.2552e+01	1.1939e+02	2.0848e+01	37.0378
SHO	**0.0000e+00**	**0.0000e+00**	**0.0000e+00**	**0.0000e+00**	**0.0000e+00**	5.25136
SSA	1.5919e+01	3.9798e+01	3.8166+01	5.1737e+01	1.0753e+01	2.52734
AEO	**0.0000e+00**	**0.0000e+00**	**0.0000e+00**	**0.0000e+00**	**0.0000e+00**	2.90343
HMPA	**0.0000e+00**	**0.0000e+00**	**0.0000e+00**	**0.0000e+00**	**0.0000e+00**	14.6411
TF10						
HHO	**8.8818e−16**	**8.8818e−16**	**8.8818e−16**	**8.8818e−16**	**0.0000e+00**	12.5164
FFA	1.3491e−08	3.5601e−08	3.7066e−08	8.1063e−08	1.5065e−08	4.96700
MFO	6.8828e−04	2.0133e+00	8.1163e+00	1.9407e+01	8.3068e+00	2.02379
ALO	9.3130e−01	2.0133e+00	2.0257e+00	3.1583e+00	5.2546e−01	37.4280
SHO	8.8818e−16	8.8818e−16	2.2788e−01	6.8366e+00	1.2481e+00	5.27194
SSA	2.0905e−05	1.7779e+00	1.6169e+00	3.0937e+00	9.9016e−01	2.79218
AEO	**8.8818e−16**	**8.8818e−16**	**8.8818e−16**	**8.8818e−16**	**0.0000e+00**	2.81257
HMPA	**8.8818e−16**	**8.8818e−16**	**8.8818e−16**	**8.8818e−16**	**0.0000e+00**	15.5893
TF11						
HHO	**0.0000e+00**	**0.0000e+00**	**0.0000e+00**	**0.0000e+00**	**0.0000e+00**	13.1575
FFA	5.5333e−07	8.1217e−06	1.5229e−05	1.0052e−04	2.1261e−05	5.09034
MFO	1.8909e−05	1.0001e−02	1.0849e+01	1.8021e+02	3.9669e+01	2.37502
ALO	3.0444e−05	1.0101e−02	1.0552e−02	3.4540e−02	8.7807e−03	37.4154
SHO	**0.0000e+00**	**0.0000e+00**	**0.0000e+00**	**0.0000e+00**	**0.0000e+00**	5.32358
SSA	1.8703e−08	3.8554e−08	6.2056e−03	3.1942e−02	8.8470e−03	2.90227
AEO	**0.0000e+00**	**0.0000e+00**	**0.0000e+00**	**0.0000e+00**	**0.0000e+00**	3.84447
HMPA	**0.0000e+00**	**0.0000e+00**	**0.0000e+00**	**0.0000e+00**	**0.0000e+00**	16.3819
TF12						
HHO	4.3702e−08	1.8335e−06	3.6155e−06	1.3021e−05	4.0857e−06	15.4125
FFA	4.4294e−08	3.3747e−06	9.1515e−06	6.4776e−05	1.4657e−05	7.21749
MFO	6.5085e−06	1.0366e+01	5.1443e−01	2.1648e+00	7.6444e−01	3.88970
ALO	3.1954e+00	7.3917e+00	8.3076e+00	1.5311e+01	3.1104e+00	37.6693
SHO	5.2445e−05	6.9714e−05	6.7554e−05	7.7207e−05	7.3433e−06	6.28763
SSA	3.2789e−02	2.8403e+00	3.4545e+00	1.0355e+01	2.6140e+00	3.62955
AEO	2.8785e−13	3.0158e−11	8.0771e−11	3.9070e−10	1.1344e−10	5.72319
HMPA	**1.5705e−32**	**1.5705e−32**	**1.5757e−32**	**1.6028e−32**	**8.9833e−35**	31.3325
TF13						
HHO	7.1677e−08	3.2164e−05	3.5770e−05	1.0822e−04	3.1856e−05	15.3583
FFA	7.4271e−09	1.3615e−07	3.6941e−07	1.9783e−06	5.5921e−07	7.10244
MFO	3.6688e−05	1.6317e−03	5.4674e−03	2.7851e−02	1.5454e−03	3.97892
ALO	2.4686e−07	1.0989e−02	9.7971e−03	3.0829e−02	9.5089e−03	37.1176

Table 7 (continued)

Algorithm	Best	Median	Average	Worst	STD	AET(s)
SHO	2.8207e+00	2.9578e+00	2.9515e+00	2.9969e+00	3.0610e−02	6.52049
SSA	3.5914e−10	6.2849e−10	6.0388e−03	2.1023e−02	7.5831e−03	3.75444
AEO	2.4805e−10	1.4115e−05	2.1509e−03	1.1122e−03	4.0586e−03	5.81502
HMPA	**1.3497e−32**	**1.3497e−32**	**1.3843e−32**	**1.8428e−32**	**1.0386e−33**	32.0575

The best results have been written in bold

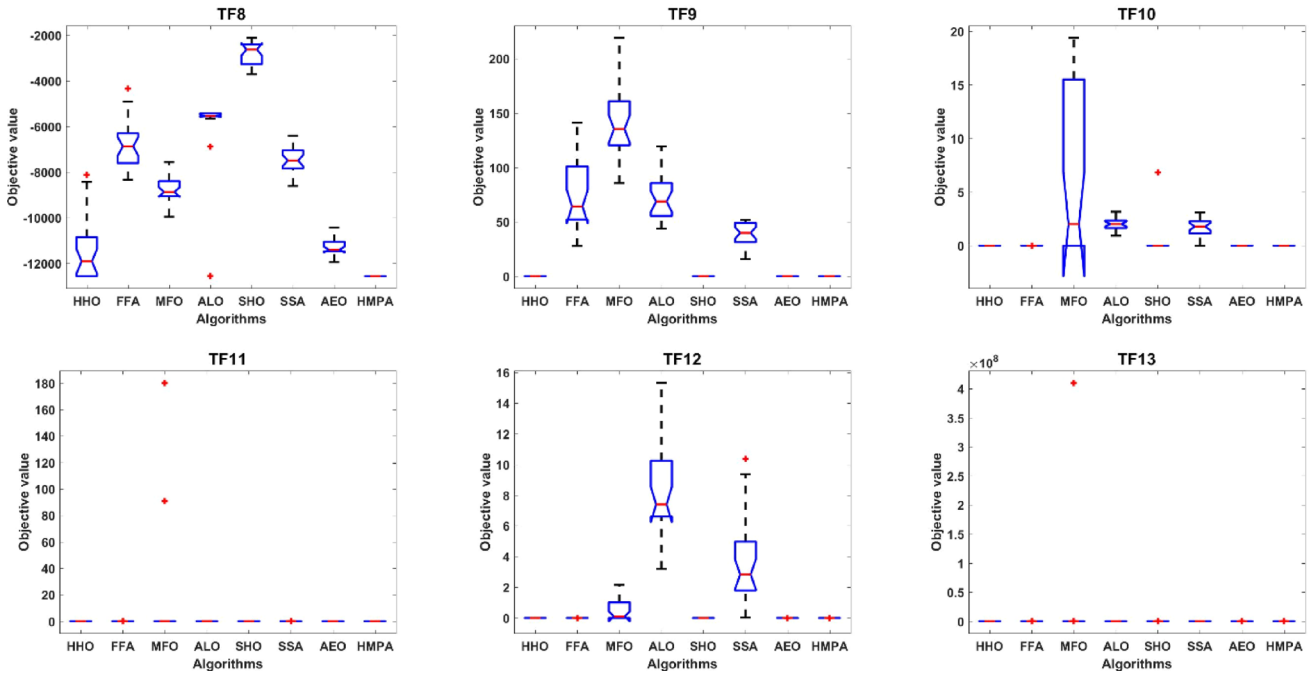

Fig. 14 Box plots of the obtained results from the algorithms on the multimodal test functions

$$\vec{v} = \left[v_1 v_2 v_3 v_4\right] = [hltb],$$

Minimize:

$$f(\vec{v}) = 1.10471 v_1^2 v_2 + 0.04811 v_3 v_4 (14.0 + v_2),$$

Subject to:

$$c_1(\vec{v}) = \tau(\vec{v}) - \tau_{\max} \le 0,$$

$$c_2(\vec{v}) = \sigma(\vec{v}) - \sigma_{\max} \le 0,$$

$$c_3(\vec{v}) v = \delta(v) - \delta_{\max} \le 0,$$

$$c_4(\vec{v}) = v_1 - v_4 \le 0,$$

$$c_5(\vec{v}) = P - P_c(\vec{v}) \le 0,$$

$$c_6(\vec{v}) = 0.125 - v_1 \le 0,$$

$$c_7(\vec{v}) = 1.10471 v_1^2 + 0.04811 v_3 v_4 (14.0 + v_2) - 5.0 \le 0,$$

where $0.1 \le v_1 \le 2$, $0.1 \le v_2 \le 10$, $0.1 \le v_3 \le 10$, $0.1 \le v_4 \le 2$,

$$\tau(\vec{v}) = \sqrt{(\tau')^2 + 2\tau'\tau'' \frac{v_2}{2R} + (\tau'')^2}, \tag{31}$$

$$\tau' = \frac{P}{\sqrt{2} v_1 v_2},$$

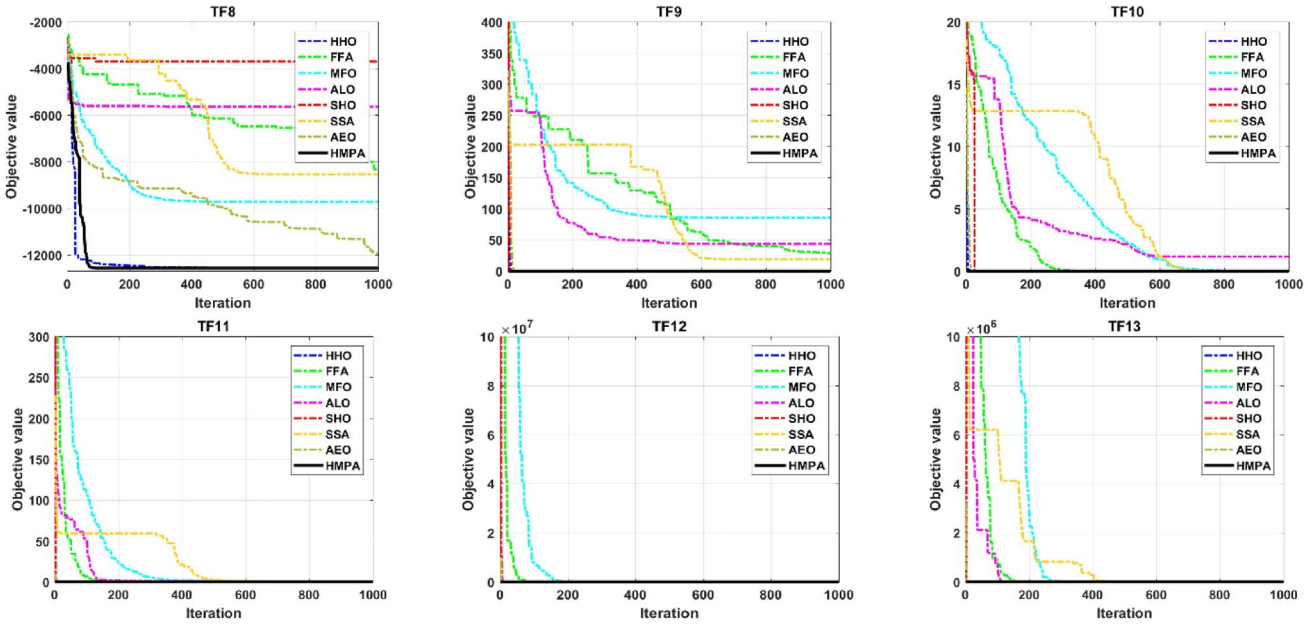

Fig. 15 Convergence graphs of the algorithms on the multimodal test functions

Table 8 Wilcoxon signed-rank test results of the HMPA versus the competitor algorithms with 5% significance level on the multimodal test functions

	HMPA vs.HHO		HMPA vs.HHO		HMPA vs.MFO		HMPA vs.ALO		HMPA vs.SHO		HMPA vs.SSA		HMPA vs.AEO	
	P value	*R*	*P* value	*R*	*P* value	*R*	*P* value	*R*	*P* value	*R*	*P* value	*R*	*P* value	*R*
TF8	1.229e−05	+	1.229e−05	+	1.229e−05	+	1.169e−05	+	1.229e−05	+	1.229e−05	+	1.229e−05	+
TF9	–	=	1.229e−05	+	1.229e−05	+	1.229e−05	+	–	=	1.229e−05	+	–	=
TF10	–	=	1.229e−05	+	1.229e−05	+	1.229e−05	+	–	=	1.229e−05	+	–	=
TF11	–	=	1.229e−05	+	1.229e−05	+	1.229e−05	+	–	=	1.229e−05	+	–	=
TF12	1.229e−05	+	1.229e−05	+	1.229e−05	+	1.229e−05	+	1.229e−05	+	1.229e−05	+	1.229e−05	+
TF13	1.229e−05	+	1.229e−05	+	1.229e−05	+	1.229e−05	+	1.229e−05	+	1.229e−05	+	1.229e−05	+

$$\tau'' = \frac{\mathrm{MR}}{J},$$

$$M = P\left(L + \frac{v_2}{2}\right),$$

$$R = \sqrt{\frac{v_2^2}{4} + \left(\frac{v_1 + v_3}{2}\right)^2},$$

$$J = 2\left\{\sqrt{2}v_1v_2\left[\frac{v_2^2}{4} + \left(\frac{v_1 + v_3}{2}\right)^2\right]\right\},$$

$$\sigma(\vec{v}) = \frac{6PL}{v_4v_3^2},$$

$$\delta(\vec{v}) = \frac{6PL^3}{Ev_3^3v_4},$$

$$P_c(\vec{v}) = \frac{4.013E\sqrt{\frac{v_3^2v_4^6}{36}}}{L^2}\left(1 - \frac{v_3}{2L}\sqrt{\frac{E}{4G}}\right), \quad P = 6000 \text{ lb.},$$

$L = 14$ inch, $E = 30 \times 10^6$ psi, $G = 12 \times 10^6$ psi, $\delta_{\max} = 0.25$ inch, $\tau_{\max} = 13,600$ psi, $\sigma_{\max} = 30,000$ psi.

In Table 15, the statistical analysis of the algorithms is conveyed. Moreover, the best points and their corresponding fitness values obtained by the algorithms on this problem are provided in Table 16.

Table 9 Details of the fixed-dimension test functions

	Function	dim	Range	$F_{\min}$
TF14	$f(x)=\left[\frac{1}{500}+\sum_{i=1}^{25}\frac{1}{i+\sum_{j=1}^{2}(x_j-a_{j,i})^6}\right]^{-1}$	2	$[-65.53,65.53]^d$	0.9980
TF15	$f(x)=\sum_{i=1}^{d}\left\lvert a_i-\frac{x_1(b_i^2+b_ix_2)}{b_i^2+b_ix_3+x_4}\right\rvert^2$	4	$[-5,5]^d$	0.0003075
TF16	$f(x)=4x_1^2-2.1x_1^4+\frac{1}{3}x_1^6+x_1x_2-4x_2^2+4x_2^4$	2	$[-5,5]^d$	− 1.0316
TF17	$f(x)=\left(x_2-\frac{5.1}{4\pi^2}x_1^2+\frac{5}{\pi}x_1-6\right)^2+10\left(1-\frac{1}{8\pi}\right)\cos x_1+10$	2	$[-5,10]^d\times[0,15]^d$	0.398
TF18	$f(x)=\left[1+(x_1+x_2+1)^2(19-14x_1+3x_1^2-14x_2+6x_1x_2+3x_2^2)\right]\times\left[30+(2x_1-3x_2)^2\times(18-32x_1+12x_1^2+48x_2-36x_1x_2+27x_2^2)\right]$	2	$[-2,2]^d$	3.0000
TF19	$f(x)=-\sum_{i=1}^{4}a_i\exp\left(-\sum_{j=1}^{3}b_{ij}(x_j-p_{ij})^2\right)$	3	$[0,1]^d$	− 3.86278
TF20	$f(x)=-\sum_{i=1}^{4}a_i\exp\left(-\sum_{j=1}^{6}b_{ij}(x_j-p_{ij})^2\right)$	6	$[0,1]^d$	− 3.322
TF21	$f(x)=-\sum_{i=1}^{5}\left\lvert(x_i-a_i)(x_i-a_i)^T+c_i\right\rvert^{-1}$	4	$[0,10]^d$	− 10.1532
TF22	$f(x)=-\sum_{i=1}^{7}\left\lvert(x_i-a_i)(x_i-a_i)^T+c_i\right\rvert^{-1}$	4	$[0,10]^d$	− 10.4028
TF23	$f(x)=-\sum_{i=1}^{10}\left\lvert(x_i-a_i)(x_i-a_i)^T+c_i\right\rvert^{-1}$	4	$[0,10]^d$	− 10.5363

For further comparison of the algorithms, the convergence rates of the algorithms are plotted in Fig. 21.

In view of the attained outcomes, HMPA outstrips other competitor algorithms.

7.2 Speed reducer design problem

This subsection describes the speed reducer design problem with the objective of minimizing the weight of reducer. The speed reducer design problem is a constrained mixed-integer optimization problem and has seven design variables: face width (b), the module of teeth (m), number of teeth in the pinion (z), length of the first shaft between bearings (l_1), length of the second shaft between bearings (l_2), the diameter of first shafts (d_1), and the diameter of the second shafts (d_2). The constraints of this problem are bending stress of the gear teeth, surface stress, transverse deflections of the shafts, and stresses in the shafts. The schematic view of this problem is represented in Fig. 22.

The constraints and the mathematical formulation of the problem are as follows:

Consider:

$$\vec{v}=\left[v_1,v_2,v_3,v_4,v_5,v_6,v_7\right]=\left[b,m,z,l_1,l_2,d_1,d_2\right],$$

Minimize:

$$\begin{aligned}f\left(\vec{V}\right)=&0.7854v_1v_2^2(3.3333v_3^2+14.9334v_3-43.0934)\\&-1.508v_1\left(v_6^2+v_7^2\right)+7.4777\left(v_6^3+v_7^3\right)\\&0.7854\left(v_4v_6^2+v_5v_7^2\right),\end{aligned}$$

Subject to:

$$c_{21}\left(\vec{v}\right)=\frac{27}{v_1v_2^2v_3}-1\le 0,$$

$$c_2\left(\vec{v}\right)=\frac{397.5}{v_1v_2^2v_3^3}-1\le 0,$$

$$c_3\left(\vec{v}\right)=\frac{1.93v_4^3}{v_2v_6^4v_3}-1\le 0,$$

$$c_4\left(\vec{v}\right)=\frac{1.93v_5^3}{v_2v_7^4v_3}-1\le 0,$$

$$c_5\left(\vec{v}\right)=\frac{\left[\left(745\left(v_4/v_2v_3\right)\right)^2+16.9\times10^6\right]^{0.5}}{110v_6^3}-1\le 0,$$

Table 10 Statistical results obtained by the algorithms on the fix-dimension test functions

Algorithm	Best	Median	Average	Worst	STD	AET(s)
TF14						
HHO	0.9980038	0.9980038	1.0311387	1.9920301	1.8148e−01	27.9639
FFA	0.9980038	0.9980038	0.9980038	0.9980038	1.0037e−16	14.7672
MFO	0.9980038	0.9980038	2.5751488	10.763180	2.4194e+00	9.48120
ALO	0.9980038	0.9980038	1.1968092	1.9920309	4.0580e−01	11.7720
SHO	1.1223405	10.961674	9.4804071	12.670505	3.8393e+00	6.89156
SSA	0.9980038	0.9980038	0.9980038	0.9980038	2.0396e−16	8.08868
AEO	0.9980038	0.9980038	0.9980038	0.9980038	9.0649e−17	13.1220
HMPA	**0.9980038**	**0.9980038**	**0.9980038**	**0.9980038**	**3.2762e−17**	42.0783
TF15						
HHO	3.0748e−04	3.0821e−04	3.0967e−04	3.2299e−04	3.4418e−06	11.5508
FFA	3.4164e−04	5.7085e−04	5.5956e−04	7.6631e−04	1.1990e−04	8.34289
MFO	3.8217e−04	7.8265e−04	9.6961e−04	1.6553e−03	3.6358e−04	1.74772
ALO	3.0761e−04	7.5594e−04	1.5660e−03	2.0363e−02	3.9244e−03	16.7860
SHO	3.0838e−04	3.1318e−04	3.1401e−04	3.2239e−04	3.7531e−06	4.72453
SSA	3.0785e−04	6.9851e−04	1.5429e−03	2.0363e−02	3.9296e−03	2.59825
AEO	3.0748e−04	3.0748e−04	3.0748e−04	3.0748e−04	2.5761e−19	3.13725
HMPA	**3.0748e−04**	**3.0748e−04**	**3.0748e−04**	**3.0748e−04**	**1.7670e−19**	19.4520
TF16						
HHO	− 1.031628	− 1.031628	− 1.031628	− 1.031628	1.7561e−15	10.7233
FFA	− 1.031628	− 1.031628	− 1.031628	− 1.031628	6.7227e−16	7.58313
MFO	− 1.031628	− 1.031628	− 1.031628	− 1.031628	6.7986e−16	1.42358
ALO	− 1.031628	− 1.031628	− 1.031628	− 1.031628	3.5739e−14	8.67291
SHO	− 1.030881	− 1.016558	−0.983392	− 0.467304	1.0399e−01	2.30476
SSA	− 1.031628	− 1.031628	− 1.031628	− 1.031628	1.3613e−14	1.88688
AEO	− 1.031628	− 1.031628	− 1.031628	− 1.031628	5.5762e−16	2.80716
HMPA	**− 1.031628**	**− 1.031628**	**− 1.031628**	**− 1.031628**	**1.7986e−17**	15.9482
TF17						
HHO	0.3978873	0.3978873	0.3978873	0.3978873	4.3137e−14	10.4722
FFA	0.3978873	0.3978873	0.3978873	0.3978873	2.0616e−10	7.39044
MFO	**0.3978873**	**0.3978873**	**0.3978873**	**0.3978873**	**0.0000e+00**	1.22944
ALO	0.3978873	0.3978873	0.3978873	0.3978873	2.7683e−14	8.62536
SHO	0.3978909	0.3980961	0.4909601	1.6411045	2.7390e−01	2.25536
SSA	**0.3978873**	**0.3978873**	**0.3978873**	**0.3978873**	1.7709e−14	1.79611
AEO	**0.3978873**	**0.3978873**	**0.3978873**	**0.3978873**	**0.0000e+00**	2.66134
HMPA	**0.3978873**	**0.3978873**	**0.3978873**	**0.3978873**	**0.0000e+00**	15.1148
TF18						
HHO	3.00000	3.00000	3.00000	3.00000	3.1266e−10	12.4338
FFA	3.00000	3.00000	3.00000	3.00000	4.5325e−16	5.65878
MFO	3.00000	3.00000	3.00000	3.00000	1.0571e−15	1.22416
ALO	3.00000	3.00000	3.00000	3.00000	2.9394e−13	8.41208
SHO	3.21886	6.86716	12.3416	92.3854	1.6717e+01	1.26389
SSA	3.00000	3.00000	3.00000	3.00000	5.2572e−14	1.79820
AEO	3.00000	3.00000	3.00000	3.00000	1.1609e−15	2.65212
HMPA	**3.00000**	**3.00000**	**3.00000**	**3.00000**	**1.0571e−16**	16.1714
TF19						
HHO	− 3.8627821	− 3.8627821	− 3.8627821	− 3.8627821	8.3536e−15	14.8745
FFA	**− 3.8627821**	**− 3.8627821**	**− 3.8627821**	**− 3.8627821**	**2.2662e−15**	7.37115
MFO	**− 3.8627821**	**− 3.8627821**	**− 3.8627821**	**− 3.8627821**	**2.2662e−15**	2.30769
ALO	− 3.8627821	− 3.8627821	− 3.8627821	− 3.8627821	1.0842e−14	12.5300

Table 10 (continued)

Algorithm	Best	Median	Average	Worst	STD	AET(s)
SHO	− 3.8541670	− 3.8020345	− 3.7871695	− 3.2442490	1.0891e−01	2.40778
SSA	− 3.8627821	− 3.8627821	− 3.8627821	− 3.8627821	1.4968e−14	2.45123
AEO	**− 3.8627821**	**− 3.8627821**	**− 3.8627821**	**− 3.8627821**	**2.2662e−15**	5.18880
HMPA	**− 3.8627821**	**− 3.8627821**	**− 3.8627821**	**− 3.8627821**	**2.2662e−15**	20.7901
TF20						
HHO	− 3.3220	− 3.3220	− 3.2704	− 3.2030	5.9929e−02	14.6737
FFA	− 3.3220	− 3.3220	− 3.3220	− 3.3218	3.1962e−05	9.16350
MFO	− 3.3220	− 3.2031	− 3.2144	− 3.1376	4.2567e−02	2.80983
ALO	− 3.3220	− 3.3220	− 3.2744	− 3.2031	5.9446e−02	23.2390
SHO	− 3.0783	− 2.8243	− 2.8067	− 2.3738	1.7356e−01	3.08541
SSA	− 3.3220	− 3.2031	− 3.2363	− 3.2030	5.4486e−02	2.68150
AEO	− 3.3220	− 3.2031	− 3.2554	− 3.2031	6.0234e+00	7.27492
HMPA	**− 3.3220**	**− 3.3220**	**− 3.3220**	**− 3.3220**	**1.2094e−15**	23.2660
TF21						
HHO	− 10.1532	− 5.0552	− 6.4146	− 5.0552	2.2929e+00	17.2298
FFA	− 10.1532	− 10.1532	− 10.1386	− 9.8938	5.4091e−02	9.73391
MFO	− 10.1532	− 10.1532	− 7.1414	− 2.6304	3.3140e+00	4.25316
ALO	− 10.1532	− 5.1007	− 7.2143	− 2.6828	2.7001e+00	16.3979
SHO	− 8.4183	− 3.9158	− 4.1620	− 2.2293	1.1867e+00	2.38617
SSA	− 10.1532	− 10.1532	− 9.3534	− 2.6828	2.2467e+00	3.72830
AEO	− 10.1532	− 10.1532	− 10.1532	− 10.1532	5.2545e−15	6.36178
HMPA	**− 10.1532**	**− 10.1532**	**− 10.1532**	**− 10.1532**	**1.5268e−15**	25.6961
TF22						
HHO	− 10.4029	− 5.0877	− 7.2138	− 5.0876	2.6484e+00	18.9138
FFA	− 10.4029	− 10.4029	− 10.4029	− 10.4029	6.9698e−09	10.5352
MFO	− 10.4029	− 10.4029	− 8.2214	− 2.7519	3.2929e+00	4.93459
ALO	− 10.4029	− 10.4029	− 7.9244	− 2.7519	2.8987e+00	16.4637
SHO	− 7.8734	− 4.3919	− 4.5252	− 2.4446	1.3691e+00	2.81735
SSA	− 10.4029	− 10.4029	− 9.7908	− 2.7519	2.1184e+00	4.16656
AEO	− 10.4029	− 10.4029	− 10.4029	− 10.4029	3.1611e−15	8.08289
HMPA	**− 10.4029**	**− 10.4029**	**− 10.4029**	**− 10.4029**	**1.8129e−15**	26.4040
TF23						
HHO	− 10.5364	− 5.1285	− 7.2916	− 5.1284	2.6946e+00	21.4889
FFA	− 10.5364	− 10.5364	− 10.5364	− 10.5364	2.3972e−09	13.7422
MFO	− 10.5364	− 10.5364	− 9.4746	− 2.42733	2.5357e+00	5.90012
ALO	− 10.5364	− 5.1756	− 6.8125	− 2.4217	3.4641e+00	17.0362
SHO	− 9.4316	− 4.5497	− 4.6808	− 2.5519	1.6647e+00	3.36700
SSA	− 10.5364	− 10.5364	− 10.3220	− 5.1756	1.0721e+00	5.00898
AEO	− 10.5364	− 10.5364	− 10.5364	− 10.5364	1.8130e−15	9.21528
HMPA	**− 10.5364**	**− 10.5364**	**− 10.5364**	**− 10.5364**	**9.8035e−16**	28.6922

The best results have been written in bold

$$c_6(\vec{v}) = \frac{\left[\left(745\left(v_5/v_2v_3\right)\right)^2 + 1575 \times 10^5\right]^{0.5}}{110v_7^3} - 1 \le 0,$$

$$c_7(\vec{v}) = \frac{v_2v_3}{40} - 1 \le 0,$$

$$c_8(\vec{v}) = \frac{5v_2}{v_1} - 1 \le 0,$$

$$c_9(\vec{v}) = \frac{v_1}{12v_2} - 1 \le 0,$$

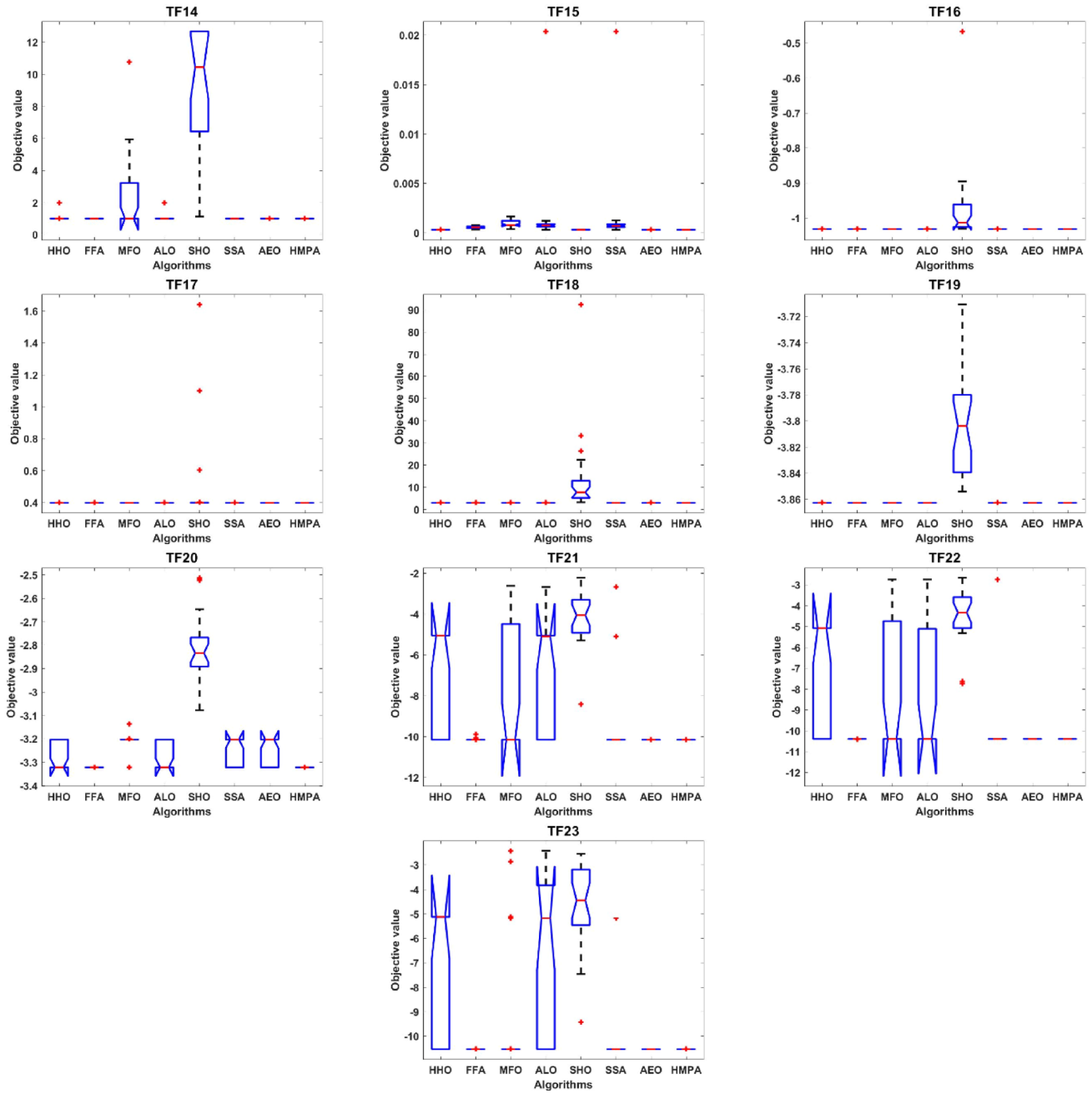

Fig. 16 Box plots of the obtained results from the algorithms on the fix-dimension test functions

$$c_{10}(\vec{v}) = \frac{1.5v_6 + 1.9}{v_4} - 1 \le 0,$$

$$c_{11}(\vec{v}) = \frac{1.1v_7 + 1.9}{v_5} - 1 \le 0, \tag{32}$$

where $2.6 \le v_1 \le 3.6$, $7.3 \le v_5 \le 8.3$, $0.7 \le v_2 \le 0.8$, $2.9 \le v_6 \le 3.9, 17 \le v_3 \le 28, 5.0 \le v_7 \le 5.5, 7.3 \le v_4 \le 8.3$.

The statistical results of the algorithms on the speed reducer design problem are presented in Table 17. Besides, the best-obtained points are represented in Table 18, and the convergence graphs of the algorithms are illustrated in Fig. 23.

As reported in Tables 17, 18, and Fig. 23, the HMPA algorithm outdid the other algorithms.

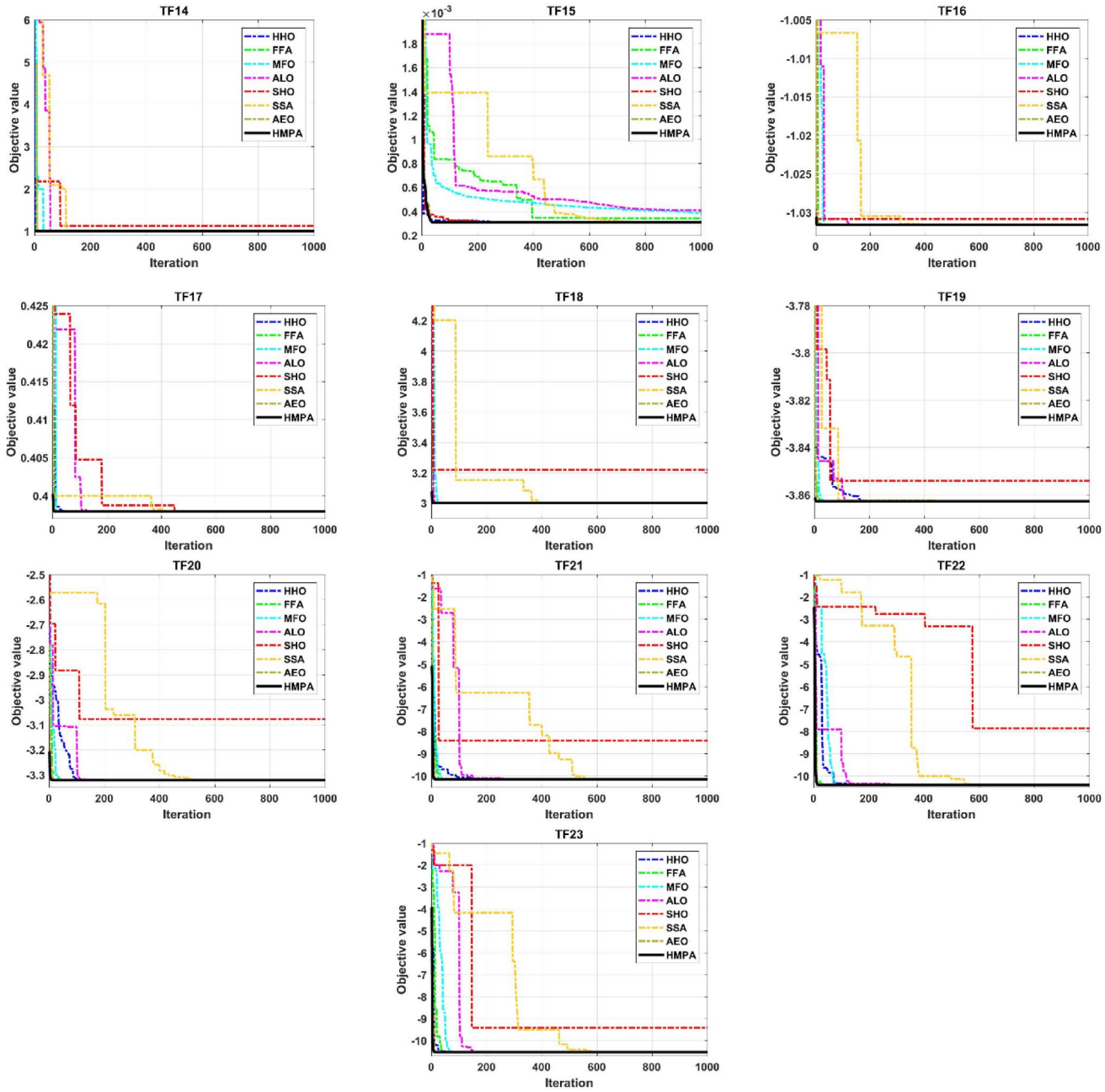

Fig. 17 Convergence graphs of the algorithms on the fix-dimension test functions

7.3 Pressure vessel design problem

The third constrained problem is the pressure vessel design problem, which tries to minimize the costs of material, forming, and welding of a cylindrical vessel. The design variables of this problem are: the thickness of the shell (T_s), the thickness of the head (T_h), inner radius (R), and length of the cylindrical section without the head (L). The pressure vessel, along with the design variables, has been presented in Fig. 24.

The constraints and the mathematical formulation of the problem are as follows:Consider:

$$\vec{v} = \left[v_1, v_2, v_3, v_4\right] = \left[T_s, T_h, R, L\right],$$

Minimize:

$$f\left(\vec{v}\right) = 0.6224 v_1 v_3 v_4 + 1.7781 v_2 v_3^2 + 3.1661 v_1^2 v_4 + 19.84 v_1^2 v_3,$$

Subject to:

Table 11 Wilcoxon signed-rank test results of the HMPA versus the competitor algorithms with 5% significance level on the fix-dimension test functions

	HMPA vs. HHO		HMPA vs. FFA		HMPA vs. MFO		HMPA vs. ALO		HMPA vs. SHO		HMPA vs. SSA		HMPA vs. AEO	
	P value	*R*	*P* value	*R*	*P* value	*R*	*P* value	*R*	*P* value	*R*	*P* value	*R*	*P* value	*R*
TF14	8.390e−05	+	1.620e−06	+	8.556e−02	−	1.562e−02	+	1.169e−05	+	–	=	2.726e−06	+
TF15	1.229e−05	+	1.229e−05	+	1.216e−05	+	1.229e−05	+	1.229e−05	+	1.229e−05	+	1.242e−04	+
TF16	9.765e−04	+	–	=	–	=	5.835e−05	+	1.229e−05	+	2.201e−05	+	–	=
TF17	1.916e−04	+	0.500	−	–	=	1.216e−05	+	1.229e−05	+	1.846e−04	+	–	=
TF18	1.216e−05	+	7.812e−03	+	9.765e−04	+	1.227e−05	+	1.229e−05	+	1.218e−05	+	1.953e−03	+
TF19	3.841e−05	+	–	=	–	=	8.796e−06	+	1.229e−05	+	1.608e−05	+	–	=
TF20	1.229e−05	+	3.088e−05	+	1.622e−05	+	1.229e−05	+	1.229e−05	+	1.229e−05	+	6.489e−04	+
TF21	1.187e−05	+	6.103e−05	+	4.882e−04	+	1.229e−05	+	1.229e−05	+	1.229e−05	+	–	=
TF22	1.154e−05	+	3.125e−02	+	7.812e−03	+	1.229e−05	+	1.229e−05	+	1.229e−05	+	–	=
TF23	1.201e−05	+	1.953e−02	+	1.250e−01	−	1.229e−05	+	1.229e−05	+	1.229e−05	+	–	=

Table 12 Brief description of CEC 2017 test functions

	Function	dim	Range	$F_{\min}$
TF24	Shifted and rotated bent cigar function	30	$[-100, 100]^d$	100
TF25	Shifted and rotated Rosenbrock's function	30	$[-100, 100]^d$	300
TF26	Shifted and rotated Rastrigin's function	30	$[-100, 100]^d$	400
TF27	Shifted and rotated expanded Scaffer's F6 function	30	$[-100, 100]^d$	500
TF28	Shifted and rotated Lunacek Bi_Rastrigin function	30	$[-100, 100]^d$	600
TF29	Shifted and rotated non-continuous Rastrigin's function	30	$[-100, 100]^d$	700
TF30	Shifted and rotated levy function	30	$[-100, 100]^d$	800
TF31	Shifted and rotated Schwefel's function	30	$[-100, 100]^d$	900
TF32	Hybrid function 1 ($N=3$)	30	$[-100, 100]^d$	1000
TF33	Hybrid Function 2 ($N=3$)	30	$[-100, 100]^d$	1100
TF34	Hybrid function 3 ($N=3$)	30	$[-100, 100]^d$	1200
TF35	Hybrid function 4 ($N=4$)	30	$[-100, 100]^d$	1300
TF36	Hybrid function 5 ($N=4$)	30	$[-100, 100]^d$	1400
TF37	Hybrid function 6 ($N=4$)	30	$[-100, 100]^d$	1500
TF38	Hybrid function 6 ($N=5$)	30	$[-100, 100]^d$	1600
TF39	Hybrid function 6 ($N=5$)	30	$[-100, 100]^d$	1700
TF40	Hybrid function 6 ($N=5$)	30	$[-100, 100]^d$	1800
TF41	Hybrid function 6 ($N=6$)	30	$[-100, 100]^d$	1900
TF42	Composition function 1 ($N=3$)	30	$[-100, 100]^d$	2000
TF43	Composition function 2 ($N=3$)	30	$[-100, 100]^d$	2100
TF44	Composition function 4 ($N=4$)	30	$[-100, 100]^d$	2300
TF45	Composition function 5 ($N=5$)	30	$[-100, 100]^d$	2400
TF46	Composition function 6 ($N=5$)	30	$[-100, 100]^d$	2500
TF47	Composition function 7 ($N=6$)	30	$[-100, 100]^d$	2600
TF48	Composition function 8 ($N=6$)	30	$[-100, 100]^d$	2700
TF49	Composition function 9 ($N=3$)	30	$[-100, 100]^d$	2800
TF50	Composition function 10 ($N=3$)	30	$[-100, 100]^d$	2900

Table 13 Statistical results obtained by the algorithms on CEC 2017 test functions

Algorithm	Best	Median	Average	Worst	STD	AET(s)
TF26						
HHO	5.2851E+02	5.9844E+02	6.9812E+02	1.1995E+03	2.1782E+02	15.8323
FFA	4.8832E+02	5.1741E+02	5.1820E+02	5.4829E+02	1.4317E+01	14.1702
MFO	5.2663E+02	6.6314E+02	8.1250E+02	1.8954E+03	3.5212E+02	2.43557
ALO	4.6438E+02	5.0741E+02	5.0147E+02	5.3446E+02	2.0234E+01	110.469
SHO	1.5259E+04	2.3217E+04	2.2840E+04	2.8384E+04	4.5147E+03	2.32570
SSA	4.2657E+02	5.0134E+02	4.9694E+02	5.2189E+02	2.4320E+01	3.16385
AEO	4.0036E+02	4.7320E+02	4.7880E+02	5.3674E+02	2.9245E+01	3.50411
HMPA	**4.0000E+02**	**4.0000E+02**	**4.0134E+02**	**4.0408E+02**	**1.9547E+00**	31.1044
TF27						
HHO	7.0127E+02	7.3836E+02	7.3976E+02	8.0170E+02	2.7410E+01	19.6034
FFA	6.4729E+02	7.2288E+02	7.1991E+02	7.5358E+02	2.4956E+01	14.5966
MFO	6.1569E+02	6.8613E+02	6.8802E+02	7.4663E+02	3.8541E+01	2.56790
ALO	6.0845E+02	6.6218E+02	6.5889E+02	7.4675E+02	4.3389E+01	113.621
SHO	9.5833E+02	9.9409E+02	1.0021E+03	1.0637E+03	2.8945E+01	2.46781
SSA	6.0348E+02	6.7412E+02	6.7140E+02	7.7162E+02	5.2914E+01	3.27216
AEO	5.9353E+02	6.4728E+02	6.5716E+02	7.0497E+02	3.6742E+01	3.81752
HMPA	**5.8457E+02**	**6.1939E+02**	**6.2112E+02**	**6.6218E+02**	**2.2740E+01**	22.1301
TF28						
HHO	6.4960E+02	6.6279E+02	6.6254E+02	6.7250E+02	6.4861E+00	21.3844
FFA	6.1832E+02	6.2712E+02	6.2859E+02	6.4706E+02	7.0332E+00	16.0577
MFO	6.1576E+02	6.3054E+02	6.3190E+02	6.6038E+02	1.1950E+01	3.18820
ALO	6.3038E+02	6.3900E+02	6.4051E+02	6.4863E+02	7.1439E+00	116.903
SHO	6.9222E+02	7.1164E+02	7.1415E+02	7.3781E+02	1.0747E+01	2.96765
SSA	6.2835E+02	6.4305E+02	6.4594E+02	6.6327E+02	1.1373E+01	3.85836
AEO	6.1408E+02	6.2815E+02	6.2789E+02	6.4299E+02	7.9484E+00	4.81158
HMPA	**6.0183E+02**	**6.0495E+02**	**6.0608E+02**	**6.1362E+02**	**4.0804E+00**	39.9061
TF29						
HHO	1.1752E+03	1.2993E+03	1.2911E+03	1.3530E+03	5.1586E+01	19.7190
FFA	8.7079E+02	9.2371E+02	9.2858E+02	9.9168E+02	3.1452E+01	15.0084
MFO	9.2020E+02	1.0617E+03	1.0826E+03	1.3801E+03	1.2319E+02	2.66821
ALO	8.7067E+02	9.4843E+02	9.7113E+02	1.1185E+03	8.4615E+01	115.969
SHO	1.4613E+03	1.5078E+03	1.5044E+03	1.5475E+03	2.6611E+01	2.49729
SSA	8.3456E+02	9.1513E+02	9.1796E+02	1.0268E+03	5.7163E+01	3.53884
AEO	9.3878E+02	1.0475E+03	1.0638E+03	1.2434E+03	7.3718E+01	3.87875
HMPA	**8.2657E+02**	**8.9295E+02**	**9.0195E+02**	**9.8979E+02**	**5.1817E+01**	22.0181
TF30						
HHO	9.1734E+02	9.6102E+02	9.5691E+02	9.8853E+02	2.0085E+01	19.9156
FFA	9.4376E+02	1.0252E+03	1.0171E+03	1.0468E+03	2.5747E+01	14.8146
MFO	9.3395E+02	9.7214E+02	9.8625E+02	1.0641E+03	4.1989E+01	2.61049
ALO	8.9253E+02	9.3631E+02	9.3291E+02	9.6417E+02	2.2967E+01	110.245
SHO	1.1820E+03	1.2138E+03	1.2176E+03	1.2834E+03	2.6568E+01	2.44799
SSA	8.8159E+02	9.1939E+02	9.2623E+02	9.9999E+02	3.3238E+01	3.37167
AEO	8.8358E+02	9.2043E+02	9.1953E+02	9.5820E+02	2.0747E+01	3.81102
HMPA	**8.6268E+02**	**9.0547E+02**	**9.0050E+02**	**9.3631E+02**	**1.9834E+01**	21.8930
TF31						
HHO	4.2823E+03	6.4143E+03	6.1568E+03	7.8172E+03	1.0629E+03	19.9806
FFA	1.7734E+03	2.1754E+03	2.5644E+03	4.1370E+03	7.8543E+02	14.6522
MFO	4.4520E+03	6.1356E+03	6.4804E+03	9.8972E+03	1.7172E+03	2.70074
ALO	2.1647E+03	3.6415E+03	3.6596E+03	5.0195E+03	1.1124E+03	114.103

Table 13 (continued)

Algorithm	Best	Median	Average	Worst	STD	AET(s)
SHO	1.4251E+04	1.8415E+04	1.8036E+04	2.4345E+04	2.7006E+03	2.44823
SSA	1.8412E+03	4.1709E+03	3.8954E+03	5.9951E+03	1.4977E+03	3.33507
AEO	2.2969E+03	3.8949E+03	3.9434E+03	5.4852E+03	8.7724E+02	3.75233
HMPA	**1.3723E+03**	**1.8717E+03**	**1.8684E+03**	**2.4695E+03**	**3.8689E+02**	33.2729
TF32						
HHO	3.8632E+03	5.4339E+03	5.3625E+03	6.5528E+03	7.3759E+02	20.1298
FFA	7.4054E+03	8.3095E+03	8.2173E+03	8.7239E+03	3.8854E+02	15.1163
MFO	4.2581E+03	5.8617E+03	5.6805E+03	6.6004E+03	6.3990E+02	2.76346
ALO	4.9647E+03	5.5585E+03	5.6633E+03	6.6959E+03	6.5105E+02	126.094
SHO	9.4404E+03	1.0276E+04	1.0297E+04	1.0923E+04	4.3678E+02	2.86138
SSA	**3.3949E+03**	5.0643E+03	5.0392E+03	6.9092E+03	9.0401E+02	3.62277
AEO	3.4927E+03	4.5905E+03	4.6758E+03	5.7705E+03	6.2264E+02	4.04666
HMPA	3.6890E+03	**4.1453E+03**	**4.2707E+03**	**5.0227E+03**	**4.2924E+02**	34.8360
TF24						
HHO	7.0660E+06	1.1812E+07	1.2071E+07	1.8773E+07	3.2686E+06	14.8938
FFA	1.8036E+05	1.5006E+06	5.1794E+06	2.1457E+07	6.7848E+06	15.3813
MFO	1.0268E+09	8.0565E+09	1.0165E+10	2.2682E+10	7.0301E+09	2.35240
ALO	7.0085E+02	5.8299E+03	5.3492E+03	1.0586E+04	3.5490E+03	99.4014
SHO	6.1500E+10	7.0135E+10	6.9855E+10	7.6328E+10	4.1859E+09	3.34776
SSA	1.1807E+02	5.6556E+03	6.5510E+03	2.0277E+04	5.7999E+03	4.08626
AEO	1.0102E+02	1.4595E+03	4.0323E+03	1.7754E+04	4.8968E+03	5.03689
HMPA	**1.0019E+02**	**1.3486E+02**	**2.2475E+02**	**1.0159E+03**	**2.3776E+02**	30.0016
TF25						
HHO	1.1968E+04	1.9641E+04	1.9307E+04	2.6527E+04	3.6315E+03	18.1841
FFA	5.4140E+04	9.1655E+04	8.7786E+04	1.1087E+05	1.6820E+04	14.3679
MFO	2.5347E+04	1.0374E+05	1.1807E+05	1.9680E+05	4.7432E+04	2.42526
ALO	6.6728E+04	8.2285E+04	1.0037E+05	1.6615E+05	3.5977E+04	104.998
SHO	9.2292E+04	2.3093E+05	3.9077E+05	1.3258E+06	3.6257E+05	2.30629
SSA	3.0651E+03	6.6836E+03	6.9876E+03	1.1305E+04	2.4893E+03	3.22374
AEO	3.0842E+02	3.2189E+02	3.5693E+02	7.3510E+02	1.0625E+02	4.20227
HMPA	**3.0000E+02**	**3.0000E+02**	**3.0000E+02**	**3.0000E+02**	**5.1514E−11**	30.7030
TF26						
HHO	5.2851E+02	5.9844E+02	6.9812E+02	1.1995E+03	2.1782E+02	15.8323
FFA	4.8832E+02	5.1741E+02	5.1820E+02	5.4829E+02	1.4317E+01	14.1702
MFO	5.2663E+02	6.6314E+02	8.1250E+02	1.8954E+03	3.5212E+02	2.43557
ALO	4.6438E+02	5.0741E+02	5.0147E+02	5.3446E+02	2.0234E+01	110.469
SHO	1.5259E+04	2.3217E+04	2.2840E+04	2.8384E+04	4.5147E+03	2.32570
SSA	4.2657E+02	5.0134E+02	4.9694E+02	5.2189E+02	2.4320E+01	3.16385
AEO	4.0036E+02	4.7320E+02	4.7880E+02	5.3674E+02	2.9245E+01	3.50411
HMPA	**4.0000E+02**	**4.0000E+02**	**4.0134E+02**	**4.0408E+02**	**1.9547E+00**	31.1044
TF27						
HHO	7.0127E+02	7.3836E+02	7.3976E+02	8.0170E+02	2.7410E+01	19.6034
FFA	6.4729E+02	7.2288E+02	7.1991E+02	7.5358E+02	2.4956E+01	14.5966
MFO	6.1569E+02	6.8613E+02	6.8802E+02	7.4663E+02	3.8541E+01	2.56790
ALO	6.0845E+02	6.6218E+02	6.5889E+02	7.4675E+02	4.3389E+01	113.621
SHO	9.5833E+02	9.9409E+02	1.0021E+03	1.0637E+03	2.8945E+01	2.46781
SSA	6.0348E+02	6.7412E+02	6.7140E+02	7.7162E+02	5.2914E+01	3.27216
AEO	5.9353E+02	6.4728E+02	6.5716E+02	7.0497E+02	3.6742E+01	3.81752
HMPA	**5.8457E+02**	**6.1939E+02**	**6.2112E+02**	**6.6218E+02**	**2.2740E+01**	22.1301

Table 13 (continued)

Algorithm	Best	Median	Average	Worst	STD	AET(s)
TF28						
HHO	6.4960E+02	6.6279E+02	6.6254E+02	6.7250E+02	6.4861E+00	21.3844
FFA	6.1832E+02	6.2712E+02	6.2859E+02	6.4706E+02	7.0332E+00	16.0577
MFO	6.1576E+02	6.3054E+02	6.3190E+02	6.6038E+02	1.1950E+01	3.18820
ALO	6.3038E+02	6.3900E+02	6.4051E+02	6.4863E+02	7.1439E+00	116.903
SHO	6.9222E+02	7.1164E+02	7.1415E+02	7.3781E+02	1.0747E+01	2.96765
SSA	6.2835E+02	6.4305E+02	6.4594E+02	6.6327E+02	1.1373E+01	3.85836
AEO	6.1408E+02	6.2815E+02	6.2789E+02	6.4299E+02	7.9484E+00	4.81158
HMPA	**6.0183E+02**	**6.0495E+02**	**6.0608E+02**	**6.1362E+02**	**4.0804E+00**	39.9061
TF29						
HHO	1.1752E+03	1.2993E+03	1.2911E+03	1.3530E+03	5.1586E+01	19.7190
FFA	8.7079E+02	9.2371E+02	9.2858E+02	9.9168E+02	3.1452E+01	15.0084
MFO	9.2020E+02	1.0617E+03	1.0826E+03	1.3801E+03	1.2319E+02	2.66821
ALO	8.7067E+02	9.4843E+02	9.7113E+02	1.1185E+03	8.4615E+01	115.969
SHO	1.4613E+03	1.5078E+03	1.5044E+03	1.5475E+03	2.6611E+01	2.49729
SSA	8.3456E+02	9.1513E+02	9.1796E+02	1.0268E+03	5.7163E+01	3.53884
AEO	9.3878E+02	1.0475E+03	1.0638E+03	1.2434E+03	7.3718E+01	3.87875
HMPA	**8.2657E+02**	**8.9295E+02**	**9.0195E+02**	**9.8979E+02**	**5.1817E+01**	22.0181
TF30						
HHO	9.1734E+02	9.6102E+02	9.5691E+02	9.8853E+02	2.0085E+01	19.9156
FFA	9.4376E+02	1.0252E+03	1.0171E+03	1.0468E+03	2.5747E+01	14.8146
MFO	9.3395E+02	9.7214E+02	9.8625E+02	1.0641E+03	4.1989E+01	2.61049
ALO	8.9253E+02	9.3631E+02	9.3291E+02	9.6417E+02	2.2967E+01	110.245
SHO	1.1820E+03	1.2138E+03	1.2176E+03	1.2834E+03	2.6568E+01	2.44799
SSA	8.8159E+02	9.1939E+02	9.2623E+02	9.9999E+02	3.3238E+01	3.37167
AEO	8.8358E+02	9.2043E+02	9.1953E+02	9.5820E+02	2.0747E+01	3.81102
HMPA	**8.6268E+02**	**9.0547E+02**	**9.0050E+02**	**9.3631E+02**	**1.9834E+01**	21.8930
TF31						
HHO	4.2823E+03	6.4143E+03	6.1568E+03	7.8172E+03	1.0629E+03	19.9806
FFA	1.7734E+03	2.1754E+03	2.5644E+03	4.1370E+03	7.8543E+02	14.6522
MFO	4.4520E+03	6.1356E+03	6.4804E+03	9.8972E+03	1.7172E+03	2.70074
ALO	2.1647E+03	3.6415E+03	3.6596E+03	5.0195E+03	1.1124E+03	114.103
SHO	1.4251E+04	1.8415E+04	1.8036E+04	2.4345E+04	2.7006E+03	2.44823
SSA	1.8412E+03	4.1709E+03	3.8954E+03	5.9951E+03	1.4977E+03	3.33507
AEO	2.2969E+03	3.8949E+03	3.9434E+03	5.4852E+03	8.7724E+02	3.75233
HMPA	**1.3723E+03**	**1.8717E+03**	**1.8684E+03**	**2.4695E+03**	**3.8689E+02**	33.2729
TF32						
HHO	3.8632E+03	5.4339E+03	5.3625E+03	6.5528E+03	7.3759E+02	20.1298
FFA	7.4054E+03	8.3095E+03	8.2173E+03	8.7239E+03	3.8854E+02	15.1163
MFO	4.2581E+03	5.8617E+03	5.6805E+03	6.6004E+03	6.3990E+02	2.76346
ALO	4.9647E+03	5.5585E+03	5.6633E+03	6.6959E+03	6.5105E+02	126.094
SHO	9.4404E+03	1.0276E+04	1.0297E+04	1.0923E+04	4.3678E+02	2.86138
SSA	**3.3949E+03**	5.0643E+03	5.0392E+03	6.9092E+03	9.0401E+02	3.62277
AEO	3.4927E+03	4.5905E+03	4.6758E+03	5.7705E+03	6.2264E+02	4.04666
HMPA	3.6890E+03	**4.1453E+03**	**4.2707E+03**	**5.0227E+03**	**4.2924E+02**	34.8360
TF33						
HHO	1.1714E+03	1.2724E+03	1.3124E+03	1.6036E+03	1.1976E+02	19.9884
FFA	1.2110E+03	1.2795E+03	1.2687E+03	1.3389E+03	3.7938E+01	13.8295
MFO	1.3779E+03	1.9018E+03	3.0933E+03	6.5291E+03	1.9940E+03	2.53544
ALO	1.2142E+03	1.3074E+03	1.3136E+03	1.4276E+03	6.6189E+01	124.533

Table 13 (continued)

Algorithm	Best	Median	Average	Worst	STD	AET(s)
SHO	1.1418E+04	2.4514E+04	2.6712E+04	6.2226E+04	1.4439E+04	2.45820
SSA	1.2152E+03	1.2609E+03	1.2708E+03	1.3507E+03	4.0338E+01	3.32137
AEO	1.1706E+03	1.2211E+03	1.2161E+03	1.3065E+03	3.7475E+01	3.71565
HMPA	**1.1507E+03**	**1.1647E+03**	**1.1792E+03**	**1.2204E+03**	**2.5963E+01**	36.7320
TF34						
HHO	6.4765E+06	3.8401E+07	6.2315E+07	2.4845E+08	6.7357E+07	17.6107
FFA	2.1116E+05	2.1720E+06	2.6205E+06	5.5573E+06	1.6063E+06	15.5679
MFO	1.3111E+06	1.5167E+07	7.8928E+07	4.6158E+08	1.5515E+08	2.66538
ALO	2.8048E+06	1.0133E+07	1.5311E+07	4.9656E+07	1.5130E+07	116.909
SHO	9.3942E+09	2.0259E+10	1.9001E+10	2.3664E+10	3.6130E+09	2.96889
SSA	7.6561E+05	3.7392E+06	4.3085E+06	1.0968E+07	2.9482E+06	3.35389
AEO	2.9425E+04	1.2834E+05	1.9255E+05	8.7355E+05	2.3492E+05	4.15805
HMPA	**4.7200E+03**	**1.0798E+04**	**1.0193E+04**	**1.7369E+04**	**4.1273E+03**	32.1631
TF35						
HHO	3.6576E+04	1.0812E+05	5.6150E+05	4.3468E+06	1.1895E+06	19.9234
FFA	1.7683E+03	2.5838E+04	1.0181E+05	1.0094E+06	2.5530E+05	16.0314
MFO	2.4158E+04	1.2137E+05	1.0814E+07	7.1750E+07	2.4808E+07	2.63315
ALO	3.9668E+04	9.1251E+04	9.7310E+04	1.9056E+05	4.8663E+04	112.641
SHO	7.8618E+09	1.9013E+10	1.8824E+10	2.8536E+10	5.7367E+09	2.92168
SSA	1.9746E+04	5.4260E+04	6.9553E+04	2.0206E+05	4.6376E+04	3.56639
AEO	1.9265E+03	2.1753E+04	2.4581E+04	6.0971E+04	2.0688E+04	4.19475
HMPA	**1.4475E+03**	**2.6474E+03**	**5.2429E+03**	**1.0622E+04**	**3.7779E+03**	33.1602
TF36						
HHO	1.4892E+04	1.2175E+05	2.4672E+05	1.0730E+06	3.1714E+05	19.5099
FFA	1.2409E+04	4.3502E+04	5.4282E+04	1.4279E+05	3.8391E+04	15.9659
MFO	9.3260E+03	7.9603E+04	3.0301E+05	2.5152E+06	6.3957E+05	3.07173
ALO	4.3461E+03	3.3145E+04	3.3301E+04	8.3884E+04	2.3460E+04	104.363
SHO	3.4074E+06	2.3696E+07	2.5545E+07	6.0603E+07	1.7353E+07	2.72007
SSA	1.9275E+03	2.8063E+04	2.3559E+04	4.3978E+04	1.3647E+04	3.73166
AEO	1.5146E+03	1.8572E+03	2.2853E+03	4.4152E+03	9.7344E+02	4.21999
HMPA	**1.4670E+03**	**1.5297E+03**	**1.5259E+03**	**1.5820E+03**	**3.0228E+01**	33.4333
TF37						
HHO	1.9320E+04	4.7232E+04	4.9351E+04	1.0700E+05	2.5382E+04	19.8232
FFA	1.6355E+03	3.5973E+03	5.8624E+03	2.6599E+04	6.8290E+03	15.0107
MFO	4.2101E+03	3.1608E+04	8.0818E+04	6.9519E+05	1.7197E+05	2.93092
ALO	1.4838E+04	4.5407E+04	5.2125E+04	1.3183E+05	3.6481E+04	105.503
SHO	3.3402E+08	2.2581E+09	2.2635E+09	3.5625E+09	9.7537E+08	2.68491
SSA	1.3105E+04	3.1637E+04	3.5277E+04	8.3794E+04	2.1111E+04	3.26063
AEO	1.6624E+03	2.4058E+03	4.3985E+03	1.6495E+04	3.8787E+03	3.71769
HMPA	**1.6326E+03**	**1.8959E+03**	**2.6322E+03**	**5.5289E+03**	**1.2333E+03**	31.5056
TF38						
HHO	2.7015E+03	3.5391E+03	3.4868E+03	4.7026E+03	5.4740E+02	17.8063
FFA	2.6038E+03	3.2874E+03	3.2279E+03	3.5461E+03	2.5032E+02	15.4890
MFO	2.3191E+03	3.1954E+03	3.1150E+03	3.8368E+03	4.8282E+02	3.23290
ALO	2.3676E+03	3.0916E+03	3.0338E+03	3.5363E+03	3.1157E+02	105.194
SHO	6.0726E+03	8.0244E+03	8.0803E+03	1.4007E+04	1.9024E+03	2.45452
SSA	2.1704E+03	2.7308E+03	2.7702E+03	3.4452E+03	3.6274E+02	3.29262
AEO	2.2060E+03	2.7909E+03	2.7710E+03	3.2985E+03	2.9654E+02	3.94091
HMPA	**2.1610E+03**	**2.3899E+03**	**2.4128E+03**	**3.0243E+03**	**2.1313E+02**	32.7070

Table 13 (continued)

Algorithm	Best	Median	Average	Worst	STD	AET(s)
TF39						
HHO	2.2070E+03	2.6427E+03	2.6291E+03	3.1238E+03	2.5702E+02	25.8047
FFA	1.9316E+03	2.2074E+03	2.1819E+03	2.3675E+03	1.5077E+02	17.1872
MFO	1.9689E+03	2.4571E+03	2.4632E+03	3.0306E+03	2.7028E+02	3.77024
ALO	2.1984E+03	2.4414E+03	2.5311E+03	2.9536E+03	2.8670E+02	107.047
SHO	4.3217E+03	5.9785E+03	7.9344E+03	2.1213E+04	4.3622E+03	3.09623
SSA	1.8131E+03	2.0295E+03	2.1393E+03	2.6878E+03	2.6655E+02	4.03814
AEO	1.7923E+03	2.0146E+03	2.0662E+03	2.3774E+03	1.9977E+02	4.60560
HMPA	**1.7707E+03**	**1.9016E+03**	**1.9078E+03**	**2.1189E+03**	**1.0369E+02**	37.7248
TF40						
HHO	1.2374E+05	4.9850E+05	1.5443E+06	1.0464E+07	2.7070E+06	20.1311
FFA	3.6616E+05	1.9617E+06	2.0267E+06	3.2729E+06	8.3839E+05	15.5899
MFO	4.4664E+05	1.4358E+06	4.7102E+06	3.1263E+07	8.1203E+06	2.99143
ALO	4.4356E+04	3.3470E+05	4.8015E+05	1.3975E+06	4.5928E+05	104.960
SHO	1.7617E+07	2.8945E+08	3.3691E+08	1.0453E+09	2.9779E+08	2.52062
SSA	3.7754E+04	1.7356E+05	3.0662E+05	1.0042E+06	3.2300E+05	3.49448
AEO	1.4350E+04	3.7096E+04	4.0178E+04	9.3230E+04	2.3387E+04	3.89934
HMPA	**2.2734E+03**	**6.4666E+03**	**9.0710E+03**	**2.5429E+04**	**7.3285E+03**	33.0094
TF41						
HHO	1.0849E+04	5.0450E+04	9.4969E+04	3.9887E+05	1.1255E+05	29.5037
FFA	2.4018E+03	5.7116E+03	1.0964E+04	3.9468E+04	1.0307E+04	24.0426
MFO	7.3841E+03	1.3409E+05	8.7179E+05	8.4464E+06	2.1498E+06	5.99880
ALO	3.0261E+05	1.8317E+06	1.6004E+06	3.3165E+06	9.4629E+05	107.302
SHO	4.2796E+08	2.3790E+09	2.4434E+09	3.7433E+09	8.4368E+08	5.69980
SSA	2.6032E+04	7.2814E+05	7.4242E+05	2.0138E+06	4.5913E+05	6.41244
AEO	2.0103E+03	3.6301E+03	6.4578E+03	1.8914E+04	5.1480E+03	8.31978
HMPA	**1.9462E+03**	**2.0817E+03**	**2.1862E+03**	**2.9972E+03**	**2.9330E+02**	62.6533
TF42						
HHO	2.3600E+03	2.7711E+03	2.7058E+03	3.0062E+03	2.0799E+02	23.4922
FFA	2.2401E+03	2.5770E+03	2.5598E+03	2.8344E+03	1.7658E+02	17.9635
MFO	2.3635E+03	2.6880E+03	2.7265E+03	2.9771E+03	2.0133E+02	3.79620
ALO	2.4725E+03	2.6598E+03	2.7151E+03	2.9712E+03	1.6718E+02	105.497
SHO	3.2635E+03	3.5243E+03	3.5456E+03	3.8009E+03	1.7784E+02	4.19834
SSA	2.2512E+03	2.4474E+03	2.4505E+03	2.6807E+03	1.3542E+02	5.08997
AEO	2.2001E+03	2.4385E+03	2.4849E+03	2.9573E+03	2.1907E+02	4.77589
HMPA	**2.1845E+03**	**2.2183E+03**	**2.2397E+03**	**2.4052E+03**	**6.0285E+01**	50.6334
TF43						
HHO	2.4371E+03	2.5177E+03	2.5178E+03	2.5957E+03	4.3912E+01	21.8738
FFA	2.4178E+03	2.5117E+03	2.4983E+03	2.5417E+03	3.6299E+01	14.7403
MFO	2.4297E+03	2.4765E+03	2.4825E+03	2.5595E+03	3.9605E+01	3.93610
ALO	2.3992E+03	2.4408E+03	2.4374E+03	2.4837E+03	2.7730E+01	118.807
SHO	2.8030E+03	2.8718E+03	2.8791E+03	2.9528E+03	4.0815E+01	4.35214
SSA	2.3719E+03	2.4289E+03	2.4249E+03	2.4648E+03	2.4336E+01	4.13002
AEO	2.3675E+03	2.4432E+03	2.4334E+03	2.4849E+03	3.9092E+01	5.17950
HMPA	**2.3658E+03**	**2.3886E+03**	**2.3939E+03**	**2.4368E+03**	**2.0169E+01**	35.7019
TF44						
HHO	2.9795E+03	3.1393E+03	3.1245E+03	3.2605E+03	9.2593E+01	24.2599
FFA	2.7847E+03	2.8326E+03	2.8328E+03	2.8835E+03	2.8571E+01	15.5739
MFO	2.7615E+03	2.8105E+03	2.8038E+03	2.8492E+03	2.2224E+01	4.37430
ALO	2.7509E+03	2.7983E+03	2.7966E+03	2.8307E+03	2.7871E+01	113.154

Table 13 (continued)

Algorithm	Best	Median	Average	Worst	STD	AET(s)
SHO	3.3732E+03	3.8165E+03	3.7769E+03	4.1579E+03	1.8321E+02	4.27944
SSA	2.7553E+03	2.8008E+03	2.8029E+03	2.8628E+03	3.5510E+01	4.73158
AEO	2.8143E+03	2.9009E+03	2.8941E+03	2.9686E+03	4.6566E+01	5.82847
HMPA	**2.7531E+03**	**2.7739E+03**	**2.7755E+03**	**2.8213E+03**	**3.1040E+01**	49.7142
TF45						
HHO	3.1051E+03	3.3003E+03	3.3079E+03	3.4588E+03	9.4410E+01	22.6299
FFA	2.9814E+03	3.0347E+03	3.0281E+03	3.0518E+03	2.0932E+01	15.5121
MFO	2.9358E+03	2.9871E+03	2.9862E+03	3.0204E+03	2.6615E+01	4.50950
ALO	2.9179E+03	2.9701E+03	2.9635E+03	2.9933E+03	2.2960E+01	111.221
SHO	3.7414E+03	4.0015E+03	4.0689E+03	4.6696E+03	2.5510E+02	4.28989
SSA	2.8906E+03	2.9806E+03	2.9706E+03	3.1062E+03	5.1070E+01	4.79790
AEO	2.9428E+03	3.0420E+03	3.0510E+03	3.1443E+03	6.6806E+01	6.17258
HMPA	**2.8832E+03**	**2.9700E+03**	**2.9629E+03**	**3.0106E+03**	**2.2731E+01**	45.8348
TF46						
HHO	2.8968E+03	2.9454E+03	2.9370E+03	2.9943E+03	3.0010E+01	22.4255
FFA	2.8902E+03	2.9040E+03	2.9047E+03	2.9251E+03	1.0384E+01	14.7527
MFO	2.9090E+03	3.1827E+03	3.2139E+03	3.6624E+03	2.2959E+02	5.22712
ALO	2.8902E+03	2.9181E+03	2.9191E+03	2.9507E+03	1.8838E+01	114.352
SHO	5.4075E+03	6.3295E+03	6.4985E+03	9.1569E+03	9.0311E+02	3.55661
SSA	2.8837E+03	2.9228E+03	2.9181E+03	2.9535E+03	2.5960E+01	4.45614
AEO	2.8841E+03	2.8903E+03	2.8998E+03	2.9377E+03	1.8428E+01	5.74323
HMPA	**2.8834E+03**	**2.8839E+03**	**2.8892E+03**	**2.9316E+03**	**1.4649E+01**	44.6638
TF47						
HHO	5.6644E+03	7.3900E+03	7.5637E+03	8.9686E+03	8.7055E+02	25.6150
FFA	3.3820E+03	4.4314E+03	4.4154E+03	5.5343E+03	6.1176E+02	15.6537
MFO	5.2765E+03	5.6007E+03	5.7090E+03	6.3986E+03	3.8334E+02	4.77885
ALO	5.1205E+03	5.4498E+03	5.6854E+03	6.5456E+03	5.5555E+02	107.987
SHO	1.0506E+04	1.2350E+04	1.2436E+04	1.4842E+04	1.0513E+03	4.10250
SSA	2.8000E+03	4.7860E+03	4.6396E+03	5.9489E+03	1.0105E+03	4.82164
AEO	2.9000E+03	5.8930E+03	5.8174E+03	7.0528E+03	9.1279E+02	6.36252
HMPA	**2.8000E+03**	**2.9000E+03**	**3.7630E+03**	**5.7144E+03**	**1.1538E+03**	50.3818
TF48						
HHO	3.5064E+03	3.7938E+03	3.7760E+03	4.1286E+03	1.7126E+02	24.5471
FFA	3.2042E+03	3.2173E+03	3.2179E+03	3.2330E+03	8.5027E+00	16.7282
MFO	3.2172E+03	3.2376E+03	3.2455E+03	3.3138E+03	2.7613E+01	5.09697
ALO	3.2964E+03	3.3500E+03	3.3775E+03	3.5366E+03	8.4895E+01	113.169
SHO	4.2306E+03	4.8897E+03	4.8919E+03	5.9053E+03	3.5548E+02	4.90668
SSA	3.2127E+03	3.2458E+03	3.2465E+03	3.2811E+03	2.3030E+01	5.09324
AEO	3.2130E+03	3.2958E+03	3.3013E+03	3.3813E+03	5.0762E+01	6.94347
HMPA	**3.1966E+03**	**3.2125E+03**	**3.2084E+03**	**3.2254E+03**	**2.2281E+00**	65.8691
TF49						
HHO	3.2407E+03	3.3342E+03	3.3521E+03	3.4847E+03	7.2555E+01	16.6886
FFA	3.2579E+03	3.2826E+03	3.2857E+03	3.3332E+03	2.0590E+01	15.4609
MFO	3.3295E+03	3.6595E+03	3.8997E+03	5.1571E+03	5.8271E+02	4.82535
ALO	3.2204E+03	3.2661E+03	3.2600E+03	3.2870E+03	2.2998E+01	111.541
SHO	7.2420E+03	8.8289E+03	8.6822E+03	9.1619E+03	4.7743E+02	3.94904
SSA	3.1991E+03	3.2203E+03	3.2303E+03	3.2665E+03	2.4860E+01	4.93789
AEO	3.1917E+03	3.2121E+03	3.2181E+03	3.2834E+03	2.6232E+01	6.48561
HMPA	**3.1000E+03**	**3.1000E+03**	**3.1000E+03**	**3.1000E+03**	**2.8451E−12**	38.7265

Table 13 (continued)

Algorithm	Best	Median	Average	Worst	STD	AET(s)
TF50						
HHO	3.9032E+03	4.7476E+03	4.7919E+03	6.1943E+03	6.0114E+02	20.8169
FFA	3.7184E+03	4.1061E+03	4.1277E+03	4.5588E+03	2.2814E+02	15.0199
MFO	3.7075E+03	4.0231E+03	4.0983E+03	4.6535E+03	2.9183E+02	4.48715
ALO	4.1460E+03	4.3790E+03	4.4660E+03	5.1809E+03	3.2793E+02	118.043
SHO	7.1167E+03	1.4124E+04	1.6157E+04	5.3542E+04	1.1888E+04	3.61199
SSA	3.7774E+03	4.1017E+03	4.1372E+03	4.6079E+03	2.5934E+02	4.56063
AEO	3.7034E+03	4.0792E+03	4.0080E+03	4.4793E+03	2.3105E+02	5.94408
HMPA	**3.3476E+03**	**3.6811E+03**	**3.6687E+03**	**4.0678E+03**	**1.9049E+02**	39.9666

The best results have been written in bold

$$
\begin{aligned}
c_1(\vec{v}) &= -v_1 + 0.0193v_3 \le 0,\\
c_2(\vec{v}) &= -v_3 + 0.00954v_3 \le 0,\\
c_3(\vec{v}) &= -\pi v_3^2 v_4 - \frac{4}{3}\pi v_3^3 + 1,296,000 \le 0,\\
c_4(\vec{v}) &= v_4 - 240 \le 0,
\end{aligned} \tag{33}
$$

where $0 \le v_1 \le 99$, $0 \le v_2 \le 99$, $10 \le v_3 \le 200$, $10 \le v_4 \le 200$.

The obtained results on this problem are presented statistically in Table 19, and the best solutions found by the algorithms are provided in Table 20. Besides, the convergence graphs of the algorithms are shown in Fig. 25.

The results show that the HMPA algorithm obtained better results, and converged more quickly in comparison with other algorithms.

7.4 Tension/compression spring design problem

The tension/compression spring design problem is another constrained engineering problem to minimize tension/compression spring weight. There are three design variables in this problem: wire diameter (d), mean coil diameter (D), and the number of active coils (P), which have been shown in Fig. 26.

The constraints and the mathematical formulation of the problem are as below:Consider:

$$\vec{v} = [v_1, v_2, v_3] = [d, D, P],$$

Minimize:

$$f(\vec{v}) = (v_3 + 2)v_2 v_1^2,$$

Subject to:

$$
\begin{aligned}
c_1(\vec{v}) &= 1 - \frac{v_2^3 v_3}{71785 v_1^4} \le 0,\\
c_2(\vec{v}) &= \frac{4v_2^2 - v_1 v_2}{12,566\left(v_2 v_1^3 - v_1^4\right)} + \frac{1}{5108 v_1^2} \le 0,\\
c_3(\vec{v}) &= 1 - \frac{140.45 v_1}{v_2^2 v_3} \le 0,\\
c_4(\vec{v}) &= \frac{v_1 + v_2}{1.5} - 1 \le 0,
\end{aligned} \tag{34}
$$

where $0.05 \le v_1 \le 2.0$, $0.25 \le v_2 \le 1.3$, $2.0 \le v_3 \le 15.0$.

Tables 21 and 22 give the statistical results and the best points obtained by the algorithms, respectively. Furthermore, Fig. 27 depicts the convergence graphs of the algorithms.

The results state that HMPA is the preeminent algorithm among the competitor algorithms.

7.5 Gear train design problem

Gear train design problem is an unconstrained real-life engineering problem with the aim of finding the optimal number of teeth in the gears between the driver and driveshafts. As depicted in Fig. 28, this problem has four gears:T_d, T_b, T_a, and T_f. It is evident that the number of teeth in the gears must be an integer.

The objective and mathematical formulation of this problem are as follows:Consider:

$$\vec{v} = [v_1, v_2, v_3, v_4] = [T_d, T_b, T_a, T_f],$$

Objective is to minimize:

$$f(\vec{v}) = \left[\frac{1}{6.931} - \frac{v_1 v_2}{v_3 v_4}\right]^2, \tag{35}$$

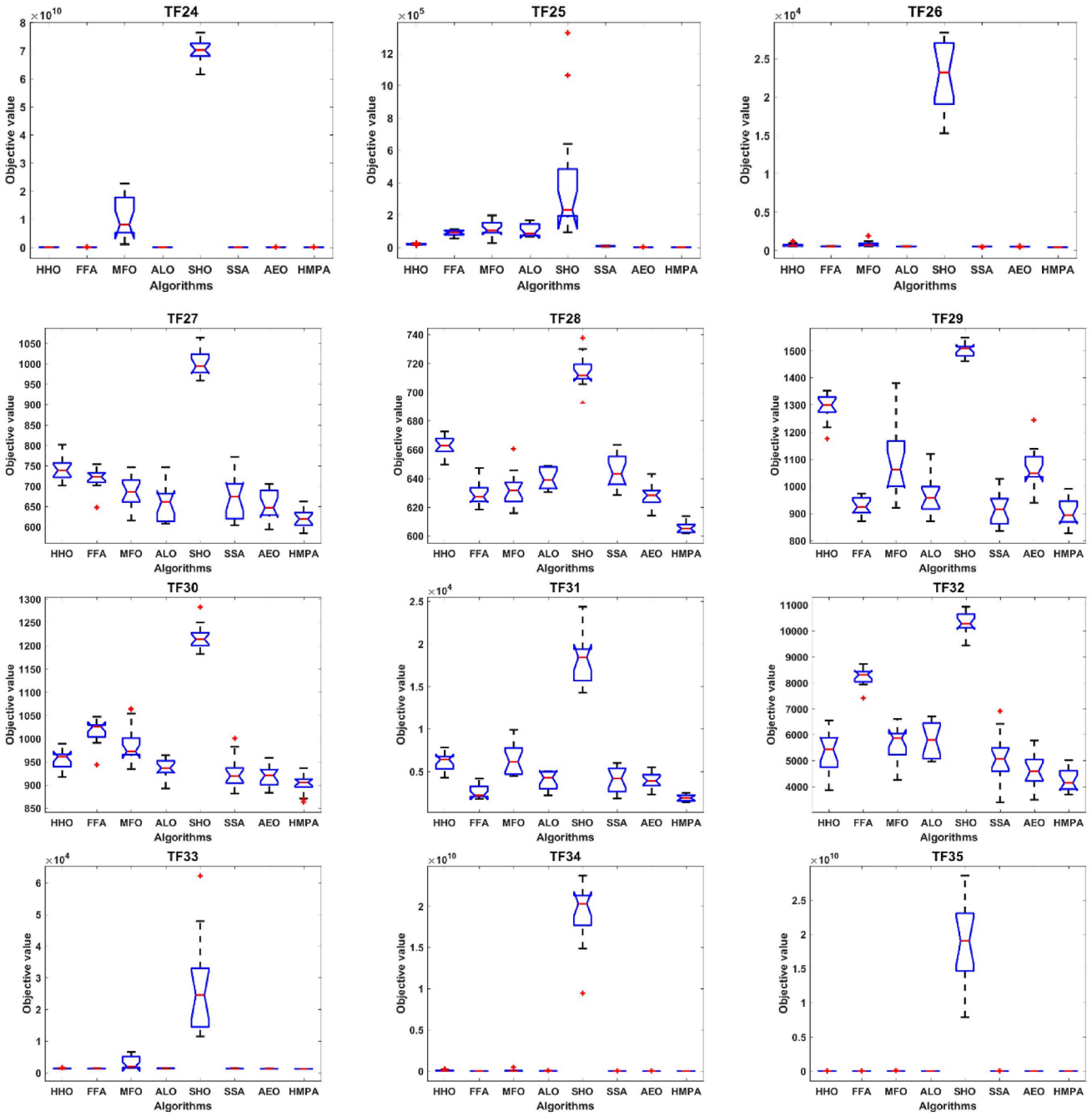

Fig. 18 Box plots of the obtained results from the algorithms on CEC 2017 test functions

where $12 \leq v_1 \leq 60$, $12 \leq v_2 \leq 60$, $12 \leq v_3 \leq 60$, $12 \leq v_4 \leq 60$.

The statistical results of the algorithms and the best solutions are expressed in Table 23 and Table 24, respectively. In addition, the result of convergence evaluation is illustrated in Fig. 29.

The results demonstrate that the HMPA has been more triumphant in solving gear train design problem.

7.6 Spread spectrum radar poly-phase design problem

Spread spectrum radar poly-phase design problem is a complex continuous optimization problem to minimize the envelope module of the compressed radar pulse at the receiver output. The objective and the mathematical formulation of this problem are as below:Objective is to minimize:

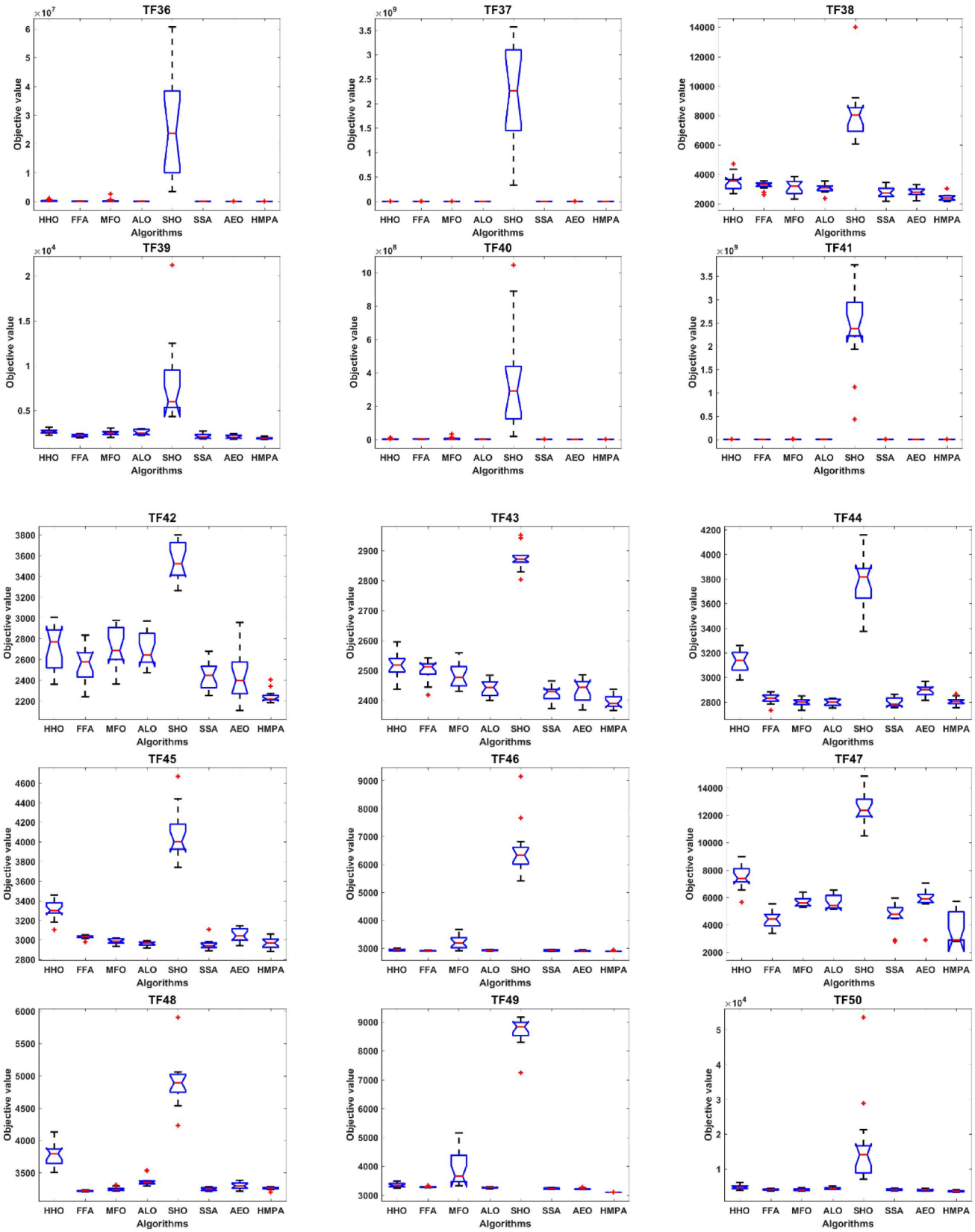

Fig. 18 (continued)

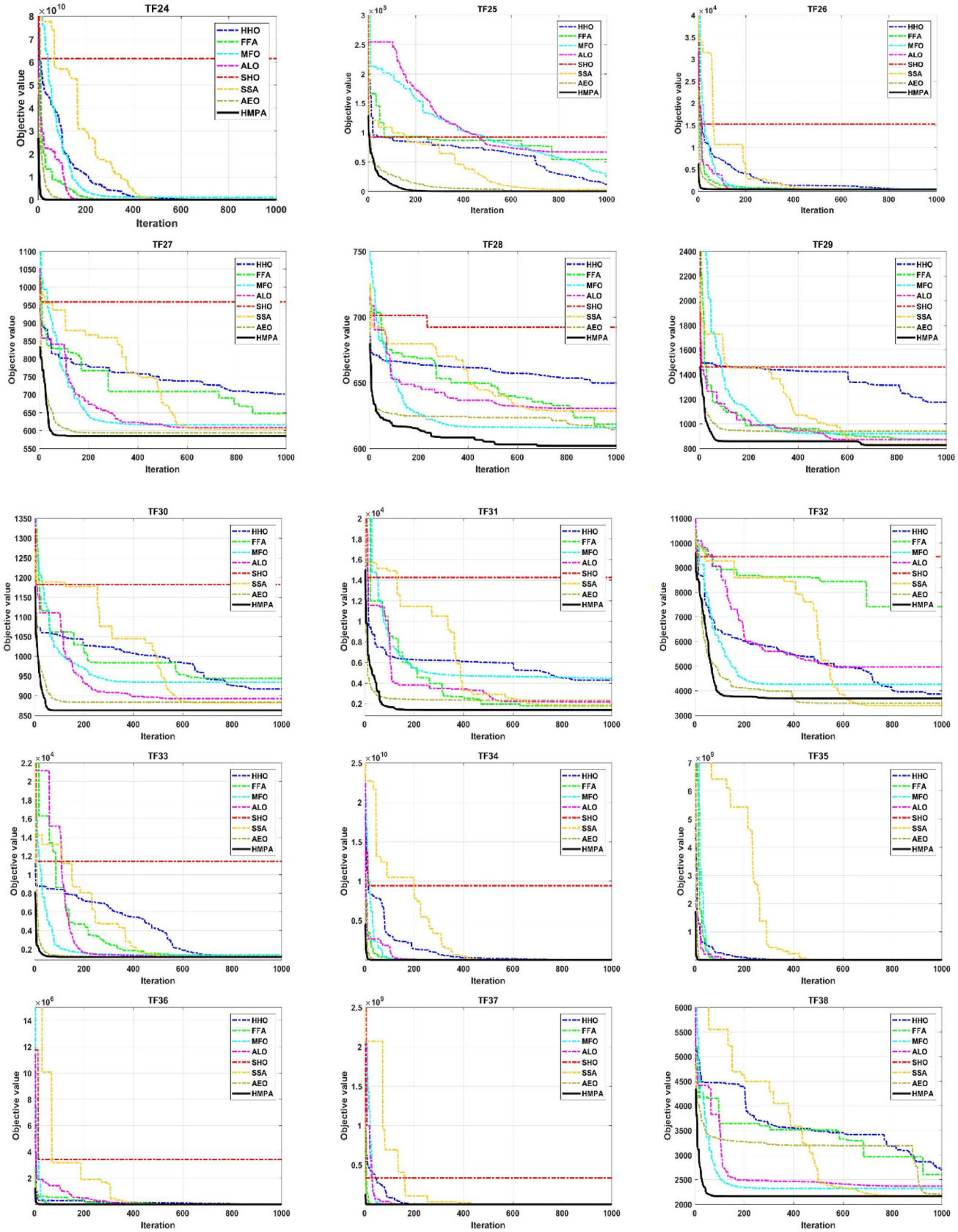

Fig. 19 Convergence graphs of the algorithms on CEC 2017 test functions

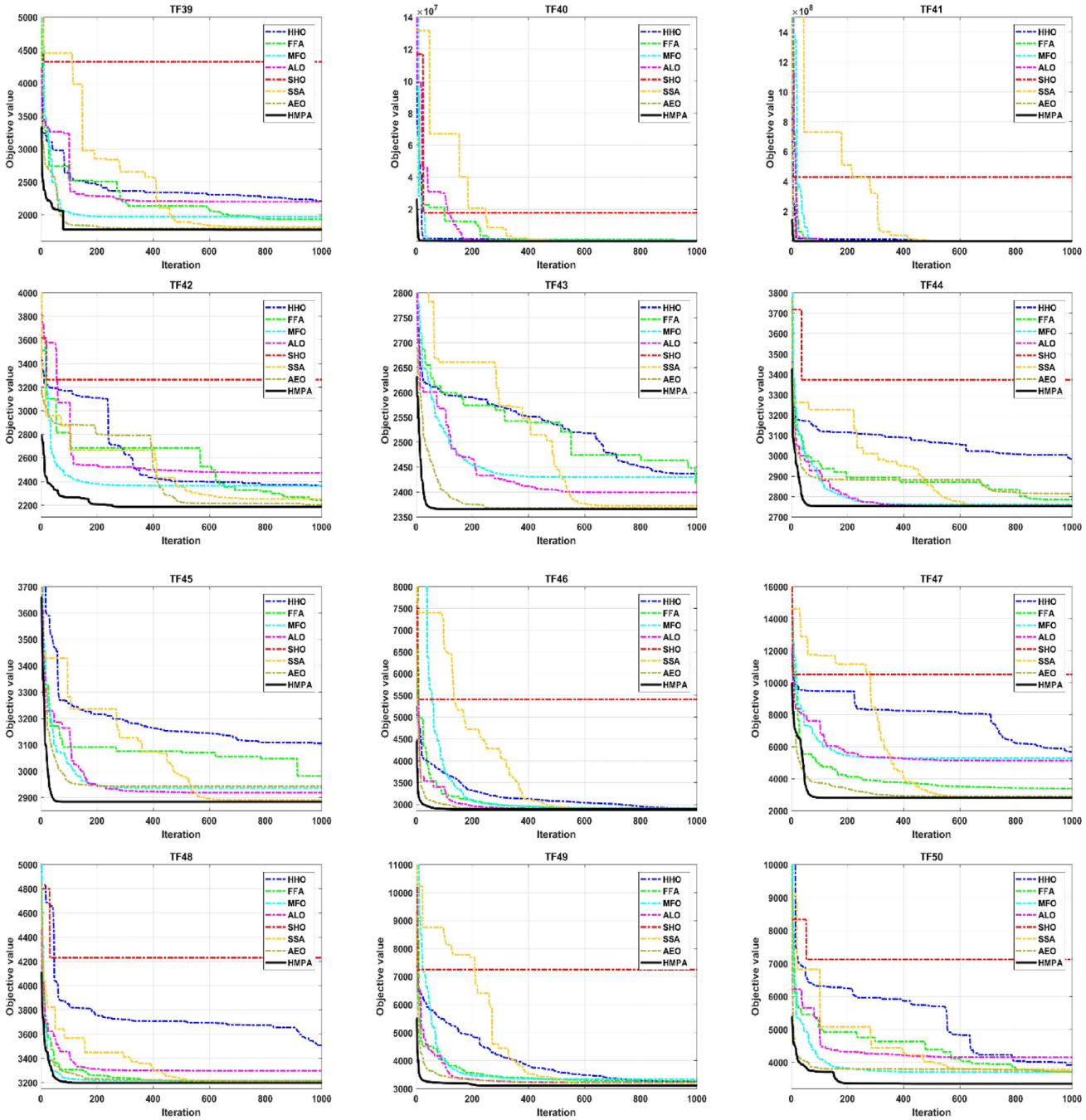

Fig. 19 (continued)

$$F(\vec{v}) = \max\{f_1(\vec{v}), f_2(\vec{v}), \ldots, f_{2m}(\vec{v})\}, \tag{36}$$

where $N = 10$, $m = 2N - 1$, $\vec{v} = (v_1, v_2, \ldots, v_N) \in R^N | 0 \le v_i \le 2\pi, i = 1, 2, \ldots, N$, $f_{2i-1}(\vec{v}) = \sum_{j=i}^{N} \cos \sum_{k=|2i-j-1|+1}^{j} v_k, i = 1, 2, \ldots, N$,

$$f_{2i}(\vec{v}) = 0.5 \sum_{j=i+1}^{N} \cos \sum_{k=|2i-j|+1}^{j} v_k, \quad i = 1, 2, \ldots, N-1,$$

$f_{m+i}(\vec{v}) = -f_i(\vec{v}), \quad i = 1, 2, \ldots, m.$

Tables 25 and 26 represent the statistical results, and the solutions found by the algorithms, respectively. Figure 30 presents the convergence rates of the algorithms on this problem.

Table 14 Wilcoxon signed-rank test results of the HMPA versus the competitor algorithms with 5% significance level on CEC 2017 test functions

	HMPA vs. HHO		HMPA vs. FFA		HMPA vs. MFO		HMPA vs. ALO		HMPA vs. SHO		HMPA vs. SSA		HMPA vs. AEO	
	P value	*R*	*P* value	*R*	*P* value	*R*	*P* value	*R*	*P* value	*R*	*P* value	*R*	*P* value	*R*
TF24	6.104E−05	+	6.104E−05	+	6.104E−05	+	6.104E−05	+	6.104E−05	+	1.221E−04	+	1.221E−04	+
TF25	6.104E−05	+	6.104E−05	+	6.104E−05	+	6.104E−05	+	6.104E−05	+	6.104E−05	+	6.104E−05	+
TF26	6.104E−05	+	6.104E−05	+	6.104E−05	+	6.104E−05	+	6.104E−05	+	6.104E−05	+	1.221E−04	+
TF27	6.104E−05	+	6.104E−05	+	6.104E−05	+	8.362E−03	+	6.104E−05	+	1.526E−03	+	1.025E−02	+
TF28	6.104E−05	+	6.104E−05	+	6.104E−05	+	6.104E−05	+	6.104E−05	+	6.104E−05	+	6.104E−05	+
TF29	6.104E−05	+	1.688E−01	–	1.831E−04	+	2.625E−03	+	6.104E−05	+	5.245E−01	–	1.221E−04	+
TF30	1.831E−04	+	6.104E−05	+	6.104E−05	+	1.526E−03	+	6.104E−05	+	1.245E−02	+	4.272E−03	+
TF31	6.104E−05	+	5.371E−03	+	6.104E−05	+	6.104E−05	+	6.104E−05	+	4.272E−04	+	6.104E−05	+
TF32	1.221E−04	+	6.104E−05	+	6.104E−05	+	6.104E−05	+	6.104E−05	+	2.155E−02	+	1.245E−02	+
TF33	1.221E−04	+	6.104E−05	+	6.104E−05	+	6.104E−05	+	6.104E−05	+	6.104E−05	+	2.625E−03	+
TF34	6.104E−05	+	6.104E−05	+	6.104E−05	+	6.104E−05	+	6.104E−05	+	6.104E−05	+	6.104E−05	+
TF35	6.104E−05	+	1.025E−02	+	6.104E−05	+	6.104E−05	+	6.104E−05	+	6.104E−05	+	8.362E−03	+
TF36	6.104E−05	+	6.104E−05	+	6.104E−05	+	6.104E−05	+	6.104E−05	+	6.104E−05	+	1.221E−04	+
FT37	6.104E−05	+	1.514E−01	–	6.104E−05	+	6.104E−05	+	6.104E−05	+	6.104E−05	+	1.205E−01	–
TF38	1.221E−04	+	1.221E−04	+	1.221E−04	+	1.221E−04	+	6.104E−05	+	1.508E−02	+	3.357E−03	+
TF39	6.104E−05	+	6.104E−05	+	6.104E−05	+	6.104E−05	+	6.104E−05	+	6.714E−03	+	3.534E−02	+
TF40	6.104E−05	+	6.104E−05	+	6.104E−05	+	6.104E−05	+	6.104E−05	+	6.104E−05	+	1.221E−04	+
TF41	6.104E−05	+	6.104E−05	+	6.104E−05	+	6.104E−05	+	6.104E−05	+	6.104E−05	+	1.526E−03	+
TF42	6.104E−05	+	1.831E−04	+	6.104E−05	+	6.104E−05	+	6.104E−05	+	6.104E−05	+	6.104E−04	+
TF43	6.104E−05	+	6.104E−05	+	6.104E−05	+	6.104E−04	+	6.104E−05	+	5.371E−03	+	2.014E−03	+
TF44	6.104E−05	+	5.536E−02	–	9.341E−01	–	6.387E−01	–	6.104E−05	+	8.040E−01	–	3.052E−04	+
TF45	6.104E−05	+	6.104E−04	+	9.460E−02	–	9.341E−01	–	6.104E−05	+	5.614E−01	–	5.371E−03	+
TF46	8.545E−04	+	6.714E−03	+	6.104E−05	+	1.221E−04	+	6.104E−05	+	2.625E−03	+	8.362E−03	+
TF47	6.104E−05	+	8.325E−02	–	6.104E−05	+	6.104E−05	+	6.104E−05	+	2.557E−02	+	6.104E−05	+
TF48	6.104E−05	+	1.831E−04	+	9.460E−02	–	6.104E−05	+	6.104E−05	+	2.078E−01	–	2.625E−03	+
TF49	6.104E−05	+	6.104E−05	+	6.104E−05	+	6.104E−05	+	6.104E−05	+	6.104E−05	+	6.104E−05	+
TF50	6.104E−05	+	1.221E−04	+	3.052E−04	+	6.104E−05	+	6.104E−05	+	1.831E−04	+	4.272E−04	+

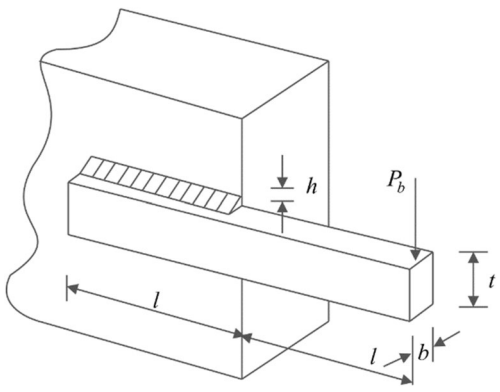

Fig. 20 Welded beam design problem

Table 15 Statistical results of the algorithms on the welded beam design problem

Algorithm	Best	Worst	Mean	Std.
HMPA	**1.695247**	**1.695247**	**1.695247**	**0.0000e+00**
HHO	1.722109	1.970076	1.818944	0.057866
FFA	1.695503	1.986527	1.752352	0.079615
MFO	1.695247	1.873179	1.716946	0.052377
ALO	1.695426	1.859499	1.723084	0.054830
SHO	1.817368	2.252941	1.972993	0.119536
SSA	1.700480	1.867176	1.739649	0.052245
AEO	1.695247	1.712678	1.696428	0.004495
TSA	1.709622	1.910382	1.851006	0.003245
MRFO	**1.695247**	**1.695247**	**1.695247**	4.9068e−09
SCA	1.759173	1.873408	1.817657	0.027543
WOA	1.722972	1.931557	1.836738	0.060294

Table 16 The best-obtained results on the welded beam design problem

Algo.	Optimum variables				Optimal fitness
	h	*l*	*t*	*b*	
HMPA	0.205729	3.253120	9.036623	0.205729	1.695247
HHO	0.195173	3.441696	9.071659	0.207203	1.722109
FFA	0.201977	3.276407	9.036130	0.208602	1.695503
MFO	0.205729	3.253120	9.036623	0.205729	1.695247
ALO	0.205540	3.256487	9.036624	0.205729	1.695426
SHO	0.173653	3.722985	9.809483	0.202454	1.817368
SSA	0.207176	3.236116	9.005000	0.207177	1.700480
AEO	0.205729	3.253120	9.036623	0.205729	1.695247
TSA	0.192162	3.512430	9.036612	0.205730	1.709622
MRFO	0.205729	3.470488	9.036623	0.205729	1.724852
SCA	0.204695	3.536291	9.004290	0.210025	1.759173
WOA	0.183843	3.701841	9.028197	0.206113	1.722972

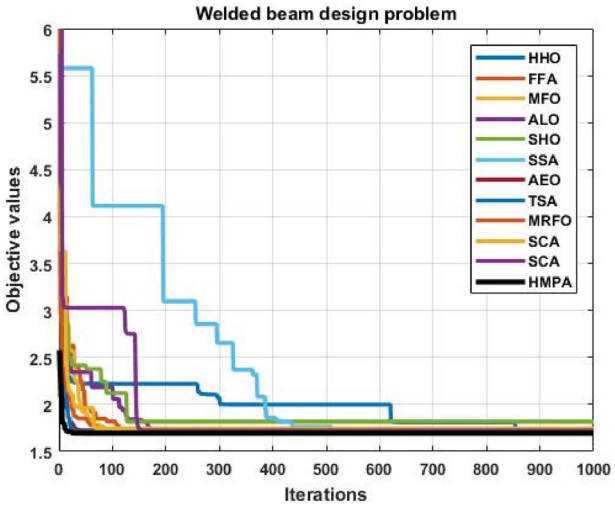

Fig. 21 Convergence graphs of the algorithms on the welded beam design problem

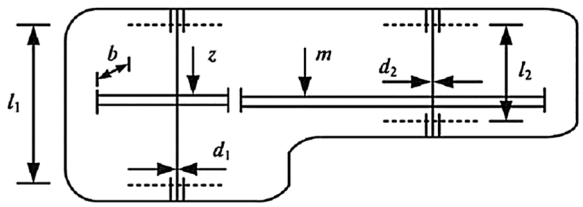

Fig. 22 Speed reducer design problem

Table 17 Statistical results of the algorithms on the speed reducer design problem

Algorithm	Best	Worst	Mean	Std.
HMPA	**2895.3333**	**2895.3333**	**2895.3333**	**0.0000e+00**
HHO	2918.9686	3065.9907	2978.6833	47.3050
FFA	2895.3356	2901.7623	2896.6489	2.01160
MFO	**2895.3333**	2906.4217	2896.0725	2.86300
ALO	2895.3335	2895.7423	2895.4296	0.15658
SHO	2996.5819	3087.6335	3038.3867	31.9255
SSA	2895.4881	2963.1217	2917.3115	19.7195
AEO	2895.3333	2895.6742	2895.3627	0.08808
TSA	2904.3056	2999.9241	2930.0140	13.5527
MRFO	**2895.3333**	**2895.3333**	**2895.3333**	5.8308e−07
SCA	3030.5630	3104.7790	3065.9172	18.0742
WOA	2899.7256	2995.8775	2917.5164	18.6605

It can be inferred from the statistical results of Tables 25 and 26 that the HMPA obtained better results, and considering the graphs of Fig. 30, the HMPA converged prier competitor algorithms.

7.7 Optimal thermo-hydraulic performance of an artificially roughened air heater problem

In this subsection, the performance of the algorithms is tested on a maximization problem, contrariwise, other subsections that deal with minimization issues. Optimal thermo-hydraulic performance of an artificially roughened air heater problem is a maximization design problem intended to maximize the heat transfer rate and maintaining the slightest amount of frictions losses. This problem consists of three variables: relative roughness pitch (*p/e*), relative roughness height (*e/D*), and Reynolds number (Re) that have been illustrated in Fig. 31.

The objective and the mathematical formulation of this problem are as below:Consider:

$$\vec{v} = \left[v_1, v_2, v_3\right] = \left[e/D, p/e, \mathrm{Re}\right],$$

Objective is to maximize:

$$\eta = 2.51\ln(e^{+}) + 5.5 - 0.1R_{\mathrm{M}} - G_{\mathrm{H}},$$

where $R_{\mathrm{M}} = 0.95v_2^{0.53}$, $G_{\mathrm{H}} = 4.5\left(e^{+}\right)^{0.28}(0.7)^{0.57}$, $e^{+} = v_1 v_3\sqrt{\frac{\bar{f}}{2}}$, $\bar{f} = \frac{f_{\mathrm{s}}+f_{\mathrm{r}}}{2}$, $f_{\mathrm{s}} = 0.079v_3^{-0.25}$, $f_{\mathrm{r}} = \frac{2}{\left(0.95v_3^{0.53}+2.5\ln\left(\frac{1}{2}v_1\right)^2-3.75\right)^2}$,

$0.02 \le v_1 \le 0.8, 10 \le v_2 \le 40, 3000 \le v_3 \le 20000.$

Table 18 The best-obtained results of the algorithms on the speed reducer design problem

Algorithms	Optimum variables							Optimal fitness
	b	m	z	l_1	l_2	d_1	d_2	
HMPA	3.50000	0.70000	17.00000	7.30000	7.80000	2.90000	5.28668	2895.3333
HHO	3.50843	0.70156	17.00000	7.50689	8.10234	2.92636	5.28678	2918.9686
FFA	3.50001	0.70000	17.00000	7.00001	7.80000	2.90000	5.28668	2895.3356
MFO	3.50000	0.70000	17.00000	7.00000	7.80000	3.90000	5.28668	2895.3333
ALO	3.50000	0.70000	17.00000	7.30000	7.80000	2.90001	5.28668	2895.3335
SHO	3.54721	0.70141	17.25842	7.81773	7.82436	2.95651	5.31054	2996.5819
SSA	3.50002	0.70000	17.00000	7.30049	7.80607	2.90005	5.28668	2895.4881
AEO	3.50000	0.70000	17.00000	7.30000	7.80000	2.90000	5.28668	2895.3333
TSA	3.50107	0.70010	17.00000	7.63893	7.84218	2.92479	5.28682	2904.3056
MRFO	3.50000	0.70000	17.00000	7.30000	7.80000	2.90000	5.28668	2895.3333
SCA	3.50875	0.70000	17.00000	7.30000	7.80000	3.46102	5.28921	3030.5630
WOA	3.50287	0.70000	17.00000	7.48038	7.88865	2.90000	5.28671	2899.7256

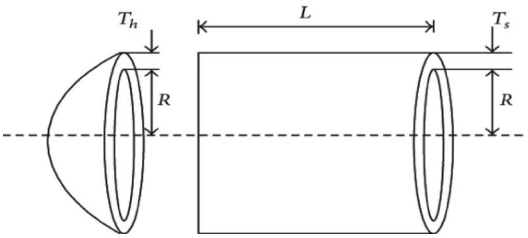

Fig. 24 Pressure vessel design problem

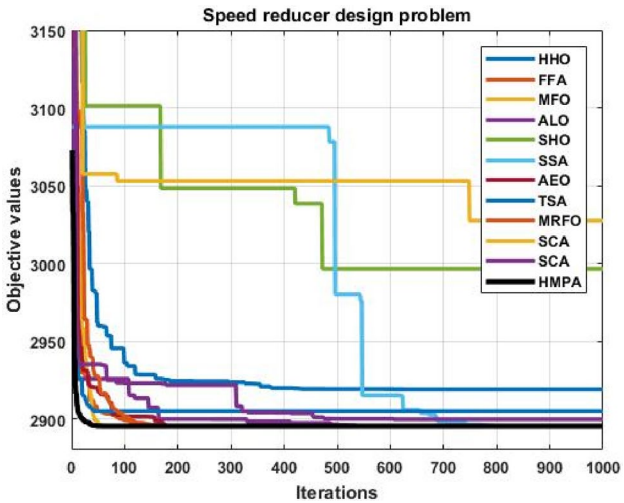

Fig. 23 Convergence graphs of the algorithms on the speed reducer design problem

Analogously, the statistical results are written in Table 27, and the best-obtained solutions are provided in Table 28. Furthermore, the convergence graphs are illustrated in Fig. 32.

Table 19 Statistical results of the algorithms on the pressure vessel design problem

Algorithm	Best	Worst	Mean	Std.
HMPA	**5885.3327**	**5885.3327**	**5885.3327**	**1.959e−12**
HHO	5966.5840	6814.2746	6358.6139	311.815
FFA	5885.9743	6453.3521	5973.1010	149.432
MFO	5885.3327	8344.0911	6228.1824	1.010e+03
ALO	5898.5516	6346.4962	6029.3359	180.245
SHO	5887.5773	5972.3207	5910.2141	14.8130
SSA	5888.7418	6239.0690	5960.6682	107.021
AEO	5885.3328	6509.7504	6020.4548	177.599
TSA	5892.2241	6139.5159	5943.1839	63.1080
MRFO	5885.5215	5892.2159	5886.9095	1.93356
SCA	6239.0690	6652.3541	6426.5906	131.609
WOA	6066.7024	6745.1734	6318.0960	97.9601

Table 20 The best-obtained results on the pressure vessel design problem

Algo.	Optimum variables				Optimal fitness
	T_s	T_h	R	L	
HMPA	0.778168	0.384649	40.31961	200.0000	5885.3327
HHO	0.822947	0.406761	42.63744	170.0701	5966.5840
FFA	0.778342	0.384856	40.32862	199.8597	5885.9743
MFO	0.778168	0.384649	40.31961	200.0000	5885.3327
ALO	0.785817	0.388430	40.71595	194.5557	5898.5516
SHO	0.780152	0.385631	40.42242	198.5739	5887.5773
SSA	0.780152	0.385631	40.42242	198.5739	5888.7418
AEO	0.778168	0.384649	40.31962	199.9999	5885.3328
TSA	0.778415	0.385684	40.38315	199.1565	5892.2241
MRFO	0.778217	0.384681	40.32240	199.9643	5885.5215
SCA	0.946210	0.467712	49.02644	106.2619	6239.0690
WOA	0.799025	0.437658	41.60884	182.7994	6066.7024

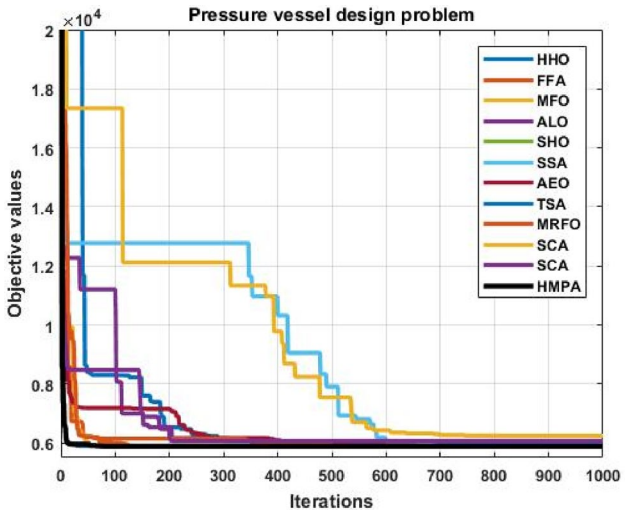

Fig. 25 Convergence graphs of the algorithms on the speed reducer design problem

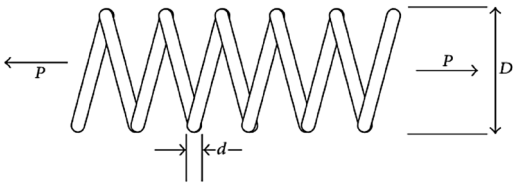

Fig. 26 Tension/compression spring design problem

Table 21 Statistical results of the algorithms on the tension/compression spring design problem

Algorithm	Best	Worst	Mean	Std.
HMPA	**0.01266535**	**0.01268822**	**0.01267299**	**6.6537e−06**
HHO	0.01266658	0.01369246	0.01308014	3.6809e−04
FFA	0.01266991	0.01321315	0.01275611	1.3438e−04
MFO	0.01268891	0.01515373	0.01331337	7.8862e−04
ALO	0.01271178	0.01737642	0.01349741	1.4539e−03
SHO	0.01274521	0.01319101	0.01300044	1.2909e−04
SSA	0.01296200	0.01319258	0.01314063	7.3959e−05
AEO	0.01266776	0.01354632	0.01290087	2.6881e−04
TSA	0.01266545	0.01298145	0.01276719	9.6949e−05
MRFO	0.01266605	0.01276648	0.01270041	3.2869e−05
SCA	0.01276188	0.01299844	0.01299772	1.5449e−04
WOA	0.01277431	0.01319508	0.01386738	1.4226e−03

According to the statistical results, it can be subsumed that most of the algorithms obtained optimal solution of the problem, and their results are close to each other. Similarly, given Fig. 32, the convergence rate of HMPA is relatively frail than several competitor algorithms.

Table 22 The best-obtained results of the algorithms on the tension/compression spring design problem

Algorithms	Optimum variables			Optimal fitness
	d	*D*	*P*	
HMPA	0.051608	0.354788	11.40295	0.01266535
HHO	0.051865	0.360985	11.04386	0.01266658
FFA	0.052306	0.317326	10.33072	0.01266991
MFO	0.052839	0.385022	9.803924	0.01268891
ALO	0.053307	0.396903	9.270784	0.01271178
SHO	0.050900	0.336987	12.59796	0.01274521
SSA	0.050000	0.313764	14.52448	0.01296200
AEO	0.051318	0.347858	11.82792	0.01266776
TSA	0.051798	0.359368	11.13524	0.01266545
MRFO	0.051902	0.361863	10.99356	0.01266605
SCA	0.050804	0.334702	12.77230	0.01277431
WOA	0.054179	0.419654	8.369768	0.01277431

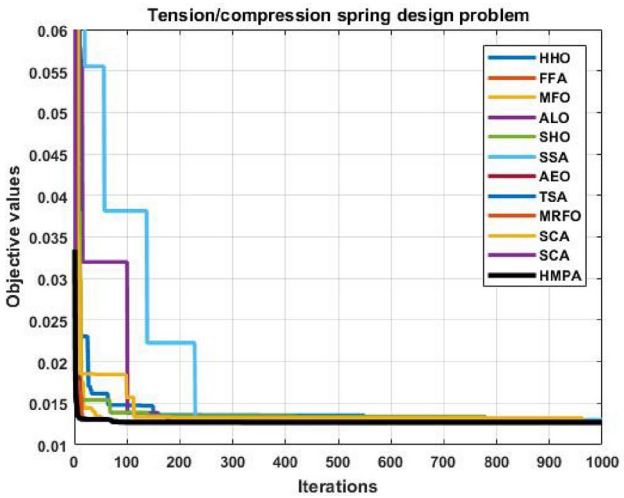

Fig. 27 Convergence graphs of the algorithms on the tension/compression spring design problem

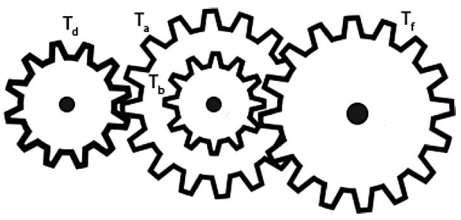

Fig. 28 Gear train design problem

8 Conclusion and future perspectives

This paper presents an innovative hybrid multi-population algorithm called HMPA. In HMPA, the initial population is

Table 23 Statistical results of the algorithms on the gear train design problem

Algorithm	Best	Worst	Mean	Std.
HMPA	**2.7008e−12**	**2.3078e−11**	**4.0593e−12**	**5.2613e−12**
HHO	2.7008e−12	2.3576e−09	8.6138e−10	1.0305e−09
FFA	2.7008e−12	1.1661e−10	2.7609e−11	3.4165e−11
MFO	9.9215e−10	2.7264e−08	5.5686e−09	8.7883e−09
ALO	8.8876e−10	1.8273e−08	8.3759e−09	7.8885e−09
SHO	2.3576e−09	1.0138e−06	1.7103e−07	3.0813e−07
SSA	9.9398e−11	1.1172e−08	3.5192e−09	4.2704e−09
AEO	2.7008e−12	1.0935e−09	2.4320e−10	4.1048e−10
TSA	2.7008e−12	9.7456e−10	8.7312e−11	2.4695e−10
MRFO	2.7008e−12	3.0675e−10	3.1122e−11	7.6915e−11
SCA	1.5450e−10	2.3576e−09	1.2606e−09	6.3148e−10
WOA	2.7008e−12	2.3576e−09	6.5324e−10	7.3375e−10

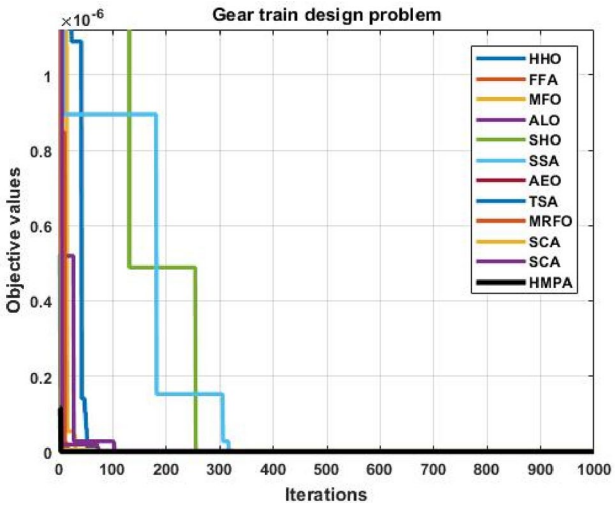

Fig. 29 Convergence graphs of the algorithms on the gear train design problem

Table 24 The best obtained results of the algorithms on the gear train design problem

Algo.	Optimum variables				Optimal fitness
	T_d	T_b	T_a	T_f	
HMPA	19	16	43	49	2.7008e−12
HHO	16	19	43	49	2.7008e−12
FFA	19	16	43	49	2.7008e−12
MFO	12	26	46	47	9.9215e−10
ALO	37	12	54	57	8.8876e−10
SHO	26	15	52	52	2.3576e−09
SSA	13	31	49	57	9.9398e−11
AEO	19	16	49	43	2.7008e−12
TSA	16	19	49	43	2.7008e−12
MRFO	16	19	49	43	2.7008e−12
SCA	21	13	43	44	1.5450e−10
WOA	16	19	49	43	2.7008e−12

Table 25 Statistical results of the algorithms on the spread spectrum radar poly-phase code design problem

Algorithm	Best	Worst	Mean	Std.
HMPA	**2.863416**	**2.863416**	**2.863416**	**2.3382e−14**
HHO	3.257884	4.507490	3.526011	3.1943e−01
FFA	2.864468	2.888421	2.875406	7.5426e−03
MFO	2.863416	3.008403	2.876389	3.8691e−02
ALO	2.863560	3.018374	2.932862	6.7822e−02
SHO	4.536872	4.855013	4.681426	1.1242e−01
SSA	2.863433	2.975245	2.880561	3.7375e−02
AEO	2.863440	3.008360	2.901156	6.4030e−02
TSA	2.872764	3.034620	2.958065	7.7604e−03
MRFO	2.863419	3.008958	2.883453	4.9997e−02
SCA	2.965197	4.584032	3.962797	3.1820e−01
WOA	2.867564	4.862673	3.686272	5.3895e−01

portioned into three sub-population. The sub-populations use an information exchange method to trade the solutions according to the

predefined principles. Furthermore, artificial ecosystem-based optimization (AEO), and Harris Hawks optimization (HHO) algorithms, which are the most recently developed powerful population-based optimization algorithms, are utilized in a hybrid model. Afterwards, some enhancement techniques are appended to the proposed framework to increase the potencies of the different aspects of the algorithm. In each round, solutions of the sub-populations are updated by only two techniques.

The HMPA is tested on fifty test functions, and the results are compared statistically and visually with well-known state-of-the-art algorithms. The experimental results reveal that the HMPA has extraordinary exploitation, exploration, and local optima departure capabilities. Moreover, the obtained results are inferentially corroborated using a nonparametric test called the Wilcoxon signed-rank test to investigate the conjectured dominance of the HMPA. The test divulges that the HMPA has a significant difference with the competitor algorithms.

In addition, HMPA is applied to seven constrained and unconstrained real-world engineering problems for further investigation of HMPA's performance. The results demonstrated that HMPA could solve real-life problems more efficiently.

Table 26 The best-obtained results of the algorithms on spread spectrum radar poly-phase code design problem

Algo.	Optimum variables										Optimal fitness
	v_1	v_2	v_3	v_4	v_5	v_6	v_7	v_8	v_9	v_{10}	
HMPA	2.378e−16	2.321e−15	3.743e−15	2.633e−16	2.004e−16	2.3634	4.988e−16	2.3634	2.3634	3.1416	2.863416
HHO	6.096e−02	8.548e−02	7.719e−02	0.4609	0.6706	1.2141	0.1029	2.5747	2.7304	3.0550	3.257884
FFA	8.086e−06	1.524e−03	6.911e−07	2.874e−05	2.210e−05	2.3612	0.0000	2.3644	2.3644	3.0967	2.864468
MFO	0.0000	0.0000	0.0000	2.3634	0.0000	0.0000	0.0000	2.3634	2.3634	3.1415	2.863416
ALO	0.0000	0.0000	0.0000	2.3635	3.239e−08	1.658e−06	0.0000	2.3635	2.3635	3.1714	2.863560
SHO	2.048e−01	8.613e−03	7.718e−01	3.938e−01	1.0705	9.494e−01	3.639e−03	4.0332	2.2355	2.4063	4.536872
SSA	2.740e−06	0.0000	0.0000	0.0000	6.032e−07	2.3634	0.0000	2.3634	2.3634	3.1515	2.863433
AEO	3.910e−05	4.318e−07	5.425e−08	2.3633	5.716e−10	2.202e−07	3.723e−07	2.3633	2.3634	3.1425	2.863440
TSA	2.3386	4.741e−03	1.984e−03	7.323e−03	4.685e−03	2.757e−03	2.573e−11	2.3727	2.3727	3.1273	2.872764
MRFO	9.708e−07	1.999e−07	5.719e−07	2.049e−06	7.840e−07	2.3634	2.983e−07	2.3634	2.3634	3.1448	2.863419
SCA	0.0000	0.0000	0.0000	0.0000	2.4371	0.0000	0.0000	2.1083	2.4651	3.2531	2.965197
WOA	2.3511	0.0000	0.0000	0.0000	0.0000	0.0000	0.0000	2.3670	2.3675	3.1858	2.867564

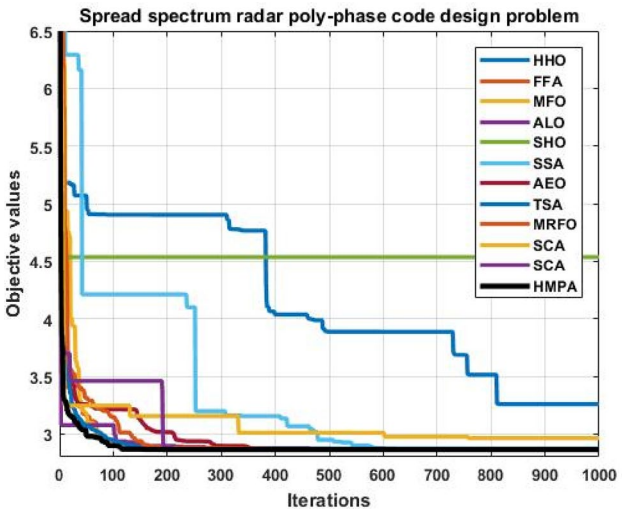

Fig. 30 Convergence graphs of the algorithms on the spread spectrum radar poly-phase code design problem

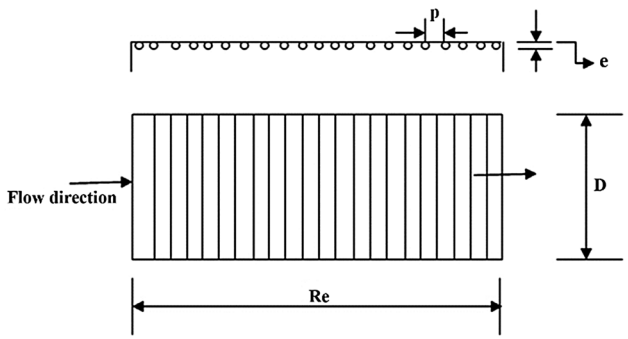

Fig. 31 Optimal thermo-hydraulic performance of an artificially roughened air heater problem

Table 27 Statistical results of the algorithms on optimal thermo-hydraulic performance of an artificially roughened air heater problem

Algorithm	Best	Worst	Mean	Std.
HMPA	**4.21421995**	**4.21421995**	**4.21421995**	**1.5439e−10**
HHO	4.21419764	4.21411714	4.21414264	7.3895e−06
FFA	4.21415627	4.21400125	4.21414305	2.9800e−06
MFO	**4.21421995**	**4.21421995**	**4.21421995**	9.1935e−09
ALO	**4.21421995**	**4.21421995**	**4.21421995**	5.9211e−09
SHO	4.21317361	4.21301246	4.21308535	3.1382e−04
SSA	**4.21421995**	**4.21421995**	**4.21421995**	6.7139e−09
AEO	**4.21421995**	**4.21421995**	**4.21421995**	9.1935e−09
TSA	4.21418159	4.21418005	4.21418039	9.9041e−06
MRFO	**4.21421995**	**4.21421995**	**4.21421995**	8.6485e−09
SCA	4.21421982	4.21421955	4.21421964	3.3404e−08
WOA	**4.21421995**	**4.21421995**	**4.21421995**	8.2229e−09

Table 28 The best-obtained results of the algorithms on optimal thermo-hydraulic performance of an artificially roughened air heater problem

Algorithms	Optimum variables			Optimal fitness
	e/D	p/e	Re	
HMPA	0.0600275	10.0002477	8803.1182	4.21421995
HHO	0.0811927	10.0000000	6344.0528	4.21419764
FFA	0.0614347	10.0021481	8576.8218	4.21415627
MFO	0.0665755	10.0000000	7899.1271	4.21418545
ALO	0.1379706	10.0000000	3408.1774	4.21418545
SHO	0.0524155	10.0317549	10858.295	4.21317361
SSA	0.0855700	10.0000000	5917.3500	4.21418545
AEO	0.0505278	10.0000000	10844.342	4.21421995
TSA	0.0642137	10.0010959	8163.6449	4.21418159
MRFO	0.0953062	10.0000000	5226.2444	4.21421995
SCA	0.1539215	10.0000000	3000.0000	4.21421982
WOA	0.0910979	10.0000000	5505.5379	4.21421995

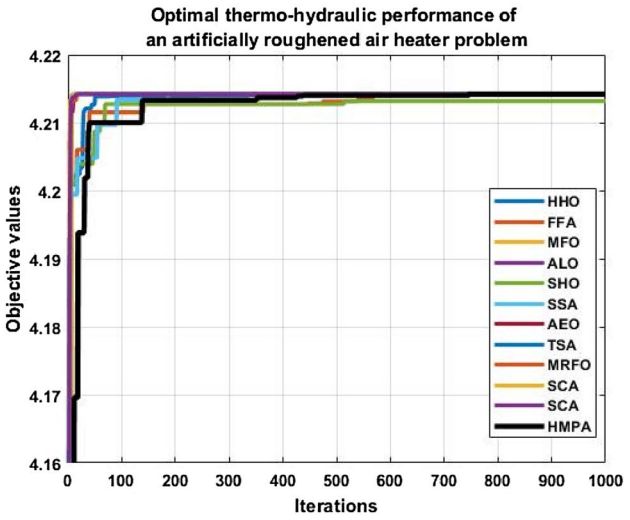

Fig. 32 Convergence graphs of the algorithms on the optimal thermo-hydraulic performance of an artificially roughened air heater problem

It is a question of future research to investigate the discretization and binarization of the HMPA. Besides, the HMPA can be extended to solve multi-objective problems.

References

1. Barshandeh S, Haghzadeh M (2020) A new hybrid chaotic atom search optimization based on tree-seed algorithm and Levy flight for solving optimization problems. Eng Comput. https://doi.org/10.1007/s00366-020-00994-0
2. Chandrawat RK, Kumar R, Garg B, Dhiman G, Kumar S (2017) An analysis of modeling and optimization production cost through fuzzy linear programming problem with symmetric and right angle triangular fuzzy number. In: Proceedings of sixth international conference on soft computing for problem solving. Springer, pp 197–211
3. Kaur A, Dhiman G (2019) A review on search-based tools and techniques to identify bad code smells in object-oriented systems. In: Yadav N, Yadav A, Bansal J, Deep K, Kim J (eds) Harmony search and nature inspired optimization algorithms, vol 741. Springer, Singapore. https://doi.org/10.1007/978-981-13-0761-4_86
4. Moghdani R, Abd Elaziz M, Mohammadi D et al (2020) An improved volleyball premier league algorithm based on sine cosine algorithm for global optimization problem. Eng Comput. https://doi.org/10.1007/s00366-020-00962-8
5. Sattar D, Salim R (2020) A smart metaheuristic algorithm for solving engineering problems. Eng Comput. https://doi.org/10.1007/978-3-030-16339-6_5
6. Zhang Y, Jin Z (2020) Group teaching optimization algorithm: a novel metaheuristic method for solving global optimization problems. Expert Syst Appl 148:113246
7. Cuevas E, Fausto F, González A (2020) The locust swarm optimization algorithm. In: New advancements in swarm algorithms: operators and applications. Springer, pp 139–159
8. Zhao W, Zhang Z, Wang L (2020) Manta ray foraging optimization: an effective bio-inspired optimizer for engineering applications. Eng Appl Artif Intell 87:103300
9. Zhao W, Wang L, Zhang Z (2019) Supply-demand-based optimization: a novel economics-inspired algorithm for global optimization. IEEE Access 7:73182–73206
10. Yadav A (2019) AEFA: artificial electric field algorithm for global optimization. Swarm Evolut Comput 48:93–108
11. Faramarzi A, Heidarinejad M, Stephens B, Mirjalili S (2020) Equilibrium optimizer: a novel optimization algorithm. Knowl-Based Syst 191:105190
12. Dhiman G, Kaur A (2019) STOA: a bio-inspired based optimization algorithm for industrial engineering problems. Eng Appl Artif Intell 82:148–174
13. Hashim FA, Houssein EH, Mabrouk MS, Al-Atabany W, Mirjalili S (2019) Henry gas solubility optimization: a novel physics-based algorithm. Future Gener Comput Syst 101:646–667
14. Abdullah JM, Ahmed T (2019) Fitness dependent optimizer: inspired by the bee swarming reproductive process. IEEE Access 7:43473–43486
15. Mohamed AAA, Hassan SA, Hemeida AM, Alkhalaf S, Mahmoud MMM, Baha Eldin AM (2019) Parasitism–Predation algorithm (PPA): a novel approach for feature selection. Ain Shams Eng J 11(2):293–308. https://doi.org/10.1016/j.asej.2019.10.004
16. Dhiman G, Kumar V (2018) Emperor penguin optimizer: a bio-inspired algorithm for engineering problems. Knowl-Based Syst 159:20–50
17. Dhiman G, Kumar V (2018) Multi-objective spotted hyena optimizer: a multi-objective optimization algorithm for engineering problems. Knowl-Based Syst 150:175–197
18. Dhiman G, Kumar V (2019) Seagull optimization algorithm: theory and its applications for large-scale industrial engineering problems. Knowl-Based Syst 165:169–196
19. Dhiman G, Kaur A Spotted hyena optimizer for solving engineering design problems. In: 2017 international conference on machine learning and data science (MLDS), 2017. IEEE, pp 114–119
20. Dhiman G, Kumar V (2019) Spotted hyena optimizer for solving complex and non-linear constrained engineering problems. In: Yadav N, Yadav A, Bansal J, Deep K, Kim J (eds) Harmony search and nature inspired optimization algorithms, vol 741. Springer, Singapore. https://doi.org/10.1007/978-981-13-0761-4_81
21. Faramarzi A, Heidarinejad M, Mirjalili S, Gandomi AH (2020) Marine predators algorithm: a nature-inspired metaheuristic. Expert Syst Appl 152:113377. https://doi.org/10.1016/j.eswa.2020.113377
22. Singh P, Dhiman G (2018) A hybrid fuzzy time series forecasting model based on granular computing and bio-inspired optimization approaches. J Comput Sci 27:370–385
23. Singh P, Dhiman G (2017) A fuzzy-LP approach in time series forecasting. In: International conference on pattern recognition and machine intelligence. Springer, pp 243–253
24. Singh P, Dhiman G, Kaur A (2018) A quantum approach for time series data based on graph and Schrödinger equations methods. Mod Phys Lett A 33(35):1850208
25. Dhiman G, Kaur A (2018) Optimizing the design of airfoil and optical buffer problems using spotted hyena optimizer. Designs 2(3):28
26. Dhiman G, Guo S, Kaur S (2018) ED-SHO: a framework for solving nonlinear economic load power dispatch problem using spotted hyena optimizer. Mod Phys Lett A 33(40):1850239
27. Kaur A, Kaur S, Dhiman G (2018) A quantum method for dynamic nonlinear programming technique using Schrödinger equation and Monte Carlo approach. Mod Phys Lett B 32(30):1850374
28. Singh P, Rabadiya K, Dhiman G (2018) A four-way decision-making system for the Indian summer monsoon rainfall. Mod Phys Lett B 32(25):1850304
29. Singh P, Dhiman G (2018) Uncertainty representation using fuzzy-entropy approach: special application in remotely sensed

high-resolution satellite images (RSHRSIs). Appl Soft Comput 72:121–139
30. Dhiman G, Kumar V (2018) Astrophysics inspired multi-objective approach for automatic clustering and feature selection in real-life environment. Mod Phys Lett B 32(31):1850385
31. Zhao W, Wang L, Zhang Z (2020) Artificial ecosystem-based optimization: a novel nature-inspired meta-heuristic algorithm. Neural Comput Appl 32:9383–9425. https://doi.org/10.1007/s00521-019-04452-x
32. Heidari AA, Mirjalili S, Faris H, Aljarah I, Mafarja M, Chen H (2019) Harris hawks optimization: algorithm and applications. Future Gener Comput Syst 97:849–872
33. Ma Y, Bai Y (2020) A multi-population differential evolution with best-random mutation strategy for large-scale global optimization. Appl Intell 50:1510–1526. https://doi.org/10.1007/s10489-019-01613-2
34. Babalik A (2018) A novel multi-swarm approach for numeric optimization. Int J Intell Syst Appl Eng 6(3):220–227
35. Ye W, Feng W, Fan S (2017) A novel multi-swarm particle swarm optimization with dynamic learning strategy. Appl Soft Comput 61:832–843
36. Arora S, Anand P (2019) Chaotic grasshopper optimization algorithm for global optimization. Neural Comput Appl 31(8):4385–4405
37. Demir FB, Tuncer T, Kocamaz AF (2020) A chaotic optimization method based on logistic-sine map for numerical function optimization. Neural Comput Appl. https://doi.org/10.1007/s00521-020-04815-9
38. Zhang X, Xu Y, Yu C, Heidari AA, Li S, Chen H, Li C (2020) Gaussian mutational chaotic fruit fly-built optimization and feature selection. Expert Syst Appl 141:112976
39. Dhiman G (2019) ESA: a hybrid bio-inspired metaheuristic optimization approach for engineering problems. Eng Comput. https://doi.org/10.1007/s00366-019-00826-w
40. Gupta S, Deep K, Moayedi H et al (2020) Sine cosine grey wolf optimizer to solve engineering design problems. Eng Comput. https://doi.org/10.1007/s00366-020-00996-y
41. Kaur S, Awasthi LK, Sangal AL (2020) HMOSHSSA: a hybrid meta-heuristic approach for solving constrained optimization problems. Eng Comput. https://doi.org/10.1007/s00366-020-00989-x
42. Shehab M, Alshawabkah H, Abualigah L, Nagham A-M (2020) Enhanced a hybrid moth-flame optimization algorithm using new selection schemes. Eng Comput. https://doi.org/10.1007/s00366-020-00971-7
43. Dhiman G, Kaur A (2019) A hybrid algorithm based on particle swarm and spotted hyena optimizer for global optimization. In: Bansal J, Das K, Nagar A, Deep K, Ojha A (eds) Soft computing for problem solving, vol 816. Springer, Singapore, pp 599–615. https://doi.org/10.1007/978-981-13-1592-3_47
44. Dhiman G, Kumar V (2019) KnRVEA: a hybrid evolutionary algorithm based on knee points and reference vector adaptation strategies for many-objective optimization. Appl Intell 49(7):2434–2460
45. Debnath S, Baishya S, Sen D et al (2020) A hybrid memory-based dragonfly algorithm with differential evolution for engineering application. Eng Comput. https://doi.org/10.1007/s00366-020-00958-4
46. Parouha RP, Das KN (2016) A memory based differential evolution algorithm for unconstrained optimization. Appl Soft Comput 38:501–517
47. Sree Ranjini KS, Murugan S (2017) Memory based hybrid dragonfly algorithm for numerical optimization problems. Expert Syst Appl 83:63–78
48. Cheng J, Wang L, Xiong Y (2019) Cuckoo search algorithm with memory and the vibrant fault diagnosis for hydroelectric generating unit. Eng Comput 35(2):687–702
49. Gupta S, Deep K (2019) Enhanced leadership-inspired grey wolf optimizer for global optimization problems. Eng Comput. https://doi.org/10.1007/s00366-019-00795-0
50. Zhou Z, Li F, Zhu H, Xie H et al (2020) An improved genetic algorithm using greedy strategy toward task scheduling optimization in cloud environments. Neural Comput Appl. https://doi.org/10.1007/s00521-019-04119-7
51. Roslan NB (2019) Lecturer timetable optimizer using genetic algorithm with hill climbing optimization method (LETO 2.0). Submitted in fulfilment of the requirement for Bachelor of Information Technology (Hons.), Intelligent System Engineering Faculty of Computer and Mathematical Science
52. Kesavan S, Sivaraj K, Palanisamy A, Murugasamy R (2019) Distributed localization algorithm using hybrid cuckoo search with hill climbing (CS-HC) algorithm for internet of things. Int J Psychosoc Rehabil 23(4)
53. Rao RV, Keesari HS, Oclon P, Taler J (2020) An adaptive multi-team perturbation-guiding Jaya algorithm for optimization and its applications. Eng Comput 36(1):391–419
54. Ang KM, Lim WH, Isa NAM, Tiang SS, Wong CH (2020) A constrained multi-swarm particle swarm optimization without velocity for constrained optimization problems. Expert Syst Appl 140:112882
55. Rao R, Pawar R (2020) Self-adaptive multi-population Rao algorithms for engineering design optimization. Appl Artif Intell 34(3):187–250
56. Vafashoar R, Meybodi MR (2020) A multi-population differential evolution algorithm based on cellular learning automata and evolutionary context information for optimization in dynamic environments. Appl Soft Comput 88:106009
57. Chen H, Heidari AA, Zhao X, Zhang L, Chen H (2020) Advanced orthogonal learning-driven multi-swarm sine cosine optimization: framework and case studies. Expert Syst Appl 144:113113
58. Darwish A, Ezzat D, Hassanien AE (2020) An optimized model based on convolutional neural networks and orthogonal learning particle swarm optimization algorithm for plant diseases diagnosis. Swarm Evolut Comput 52:100616
59. Xu Z, Hu Z, Heidari AA, Wang M, Zhao X, Chen H, Cai X (2020) Orthogonally-designed adapted grasshopper optimization: a comprehensive analysis. Expert Syst Appl 150:113282
60. Ozsoydan FB, Baykasoğlu A (2019) Quantum firefly swarms for multimodal dynamic optimization problems. Expert Syst Appl 115:189–199
61. Vijay RK, Nanda SJ (2019) A Quantum Grey Wolf Optimizer based declustering model for analysis of earthquake catalogs in an ergodic framework. J Comput Sci 36:101019
62. Liao Y, Qin G, Liu F (2019) Particle swarm optimization research base on quantum self-learning behavior. J Comput Methods Sci Eng. https://doi.org/10.3233/JCM-193644
63. Turgut MS, Turgut OE (2020) Global best-guided oppositional algorithm for solving multidimensional optimization problems. Eng Comput 36(1):43–73
64. Xu Y, Yang Z, Li X, Kang H, Yang X (2020) Dynamic opposite learning enhanced teaching–learning-based optimization. Knowl-Based Syst 188:104966
65. Chen H, Jiao S, Heidari AA, Wang M, Chen X, Zhao X (2019) An opposition-based sine cosine approach with local search for parameter estimation of photovoltaic models. Energy Convers Manag 195:927–942
66. Aslan S (2019) Time-based information sharing approach for employed foragers of artificial bee colony algorithm. Soft Comput 23(16):7471–7494

67. Tian M, Gao X (2019) An improved differential evolution with information intercrossing and sharing mechanism for numerical optimization. Swarm Evolut Comput 50:100341
68. Ning Y, Peng Z, Dai Y, Bi D, Wang J (2019) Enhanced particle swarm optimization with multi-swarm and multi-velocity for optimizing high-dimensional problems. Appl Intell 49(2):335–351
69. Truong KH, Nallagownden P, Baharudin Z, Vo DN (2019) A quasi-oppositional-chaotic symbiotic organisms search algorithm for global optimization problems. Appl Soft Comput 77:567–583
70. Guha D, Roy P, Banerjee S (2019) Quasi-oppositional backtracking search algorithm to solve load frequency control problem of interconnected power system. Iran J Sci Technol Trans Electr Eng 44:781–804. https://doi.org/10.1007/s40998-019-00260-0
71. Shiva CK, Kumar R (2020) Quasi-oppositional harmony search algorithm approach for ad hoc and sensor networks. In: De D, Mukherjee A, Kumar Das S, Dey N (eds) Nature inspired computing for wireless sensor networks. Springer tracts in nature-inspired computing. Springer, Singapore. Springer, pp 175–194. https://doi.org/10.1007/978-981-15-2125-6_9
72. Yi J, Li X, Chu C-H, Gao L (2019) Parallel chaotic local search enhanced harmony search algorithm for engineering design optimization. J Intell Manuf 30(1):405–428
73. Gao S, Yu Y, Wang Y, Wang J, Cheng J, Zhou M (2019) Chaotic local search-based differential evolution algorithms for optimization. IEEE Trans Syst Man Cybern Syst. https://doi.org/10.1109/TSMC.2019.2956121
74. Zhao R, Wang Y, Liu C, Hu P, Li Y, Li H, Yuan C (2020) Selfish herd optimizer with levy-flight distribution strategy for global optimization problem. Physica A 538:122687
75. Xie W, Wang J, Tao Y (2019) Improved black hole algorithm based on golden sine operator and levy flight operator. IEEE Access 7:161459–161486
76. Wu H, Wu P, Xu K, Li F (2020) Finite element model updating using crow search algorithm with levy flight. Int J Numer Methods Eng. https://doi.org/10.1002/nme.6338
77. Qiu C (2019) A novel multi-swarm particle swarm optimization for feature selection. Genet Program Evolvable Mach 20(4):503–529
78. Sedarous S, El-Gokhy SM, Sallam E (2018) Multi-swarm multi-objective optimization based on a hybrid strategy. Alexandria Eng J 57(3):1619–1629
79. Nie W, Xu L Multi-swarm hybrid optimization algorithm with prediction strategy for dynamic optimization problems. In: 2016 international forum on mechanical, control and automation (IFMCA 2016), 2017. Atlantis Press
80. Li J, Xiao D-d, Zhang T, Liu C, Li Y-x, Wang G-g (2020) Multi-swarm cuckoo search algorithm with Q-learning model. Comput J. https://doi.org/10.1093/comjnl/bxz149
81. Ali MZ, Awad NH, Suganthan PN (2015) Multi-population differential evolution with balanced ensemble of mutation strategies for large-scale global optimization. Appl Soft Comput 33:304–327
82. Biswas S, Das S, Debchoudhury S, Kundu S (2014) Co-evolving bee colonies by forager migration: a multi-swarm based Artificial Bee Colony algorithm for global search space. Appl Math Comput 232:216–234
83. Di Carlo M, Vasile M, Minisci E (2020) Adaptive multi-population inflationary differential evolution. Soft Comput 24:3861–3891. https://doi.org/10.1007/s00500-019-04154-5
84. Xiang Y, Zhou Y (2015) A dynamic multi-colony artificial bee colony algorithm for multi-objective optimization. Appl Soft Comput 35:766–785
85. Bao H, Han F A hybrid multi-swarm PSO algorithm based on shuffled frog leaping algorithm. In: International conference on intelligent science and big data engineering, 2017. Springer, pp 101–112
86. Wu G, Mallipeddi R, Suganthan PN, Wang R, Chen H (2016) Differential evolution with multi-population based ensemble of mutation strategies. Inf Sci 329:329–345
87. Saha S, Mukherjee V (2018) A novel quasi-oppositional chaotic antlion optimizer for global optimization. Appl Intell 48(9):2628–2660
88. Dhiman G, Kumar V (2017) Spotted hyena optimizer: a novel bio-inspired based metaheuristic technique for engineering applications. Adv Eng Softw 114:48–70
89. Shayanfar H, Gharehchopogh FS (2018) Farmland fertility: a new metaheuristic algorithm for solving continuous optimization problems. Appl Soft Comput 71:728–746
90. Mirjalili S, Gandomi AH, Mirjalili SZ, Saremi S, Faris H, Mirjalili SM (2017) Salp swarm algorithm: a bio-inspired optimizer for engineering design problems. Adv Eng Softw 114:163–191
91. Mirjalili S (2015) Moth-flame optimization algorithm: a novel nature-inspired heuristic paradigm. Knowl-Based Syst 89:228–249
92. Mirjalili S (2015) The ant lion optimizer. Adv Eng Softw 83:80–98
93. Awad N, Ali M, Liang J, Qu B, Suganthan P (2017) CEC 2017 Special session on single objective numerical optimization single bound constrained real-parameter numerical optimization
94. Liang J, Qu B, Suganthan P (2013) Problem definitions and evaluation criteria for the CEC 2014 special session and competition on single objective real-parameter numerical optimization. Computational Intelligence Laboratory, Zhengzhou University, Zhengzhou China and Technical Report, Nanyang Technological University, Singapore, p 635
95. Kiran MS (2015) TSA: tree-seed algorithm for continuous optimization. Expert Syst Appl 42(19):6686–6698
96. Mirjalili S (2016) SCA: a sine cosine algorithm for solving optimization problems. Knowl-Based Syst 96:120–133
97. Mirjalili S, Lewis A (2016) The whale optimization algorithm. Adv Eng Softw 95:51–67